Extraction of Flood Risk-Related Base-Data from Multi-Source Remote Sensing imagery

Hastings Shamaoma
March, 2005

Extraction of flood risk-related base-data from multi-source remote sensing imagery

By

Hastings Shamaoma

Thesis submitted to the International Institute for Geo-information Science and Earth Observation in partial fulfilment of the requirements for the degree of Master of Science in **Geoinformatics**

Thesis Assessment Board

Chairman:	Prof. Dr. J. L. Van Genderen
External examiner :	Dr. Ir. B. G. H. Gorte
Supervisor :	Dr. N. Kerle
Second supervisor :	Prof. Dr. Ir. M.G. Vosselman

INTERNATIONAL INSTITUTE FOR GEO-INFORMATION SCIENCE AND EARTH OBSERVATION
ENSCHEDE, THE NETHERLANDS

Disclaimer

This document describes work undertaken as part of a programme of study at the International Institute for Geo-information Science and Earth Observation. All views and opinions expressed therein remain the sole responsibility of the author, and do not necessarily represent those of the institute.

To my brother, Maybin Shamaoma for the inspiration he gave me.
To Andrew Mulenga, for the friendship and the dream we never fulfilled.
To Mon, Dad, and my siblings, for believing in me when I didn't believe in myself.

Abstract

Flooding is ranked as one of the most destructive disasters in the world, accounting for over one third of estimated total cost in damages world wide and responsible for two thirds of people affected by natural disasters. Developing countries, where over 90% of fatalities caused by natural disasters occur, are the worst affected partly due to their geographical location, but mainly due to lack of coping capacity, overdependence on foreign aid, urbanisation and lack of preparedness and early warning systems. One of most devastating flood disasters recorded in recent years was the Hurricane Mitch, which devastated Central America in 1998 and had long term devastating impact on the economies of the affected countries. Honduras was the worst affected with over 7000 fatalities and total damages of about 69% of the countries' gross domestic product (GDP).

The major cause of high fatalities in developing countries is lack of flood hazard risk models for identifying areas at risk, to enable effective early warning. This is largely due to lack of base-data needed to run them and scarcity and cost of image data sources. Base-data are the underlying foundation or basic framework data from which information related to risk can be derived and used as input to risk modeling. This study uses segmentation-based object-oriented image analysis techniques to extract base data from partially interchangeable image data sets. The first part of this study examines the interchangeability of QUICKBIRD imagery and a gridded light detection and ranging (LIDAR) digital surface model (DSM) to extract basedata that can be used as inputs to flood risk modeling in the city of Tegucigalpa, Honduras. Firstly, the two data sets were used to extract building foot prints and achieved provisional accuracies of 89% and 84% for LIDAR and QUICKBIRD, respectively. Secondly, the two data sets were used to extract the boundaries of informal settlements, which are a common feature in flood plains of developing countries, and where houses are most vulnerable. The results obtained in this case also showed good interchangeability of the two data sets. Thirdly, two complimentary products are generated from the imagery: a detailed land cover map for the purpose of deriving roughness values for input to flood hazard models from QUICKBIRD, and an estimation of the number of floors of buildings from LIDAR DSM, which is an important input to vulnerability assessment.

The second part was to examine the use of lower resolution imagery to extract more regional land cover maps. Land cover maps were extracted from the degraded QUICKBIRD imagery at 15 m resolution, enhanced Landsat ETM imagery, at 15 m and 30 m resolution. Land covers such as heavily built-up, built-up/bare-land, vegetation, and river (average width 14 m) were successfully extracted with accuracies of 85% and 71% for the degraded QUICKBIRD imagery and enhanced Landsat 15 m resolution imagery respectively. Due to the narrow width of the river, it was not possible to detect it at 30 m resolution. However, the other land covers were extracted with an accuracy of 68%. The 15 m and lower resolution, was particularly targeted because freely available imagery such Aster have that resolution.

The present study shows a great potential for various remote image sources to extract base-data for input to flood risk models, which are used to generate useful information for decision makers to reduce the impacts of flood disasters through sustainable and safe land use planning. Most importantly, they are useful for providing effective early warning and in the long run reduce the current high fatalities.

Key words: Flood-risk, base-data, segmentation-based, interchangeability, QUICKBIRD LIDAR DSM

Acknowledgements

I wish to extend my sincere gratitude to my first supervisor Dr. Norman Kerle for his tireless efforts. Without his guidance, constructive criticism and encouragement this project could not have seen light. I owe a special debt of thanks to my second supervisor Professor Dr. George Vosselman for his advice, critical comments and assistance in pre-processing the LIDAR DSM.

I gratefully acknowledge my debt to Drs. Dinand Alkema who first introduced me to the concepts of flood modelling and input requirements that can be extracted from remote sensing imagery, and for the advice and guidance throughout my research. My grateful thanks are due to Dr. Cees van Westen for proving me with the data and materials that were used in this research.

I express my sincere gratitude to The Netherlands government who gave me an opportunity to expand my professional carrier. I also thank the management at the Zambia Survey Department for giving a study leave. Indeed the advice, support and guidance of the Geoinformatics program director, Mr. Gerrit Huurneman, are well appreciated.

My thanks are due to my Zambian colleagues for the support and company during the hard times. My classmates, GFM.2-2003 colleagues, thanks for the company, I really enjoyed studying with you.

Above all, I owe a special debt of thanks to my parents for the support, advice and letting me make my own decisions in life. Without them I would not have gone this far. Lastly, though not the least, I would like express my gratitude to my brothers, my sisters, and my friends for the moral support and understanding.

Table of contents

List of figures

List of tables

1 Introduction

1.1 Flooding disaster overview

Natural disasters happen every year and their impact and frequency is on the increase. According to *Munich Reinsurance (2000),* the frequency of natural disasters has tripled over the last four decades. More than 18% of all Natural Disasters occur in developing countries, and 50% to 60% of these countries are extremely vulnerable *(Munich Reinsurance, 2003).* Flooding is ranked as one of the most frequent, destructive and damaging disasters *(IFRCRS, 1998; UN/ISDR, 2002).* According to *Glickman et al. (1992)* floods accounted for over 30% of all disasters between 1945 and 1986. These estimates were substantiated by a *Munich Reinsurance (2001)* review of economic losses for great natural catastrophes from 1950 to 2000, in which floods were reported to have accounted for over one third of total cost and were responsible for over two thirds of people affected by disasters. In terms of loss of life, floods are ranked third among geophysical hazards, coming after earthquakes and tropical cyclones. However, according to a report by *UNDP(2004),* between 1980 and 2000 floods killed more people than earthquakes coming second to tropical cyclones. Both the *IFRCRS (1998)* and *Munich Reinsurance (2001)* put Asia as the most affected region, accounting for about 90 % of people affected by natural disasters. These data were corroborated by the recent tsunami disaster that occurred on 26th December 2004, and affected Asian countries that border the Indian ocean, and caused a regional death toll of over 270 000 and disrupted livelihoods of millions of people.

According to data compiled by *CRED (2004),* flood disasters are on the increase with reported average annual extreme flood events ranging from 50 for the period between 1975 to 1985; 80 for the period between 1985 to 1995; to 140 for the period between 1995 to date. Yet the average death toll has remained steady with a substantial decrease in developed countries. This decrease in death toll for developed countries has been attributed to high investment in early warning systems, adequate preparation and incorporation of risk management in developmental plans *(UNDP, 2004).* On the contrary, the death toll in developing countries, where more than 4,200 million people live still remains high. The reasons for the high toll are: (i) high urbanisation rates and marginalisation of the poor, which forces people to settle in flood plains; (ii) lack of coping capacity, (iii) over-dependency on foreign aid and external borrowing; (iv) relative scarcity of early warning systems and lack of preparation; and (v) climate changes. Adequate preparation makes a big difference even among developing countries. For example Hurricane Ivan killed over 2000 in Haiti and only 11 in the neighbouring Dominican Republic, yet rains were even stronger in the latter but they were well prepared for the disaster *(UN/ISDR, 2004).* In terms of damages to infrastructure, high losses are recorded in developed countries due to the high standard of living and property value in those countries. However, the lack of coping capacity and smaller economies make developing countries suffer long impacts from damages. A good example is Hurricane Mitch, which devastated Honduras, in 1998 causing damages of over $5billion and accounted for about 69% of the countries gross domestic product (GDP). By comparison, Hurricane Andrew in 1998 caused damages of $30 billion in the USA, but this is less than 0.5% of GDP for that country *(UN/ISDR, 2002).* The disasters lead to diversion of resources meant for social services such as health care and education, to rebuilding of damaged infrastructure and increases external borrowing. The next section gives a brief overview of the impact of

Hurricane Mitch on Honduras, as an example of a developing country faced with the above cited problems.

1.1.1 Hurricane Mitch and Honduras

Hurricane Mitch, a category five hurricane, devastated Central America in 1998, causing widespread flood, storm surge, landslide, and mudslide damages. Over 3.5 million people were affected, an estimated 9,214 were killed and 12,845 were injured. Regional damages have been reported to have exceeded $US 7.5 billion *(UNDP/ECLAS, 1998)*, primarily in Honduras, Costa Rica and Nicaragua. In Honduras, 7000 people died, 33 000 homes and 95 bridges were destroyed, and 70% of the road network was destroyed *(Mastin, 2002)*.

The impact was worsened by lack of accurate up-to-date maps that clearly define areas prone to flooding, lack of preparation and early warning, and limited financial and human resources to cover the wide-spread effects of Mitch. The lack of geo-referenced maps presented difficulties even to the post Mitch impact assessment studies *(e.g. Martine and Guzman, 2002; UNDP/ECLAS, 1998),* who cited difficulties in relating socioeconomic data to their location and extent. Flood risk maps, though not a universal remedy, are an important tool for preparation and management of such phenomena. Adequate preparation and early warning system made a big difference in Costa Rica, where Mitch caused damages amounting to $222 million, yet only 9 people were reported missing or dead *(Martine and Guzman, 2002)*. Considering the large areas covered, the high cost involved in mapping, and the dynamic nature of flood risk and vulnerability, which demands for continuous updating of information, geoinformation techniques such as global positioning systems (GPS), geographical information systems (GIS) and remote sensing (RS) have been identified as important tools to satisfy this information demand. To illustrate this, the following section gives an overview on geoinformation science and disasters.

1.1.2 Geoinformation science and disasters

Disaster management is a typically multi-disciplinary endeavour, requiring many types of data with spatial and temporal attributes that should be made available to key players in the right format for decision-making. The volume of information needed for natural disasters far exceeds the capacity to deal with them manually *(van Westen, 2002)*. Moreover disaster management cuts across boundaries including organizational, political, geographic, professional, topical, and sociological. For the information from various sources to be used in the same environment, it has to be georeferenced and be in a compatible format. Geoinformation science is a set of tools dealing with collecting, processing, analysis and visualisation of georeferenced data. These tools include GIS, GPS and RS, and can be used to provide different information at various phases of a disaster.

At the disaster preparation phase, GIS, GPS and RS are used in combination to collect data and the data from different sources, and disciplines are combined in a GIS for hazard and risk assessment. Additionally, a combination of GPS and GIS on mobile GIS systems allow for collection, processing and updating of existing database while in the field. During the response phase, RS techniques provide data rapidly over extensive areas, and areas that are made inaccessible by the effects of the disaster. A combination of GPS and GIS on mobile GIS system are used in search and rescue operations *(van Westen, 2002).* During the recovery or relief phase, RS and GIS techniques are used for collecting data for damage assessment and reconstruction planning. More details on previous works on flood related RS applications are given in section 2.7.

1.1.3 Some important definitions

Before reviewing the application of RS in extracting risk related base-data for assessing hazards and disasters, it is important first to give definitions of some of the terms that are going to be used in this thesis.

A 'flood disaster event' is an excess amount of water, rising above the banks of a watercourse and perforating into adjacent areas, exposing society to severe danger, which results in disruption, damage and casualties that cannot be relieved by the unaided capacity of locally-mobilised resources *(United Nations Disaster Relief Co-ordinator, 1991).*

Elements at risk are people, buildings, roads, factories, agricultural fields, and other natural and man made features of value to humans, that are vulnerable to disasters *(Melching and Pilon, 1999).*

Base-data are the underlying foundation or basic framework data from which information related to risk can be derived and used as input to risk modelling. Examples of base-data in flood modelling are: soil data, Digital Elevation Models (DEMs), social/economic data, land cover maps, outline of water bodies, building footprints and building heights.

1.2 Problem definition

Flood risk models are important tools for simulating and predicting the flood event and analysing its consequences on the elements at risk, and provide warning to save lives *(Chapman et al., 2003)*. However, for these models to give meaningful results they need base-data to run them, which in most cases is unavailable in developing countries. This is due to the scarcity and cost of image data sources from which these data are derived. Therefore, there is a need to investigate the interchangeabilty of different image sources to provide the needed base-data. The other problem is the increasing number of people settling on the floodplains due to social reasons and difficulties in extracting quantitative information from imagery (e.g. distinguishing between settlement densities and extracting building footprints).

1.2.1 Objectives of the research

The aim of this study is to extract flood risk related base-data from multi-source RS imagery with emphasis on:

- Integrating existing tools to extract base-data from RS imagery
- investigating the interchangeability of different image data sources and
- use of RS imagery from various sensors to extract quantitative information for assessing flood hazard and vulnerability.

1.2.2 Research questions

The following research questions will help to address the above objective:

- What are the relevant base-data for flood risk assessment?
- What is the suitability of different image datasets to extract those base-data?
- What are the suitable methods for extracting these data?
- How can images of a lower resolution help in extracting the required base-data?
- How can we evaluate the accuracy and certainty of the obtained results for their correct application in risk assessment?
- How can RS imagery help us in dealing with the dynamic nature of flood risk?

- It is possible to extract quantitative information on the elements at risk from high resolution imagery?

1.3 Scope of the work

This study focused on extracting flood risk-related base-data from available RS imagery that can be used as input to flood risk models. No actual modelling was done. All the inputs were generated based on consultations from flood modellers and from literature review.

1.4 Thesis outline

The thesis is divided into seven chapters (Fig 1-1). The rest of the thesis is arranged as follows: Chapter 2 gives a review on some of the approaches used in flood risk modelling. Based on the reviewed modelling approach, inputs to flood risk models are identified and described and then a review of previous applications of RS techniques to flood risk assessment is given to show how technology has been applied.

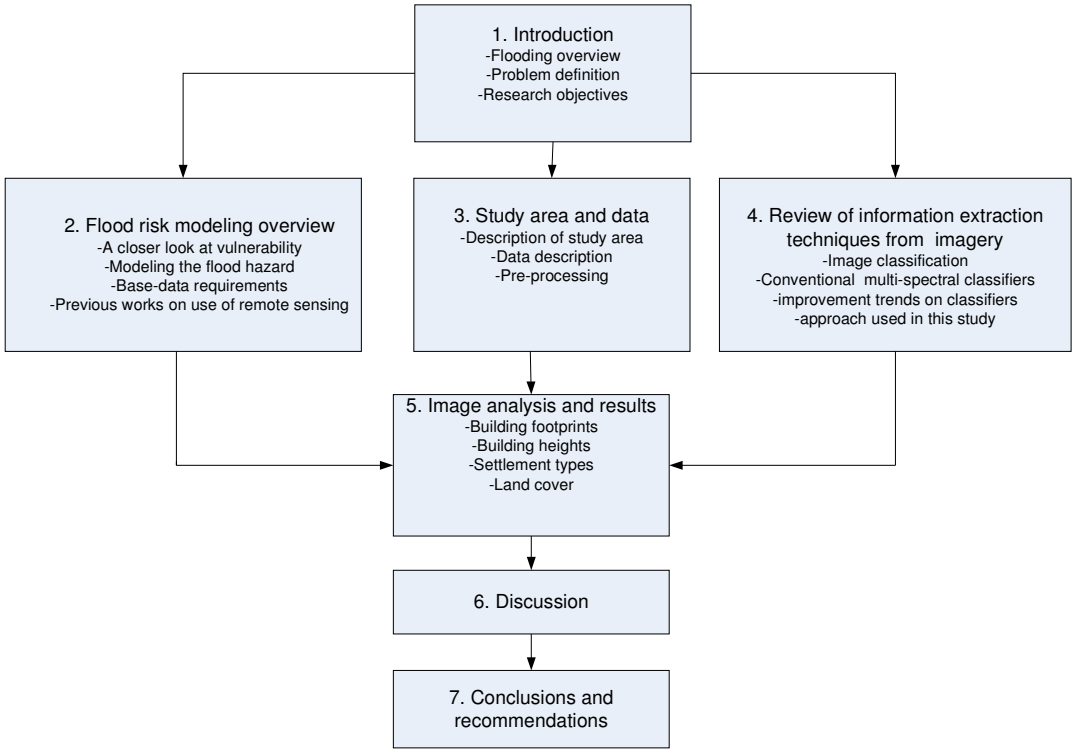

Fig. 1-1: Thesis outline flow

Chapter 3 gives the description of the study area and the reasoning behind the choice of the study area. Then the data available for the study area and pre-processing operations performed on the data are described. Chapter 4 gives a brief review of the information extraction techniques with much focus on image classification. Then the approach used in this study is introduced and briefly described. Chapter 5 gives a description of the methods followed to extract various sets of base-data, extracted in this study and presents the obtained results. Chapter 6 gives the detailed discussion of the results in relation to the set objectives. In chapter 7, the conclusion of the research is presented followed by the recommendations for future research and summary for disaster managers

2 Flood risk modelling overview

2.1 Introduction

Floodplains are areas with ecologically important wetlands, and mainly exhibit competitive advantages for human settlement. Resolving the potential conflict between ecological value and human use is consequently a major issue in determining the most appropriate flood hazard management strategy. At the same time, the strategy adopted must consider how all floods are to be managed, and not just some *(Green et al., 2000)*. The likely outcome is then that the strategy adopted will consist of a mix of options.

Floods are defined differently depending on where they occur and what causes them. A more broad and representative definition is given by *Green et al (2000)*: 'A flood is a body of water which rises to overflow land which is not normally submerged'. Table 2-1 gives a summary of some types of flood and their causes. Though the base-data to be extracted in this study could be used in many of the floods, the focus of this study will be on river flooding.

Table 2-1: types of floods

Type	Description and examples
River floods	Water exceeds the capacity of the river channel, caused by excess rainfall, snowmelt, ice melt due to rise in temperature etc.
Mud floods	Floods with high sediment content induced by volcanic activity, e.g. lava flow
Coastal/sea/tidal floods	Ocean water driven in land due to tropical storms, hurricanes or intense offshore low pressure.
	Ocean water driven inland due to a tidal sea wave induced by a geological process such as an earthquake or volcanic activity e.g. Tsunamis
Dam floods	Overflows caused by dam-break, dam overtopping or failure of natural dams, e.g. moraines
Sewer/urban drain flood	Storm discharge to sewers and rains exceeds capacity and overflows into surrounding areas (e.g. industries, commercial centres and residential houses)
Flash floods	A large amount of water floods within short period, and normally occurs locally and suddenly with little warning (caused by immoderate rainfall, dam failure, or a sudden release of water held by an ice jam).

Floods are part of the dynamic variation of the hydrological cycle, the basic causes of which are climatological. To this must be coupled the nature of the terrain which generates the runoff (e.g. geology, soil type and vegetation cover), and the antecedent conditions as well as the characteristics of the stream networks characteristics (e.g. storage capacity, channel length); and channel characteristics (e.g. channel roughness and shape) *(Green et al., 2000)*. Many of the most catastrophic floods are associated with the intense rainfalls that result from hurricanes, cyclones and typhoons. Floods have a number of measurable characteristics, including flood depth or 'stage', discharge (i.e. volume) or magnitude, frequency (usually estimated as a return period or recurrence interval), duration, velocity, extent and seasonality.

2.2 Flood risk management

Flood risk management consists of five main parts, which are depicted in Figure 2-1, and these are: (i) hazard modelling, which includes identification of the hazards and characterisation of their nature and extent, as well as the mechanics of the flood in terms of water depth, velocity and damage potential, estimation of the extent of flooding, and estimation of the probability (or frequency) of flooding; (ii) vulnerability analysis or consequence analysis, which includes estimation of the potential numbers of people impacted by the flooding, assessment of the likely property damage due to flooding, assessment of other flooding impacts such as costs to businesses, environmental damage and identification of critical buildings (hospital, schools, houses for the disabled); (iii) risk calculation and mapping; (iv) risk evaluation, which involves investigation of risk mitigation options by weighing costs and benefits of implementing them; and (v) risk treatment, where implementation and review takes place.

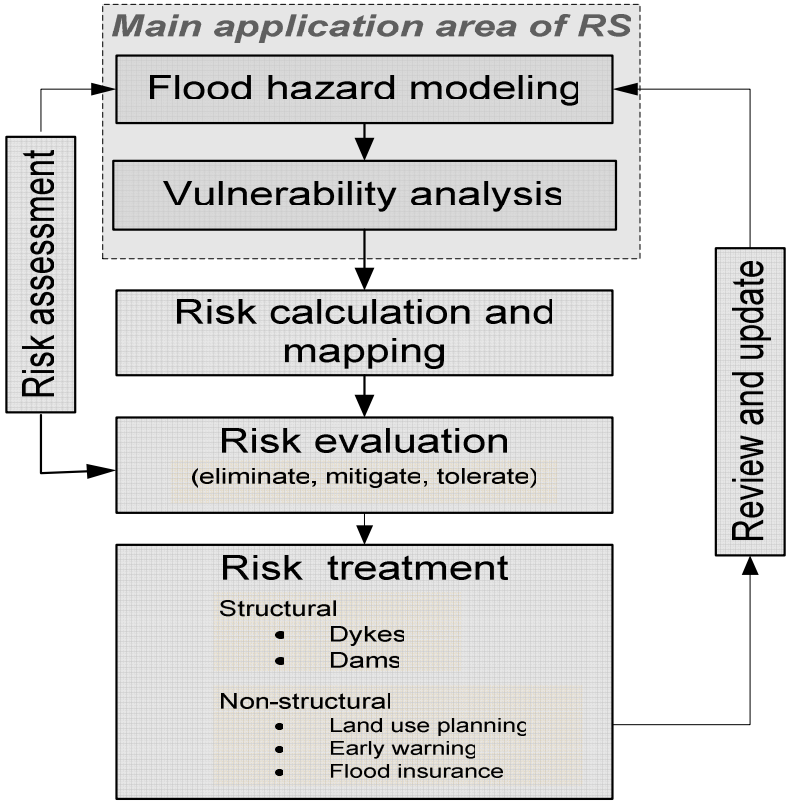

Fig. 2-1: Flood risk management ***(Modified from Chapman et al., 2003)***

The first two parts of the flood management process given in Fig. 2-1 are of prime importance when it comes to base-data requirements that can be extracted from RS imagery, which is the main focus of this study. First the role of these parts in flood risk management is discussed in more detail and then the base-data requirements are identified.

2.3 A closer look at vulnerability

The study of vulnerability related to natural disasters has been the focus of different investigations and has led to several definitions, which reflect different disciplinary and ideological positions, and different purposes. *Green et al. (2000)* identifies three main

definitions of vulnerability: (i) as a characteristic of the population at risk; (ii) as a characteristic of the flood to which that population is exposed; or (iii), as the interaction between the nature of the flood and the characteristics of the population at risk. Following this categorisation, the following studies are grouped accordingly.

Blaikie et al.(1994)) took the first approach, defining vulnerability as: 'the characteristics of a person or group in terms of their capacity to anticipate, cope with, resist, and recover from the impact of a natural hazard'. Whilst this definition of vulnerability includes recovery after a flood and capacity to recover, it also includes adaptation to floods and response during a flood. In the same category *Cannon (1993)* gives a more germane definition by considering different factors affecting or producing the vulnerability of individuals or groups. He defines vulnerability as a characteristic of individuals and groups of people who inhabit a given natural, social and economic space, within which they are differentiated according to their varying position in society into more or less vulnerable individuals and groups and divided it into three parts: (i) Livelihood resilience: the degree of resilience of the particular livelihood system of an individual or group, and their capacity for resisting the impact of a flood hazard. (ii) Health: including both the robustness of individuals, and the operation of various social measures. (iii) Preparedness: determined by the protection available for a given hazard, something that depends on people acting on their own behalf, and social factors. The weakness of this first definition is that it assumes that the community will have the same level of vulnerability regardless of the flood impact.

Some studies use the second definition of vulnerability to flooding, and interpret it as a function of the characteristics of flooding, e.g. the floods magnitude, speed of onset etc. *(Green et al., 2000).* The characteristics of the population and land use systems affected are either ignored or are only considered as peripheral matters. Using this interpretation vulnerability can be determined by a hydrological analysis only, which implies fixing the flood problem without regarding what it impacts on.

In the third category, vulnerability is generally defined as that which results when coping resources are inadequate to meet the challenge posed by a flood. It is viewed as a product of the interaction of the flood event and some of the characteristics of the affected land uses and population. The third definition has become an all-encompassing means of assessing risk and social and economic consequences associated with a hazard *(Alexander, 1993).*

2.4 Modelling the flood hazard

The necessary first step to flood management is to identify the nature and extent of the threat. This requires modelling of the flood hazard and many studies take different approaches that can be generally classified according to the definitions of vulnerability described above. The simplest form of such a model is a floodplain map. The basis of such maps may vary from an approximate interpretation of records of the largest floods of historic record to those based on comprehensive mathematical or physical models showing in accurate detail the extent, velocity and depth of flooding for defined return periods. These approaches give a picture of differing levels of accuracy and detail of the flooding hazard at a single moment in time of a historical or idealised "design" flood. Most engineering studies follow this approach, and it serves as a basis for most existing structural protective measures *(e.g. Bye and Horner, 1998).* This approach is used by land use planners and decision makers mainly at regional levels. It is in this approach, where RS imagery is used widely in the generation of basic inputs for

hydrological models; (i.e. for peak flood extent mapping and generating land cover maps for friction values and DEMs see the a review of previous works in section 2.7).

The weakness with the above modelling approach is that it implicitly assumes the second definition of vulnerability because it excludes all of the characteristics of the populations exposed to the flood. A second typical limitation of the simpler maps is that they simply draw a boundary around the flood extent for some flood of historic record or the modelled extent for a flood of a particular return period. Thus, they are static, they ignore the inherent uncertainties, and do not observe the principle that it is necessary to manage all floods and not just some, since they contain no information about the threat posed by more extreme floods as proposed by *Green et al (2000)*.

Other flood risk modelling approaches use the first definition of vulnerability by showing both critical flood features such as zones of different flood return periods and accompanying population characteristics. In this approach, flood models and resulting maps show in detail: (i) flood ways, particularly out of bank routes such as such as roads and railways; (ii) constrictions on flow such as embankments, bridges and dykes; (iii) active and passive storage areas such as depressions; and (iv) areas of high flood depths and velocities. In addition, they also show areas where the most vulnerable segments of the population are located. This approach is more robust and data intensive but it ignores vulnerability of infrastructure and economy. It is suitable for life insurance companies and flood disaster rescue teams.

The approaches that adopt the third form of vulnerability are the most useful in terms of comprehensive local flood management policy. In this case, all areas where the combination of flood characteristics, infrastructure and population result in a high degree of vulnerability are indicated. Apart from the flood characteristics mentioned above the analysis goes further to indicate: (i) areas where structures are likely to fail to provide protection to their occupiers; (ii) critical installations such as areas where toxic or flammable chemicals are stored which might trigger secondary disasters; (iii) points such as bridges and crest lines which need to be watched; (iv) points where emergency flood fighting works may protect the areas behind them; (v) those areas where warning is necessary; (vi) which areas should be evacuated in the event of a flood; (vii)where buildings should be discouraged if possible, because they lie in a flood way; (viii) where flood proofing of buildings may be satisfactory because they are only in a passive flood storage area; and (ix) public buildings such as hospitals, schools for treatment of casualties and coordination of relief efforts. This approach is data intensive and requires extensive of ground surveys, and is suitable for detailed local flood management.

The brief review of the above approaches has shown that all the modelling approaches are useful depending on the application, and level of abstraction. Common to all is that they require input of base-data to run the models. Some of these data can be derived directly from RS imagery e.g. digital elevation model (DEM), general land cover, building foot prints/height, transportation network etc. and some, such as socioeconomic data, have to be incorporated from other sources, while other data can be derived indirectly from RS imagery in combination with ground truth information (e.g. land use). Since our focus is not on modelling, but identifying the input base-data that can be derived from RS imagery, we look at a conceptual flood risk model that is representative of most but not all flood risk modelling approaches (see Fig. 2-1). The inputs are identified based on this model and, within the limits of the RS imagery available for this study; several base-data are going to be extracted.

2.5 Flood risk modelling input requirements

There are a number of models that are used for simulating and forecasting flood hazards, ranging from simple quantitative calculations based on historical flood events after calculations of back water curves *(du Plessis et al., 1999)*, to complex one-and two-dimensional modelling techniques. For the one-and two-dimensional models to run, they need base-data, which includes the following:

(i.) A **DEM** is a principal base data requirement for flood hazard modelling. Any physical or mathematical flood model requires a good representation of terrain for it to give good results. However, the accuracy requirement of the **DEM** may vary depending on the level at which the modelling is being done. In farmlands and rural areas, a relatively coarse **DEM** with resolution of 20 m or higher is enough *(Tennakoo, 2004)*, while in the urban area a fine resolution **DEM** giving a more detailed representation of: (a) out of bank water routes (roads, railways, drainage, etc.), (b) constrictions on water flow (buildings, culverts, dykes etc.) and (d) storage areas such as depressions, is needed.

(ii.) The other important base data requirement is a **land cover map** from which roughness values for input to models are derived. The level of detail required also varies as is in the above case. In urban areas a detailed land cover map can offer a good compliment where an accurate **DEM** is not available. For example, detailed representation of urban features, when combined with a terrain **DEM** will enable assignment of high roughness values for water constriction such as buildings, which will give results comparable to using a high accuracy **DEM** *(e.g. see Tennakoo, 2004)*

(iii.) Map of **surface water drainage networks**

(iv.) **Soil** and **geology maps**

(v.) Hydrological models need both **boundary** and **initial conditions** to start computations but these are hydrological condition not derivable from imagery.

(vi.) In addition to this, the model needs **historical peak flood extent maps** for calibration of the models and these can be extracted using Radar sensors at peak flood times.

2.6 Vulnerability analysis base-data requirements

Vulnerability analysis requires more detailed data to enable more reliable results, though the analysis itself is very subjective and different analysts can come up with different results depending on their personal opinions. Moreover, it is important to note that the base-data requirements may vary depending on the local conditions. Some of the essential base-data for flood vulnerability analysis include the following:

(i.) A detailed **location of buildings** and **their attributes** (age, number of floors, size, construction materials, use etc.).

(ii.) A detailed location of other **essential transportation infrastructure** such as roads, bridges, railways and airports; utilities such water and sewerage pipes, electricity, telephone and data networks.

(iii.) **Location of critical facilities** such as hospitals, police, banks, and government buildings.

(iv.) **Social/economic variables of the communities** (population, age, health status and/or mobility, savings, income, flood knowledge and cohesiveness of the community, level of education).

According to van *Westen and Montoya (2004)* the most important building attributes for flood risk assessment are building height, and ground floor and basement floor area.

Conversely, the most important social attribute for vulnerability assessment is the population at risk; that is, the total number of people potentially exposed to the flood hazard at each location and for each flood event *(Chapman et al., 2003).* Physical attributes of vulnerability such as building foot prints and height, and settlement density and pattern can be derived directly from RS imagery *(e.g. Holfman, 2001; Rottenstein and Jansa, 2002; van Westen and Montoya, 2004)*, while social attributes such as poverty can be derived by inference from characteristics of settlements (e.g. building materials for squatter compounds). Information on building types is visible and classifiable, but not the construction quality of each building. The building type may have a strong link to a structural quality typology and as such be a basis for sampling.

To date, the use of RS imagery for generating inputs for vulnerability analysis is still at an infant stage. Just like in the case of flood modelling, vulnerability assessment at a regional level needs a coarse representation of the required details and it is this level where remote sensing gives more promising results (e.g. population estimates *Dobson et al., 2000; Lo, 2001; Sutton, 1997).* The base-data requirements listed above are meant for urban areas since that is where most people live and flood risk analysis takes place.

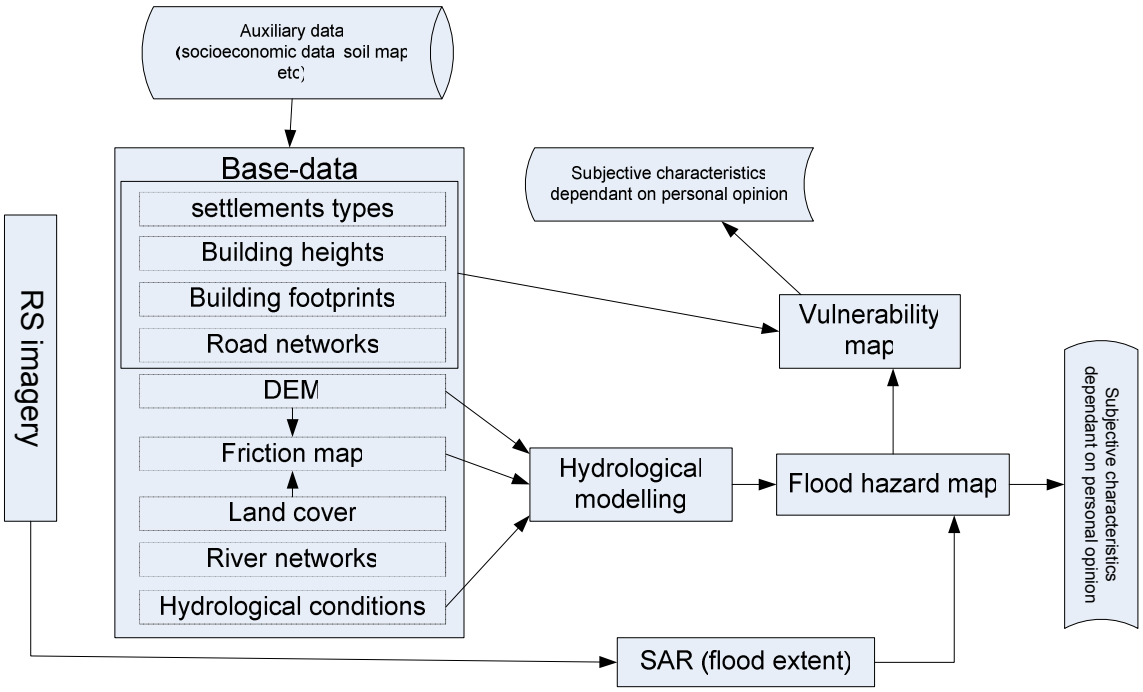

Fig. 2-2: Relationship between base-data, vulnerability, hazard and risk

The focus of this study will be on the extraction of base-data that are necessary for flood risk mapping and which can be derived from RS imagery. This is a generic study which will try to satisfy all the flood risk modelling base-data requirements extractable from the available imagery. Fig 2-2 gives a schematic relationship of base-data and flood risk modelling. The data to be extracted will include building foot prints, land cover maps at different resolutions, settlement types and estimation of building heights. Below is a section on previous application of remote sensing to flood risk modelling.

2.7 Previous applications of remote sensing in flood-risk mapping

The ability to provide large volumes of information on a timely basis and in a cost effective manner, and to acquire information on hazardous or difficult to reach regions, has made RS imagery a principal source of information for flood disaster management. To date, most documented successes in the application of RS imagery have been in flood extent mapping. Complex investigations such as vulnerability assessment and damage assessment are still a subject of active research. The other area where RS imagery is used widely is in the generation of basic inputs for hydrological models; land cover maps for friction values and DEMs. Below is a brief review of some of the works where RS was used.

The exclusive ability of microwave radar to penetrate clouds has made Synthetic Aperture Radar (SAR) imagery a principal tool for real time assessment of floods and mapping. Many authors have used different approaches, some of which are: (i) using multi-temporal techniques based on detection of changes between SAR images acquired before and after the inundation *(Badji et al., 1994; Wang et al., 1995)*, (ii) flood mapping using SAR images of peak flood *(Barber et al., 1996; Chapman et al., 2003; Galy and Sanders, 2000; Zhang et al., 2002a)*, and (iii) integrating results obtained from multi-temporal ESR SAR images and digital topographic data, using a GIS technique, which allows mapping of inundated areas using SAR imagery acquired days after the flooding event *(Brivo et al., 2002)*. Furthermore, other studies succeeded in using multi-temporal SAR image fusion to assess both flood extents and damage *(Lichtenegger and Calabresi, 1995; Matthews and Gaffney, 1994).*

Comprehensive applications of RS imagery in flood mapping can be found in *Zhang et al. (2002)*, where a wide range of RS imagery are used in the National Professional Operational Integrated Monitoring System (NPOIS) for monitoring and evaluating flood disasters in China. Examples of the application of RS imagery are: (i) high spatial and spectral resolution optical imagery (SPOT, Landsat) are used to derive land cover maps which, together with ancillary data from GIS (population, property value), are used to estimate damage, (ii) cloud-penetrating microwave (JERS-1, Radarsat, ERS-1/2) images are used to produce flood extent maps at peak times, which are overlaid with DEMs to estimate flood depth and produce flood hazard maps, and (iii) high temporal resolution (AVHRR/NOAA) data are used daily to monitor the status of the floods throughout the country during the flood season. The output of the system includes flood inundated area maps, land use maps and damage maps and accompanying statistical data. The system has proved very useful at providing flood related data in China, at both regional and national levels, though it does not provide the detailed data required at local level.

Other studies focused on the inputs to hydrological models: (i) extraction of Digital Surface Models (DSM) from airborne Light Detection and Ranging (LIDAR) data and aerial photographs for accurate estimation of Manning's roughness coefficient (hydraulic roughness, which develops resistance to the water flow through creating a retarding force), using automated techniques *(Smith et al., 2004)*, and (ii) using a DEM assembled from scattered elevation data sets, building foot prints map from a GIS and estimated height of buildings, which are combined to generate a DSM for input to 2D hydrodynamic models *(Tennakoo, 2004)*. The latter study demonstrated the use of alternative data sources in the absence of expensive high resolution DEMs (e.g from LIDAR).

A good example of application of high resolution RS imagery in flood damage assessment can be found in *van der Sande et al. (2003)*, where detailed land use maps were extracted from IKONOS-2 imagery using segmentation based classification methods. The land use maps were used for estimating property value and to produce a friction map that was used as input to LISFLOOD-FP model. This model is used to generate flood extent maps that are overlayed with land use maps and used for estimating damage using a damage function. It was found that damage estimate accuracy improved with accuracy in the land use map. The results obtained using this approach were of high quality because the land use maps extracted from high resolution IKONOS-2 imagery were also of high quality. However, it should be noted that the use of single source imagery in this project cannot be promulgated elsewhere, since a rich base-data set already existed.

Recently, *van Westen and Montoya (2004)* integrated gridded LIDAR data together with conventional vector digital topographic data (roads layer, and a DEM generated from 1: 2000 contour map) and a multispectral high resolution QUICKBIRD imagery to estimate the height and number of floors of buildings for the city of Tegucigalpa. This was a good attempt at directly extracting quantitative information from RS imagery, which is crucial to damage assessment and vulnerability analysis.

Another promising remote sensing technology for pre-disaster and post-disaster flood studies is airborne videography. *Mausel el at (1992)*, gives the following advantages of video remote sensing (VRS) that make it a useful data collection technology for different types of disasters:

- The ability to observe live images during data capturing.
- Analogue images can be interpreted manually from the screen, after which values can be converted to digital values by making use of image processing.
- The ability to collect data in very narrow spectral bands (5-12 μm) in the visible to near infrared band.
- The abundance of data obtained because images are recorded every 1/30 of a second or faster for new systems.
- The equipment is affordable and can be bought off the shelf.
- Allows for rapid damage assessment and reduced need for ground assessment in the work of reduced ground accessibility.

The major disadvantage of VRS is relatively low resolution as compared to conventional aerial photography and poor geometric properties, which causes problems when core-registering with other image sources. This emanates from the fact most cameras used are not designed for scientific applications. However, other studies have overcome the georeferencing problem by using GPS *(e.g. Clerke, 1994; Jacobs and Eggen-McIntosh, 1992)*. VRS technology has already been applied in post earthquake damage assessment *(Ozisik and Kerle, 2004)* and post disaster damage assessment in man made disasters *(Kerle and Stekelenburg, 2004).* Another study that explored the use video imagery for disaster management was *Montoya (2002),* who proposed a combination of remote sensing imagery and ground video images from a moving vehicle. The geographic location reference of each video image was provided by a GPS. Building attributes were extracted afterwards from the analysis of the video images and it was found to cover a large area within a few days as compared to other field methods. In relation to flood disasters, VRS technology has been in use for over a decade. An example of earlier applications is *Jacobs and Eggen-McIntosh (1992),* who used airborne VRS, and a GPS receiver for georeferencing, to assess timberland damage after Hurricane Andrew. In *du Plessis el al (1999)*, airborne VRS was used extensively to map the land cover in the flood plain between the Mflozi and Msunduzi rivers for the purpose of

developing flood damage functions for various land use types in farmlands and urban areas of South Africa, and the study results compared well with ground survey methods.

Estimating the number of inhabitants found in a certain flood prone area is very crucial to flood disaster management. Though RS methods have not been used extensively to estimate population densities specifically for this application, many studies have applied Defence Meteorological Satellite Program Operational Linescan System (DMSP OLS) to estimate population characteristics *(e.g. Dobson et al., 2000; Lo, 2001; Sutton, 1997),* and all these studies cite impressive results at regional and global levels. Particular to risk management was *Dobson et al (2000),* who established a worldwide population database at 30 x 30 arc second resolution for estimating ambient population at risk based on land cover, slope, road proximity, and night-time lights. *Qui et al. (2000)* used a combination of land use change detection based on Landsat ETM imagery and GIS derived road data to model population and like the other studies better accuracy was achieved at regional level due limited imagery resolution. *Lo (1986; 1995),* used aerial photographs to estimate population at dwelling level, and achieved good results but still experienced difficulties and poor results at micro level due to mixed building use and large variations in dwelling population densities. The advent of new satellites with high spatial resolution such as QUICKBIRD and IKONOS , which enable the extraction of individual building foot prints opens a new window of opportunity in this area of RS application especially the affected population, which is an important input to disaster risk management.

The above review indicates the limited use of RS techniques to flood extent mapping and generating DEMs and regional applications. The limitation of RS to such relatively simple applications is not only due to limited resolution of the available imagery, but also the cost of acquiring high resolution imagery and complexity of extracting important base-data from high resolution imagery. Chapter 4 gives an overview of the information extraction techniques that can be used to extract base data from imagery of different resolution, but before going to that, chapter 3 gives a description of the study area and the data available for this study including the pre-processing steps for these data.

3 Study area and data

3.1 Introduction

In this chapter a general description of the study area is given to illustrate the characteristics of a flood prone city in relation to the problems this research is going to address. These characteristics can be found in other flood prone cities in developing countries as well. Then the data available for this study and the pre-processing steps involved are described.

Table 3-1: Data available for this study

Remote sensing imagery	**Date**	**Band/Colour**	**Resolution or scale**	
LANDSAT	13 Mar. 2000	Multi-spectral	15 m PAN	28.50 m MS
QUICKBIRD	31 Dec. 2000	Multi-spectral	0.61 m PAN	2.8 m MS
Gridded LIDAR DEM	1 Mar. 2000	True height value	1 m cell resolution	
Aerial pho-tographs	Mar. 2001	True colour	1m cell resolution	
Ancillary data		**Format**	**Scale**	
Contour map	Mar-Feb. 2001	Shape file	1:2000	
Roads layer	Mar-Feb. 2001	Shape file	1: 2000	
Rivers layer	Mar-Feb. 2001	Shape file	1: 2000	
5, 25, 50 year flood maps	2001		1: 2000	

3.2 General description of the study area

The study area (Fig. 2-1), Tegucigalpa, is nestled into a bowl-shaped valley within the central highlands of Honduras, at a latitude of 15°06'N and longitude of 87°11'W. The bottom of the valley lies at 930 m above mean sea level, with peaks around the basin rising up to 1300 m In the entire basin rivers play an important morphological role; the Río Grande Choluteca separates Tegucigalpa from its sister city Comayagüela. The smaller Rio Chiquito flows into the basin from the eastern edge, dividing the capital into the old town on the northern riverside and the modern commercial district on the south side. The streambed material of all the rivers ranges from sand and gravel, to cobbles and small boulders in the main channel. The overbank areas are city streets and buildings in most areas. The slope of the river reaches varies from 0.0091 on the steepest section of the upper end of Río Chiquito to 0.0034 on the flattest section of the upper Río Cholute. Tegucigalpa has a total annual rainfall of about 1000 mm, with heaviest precipitation coming in the months of October and November due to the influence of the Hurricanes developing in the Caribbean. One of most extreme Hurricanes in recent years was Hurricane Mitch, which occurred between 25th and 31st October 1998 and had devastating effects on the population and property as already mentioned above.

Like most cities in developing countries, Tegucigalpa faces the problem of over-population due to rural-urban migration, which forces people to develop in flood prone areas due to scarcity of land. The city has diversity in terms of urban features complexity and range of building materials comprising a mixture of well planned settlements and unplanned poorly constructed settlements.

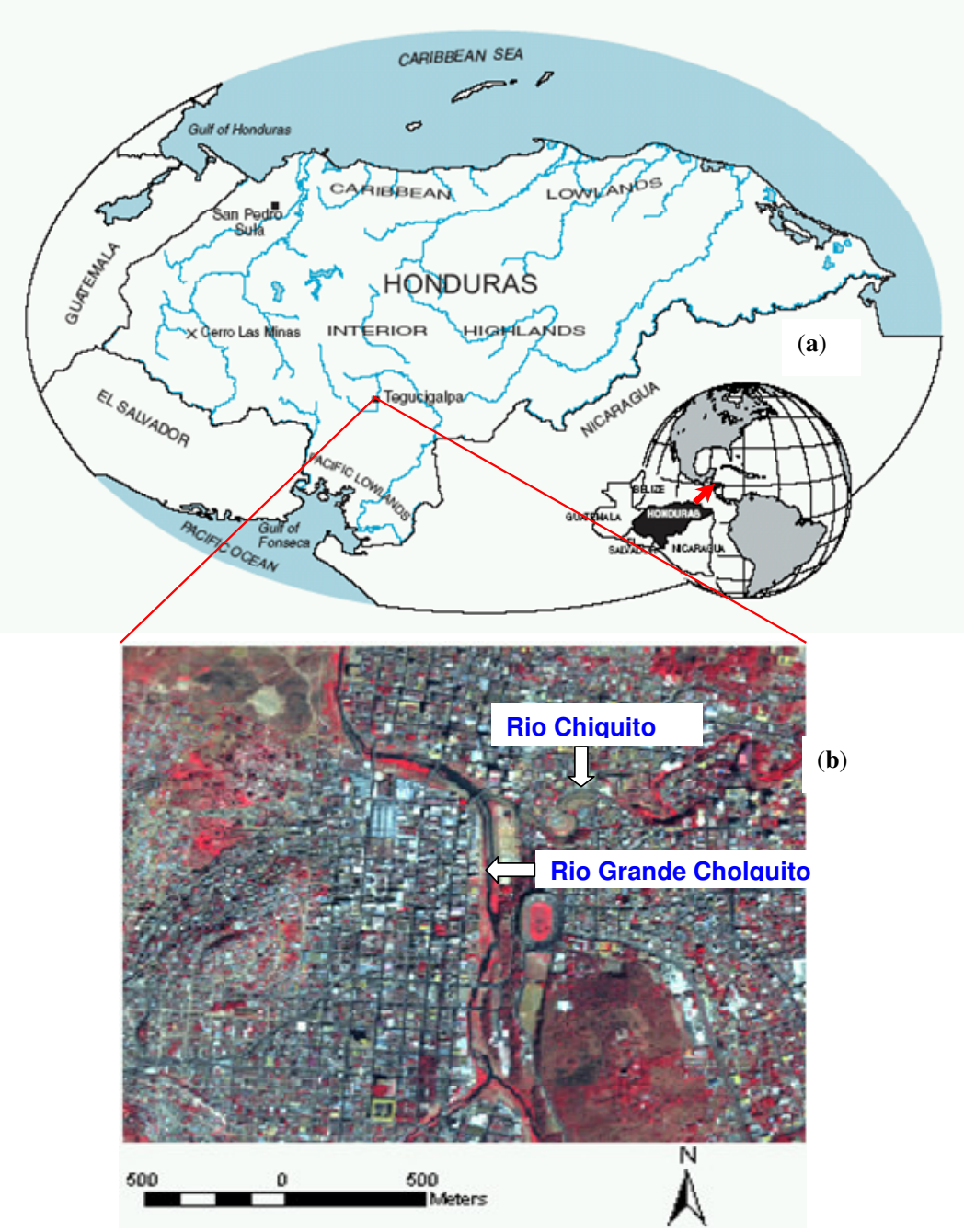

Fig. 3-1: (a) map showing location of study area, and (b), QUIKBIRD imagery showing details of urban features

The availability of a rich variety of RS imagery (LIDAR, QUICKBID and Landsat ETM), coupled with its complex urban built environment, which is a good example of most flood

disaster prone cities in developing countries makes Tegucigalpa a good case study for testing the objectives of this thesis. A wide range of data sets gives a good opportunity for the testing the interchangeability of different data sets for extracting flood-risk related base-data at different aggregation levels. Moreover, the methods used and results obtained in this study could be promulgated elsewhere.

3.3 Data

Several types of data have been used in this research, as listed in Table 2.1. However, the LIDAR DSM and QUICKBIRD imagery are the main data sources for this research. Detailed descriptions and pre-processing steps are given in sections below.

3.3.1 QUICKBIRD imagery

QUICKBIRD images are offered at various levels of processing, based on 2.44 m resolution for multi-spectral bands and 0.61 m resolution for the panchromatic band. It is designed to support applications ranging from map publishing to land and asset management to insurance risk assessment. Some of the specifications can be found in Table 3-2.

Table 3-2 Technical specifications of QUICKBIRD sensors

Launch	2004	
PAN	0.455 – 0.900 microns	
MS	Band 1: Blue 0.45 -0.52 microns Band 2: Green 0.52 -0.60 microns Band 3: Red 0.63 -0.69 microns Band 4: Near IR 0.76 -0.90 microns	
Resolution at nadir	0.61 m PAN	2.44 m MS
Swath widths and	Nominal swath width: 16.5 km at nadir	
scene sizes	a nominal single image at 16.5 km × 16.5 km	
Metric accuracy	14 m Root Mean Square Error no ground control	
Altitude	450 km	
Inclination	98.1 degrees	
Dynamic range	11 bits	
Revisit time	1 to 3.5 days depending on latitude at 70 cm	
Periods	93.4 minutes	
Orbit type	sun-synchronous	

Source: (Digital Globe, 2004)

3.3.2 LIDAR data

An airborne Light Detection and Ranging (LIDAR) system, was used to acquire high-resolution elevation data for flood-hazard mapping. This work was done by the Bureau of Economic Geology, Coastal Studies, at the University of Texas (UT). They used an Optech ALTM 1225 module mounted in a fixed-winged airplane and flew over Tegucigalpa in March 2000. Data were first acquired along densely spaced parallel flight paths and then again along flight paths orthogonal to the original flight paths. Reported vertical accuracy is 0.15 meter at a 1,200-meter operating altitude. Precise GPS operated on the aircraft during LIDAR operation and on the ground at survey control benchmarks. The final DEM derived from the irregularly positioned LIDAR data was resampled to a regular grid with a cell (horizontal) resolution of 1.5 m in Arc/Info Grid format using TopoGrid software. The data accuracy of the

LIDAR was assessed with two sets of independent field surveys. One set was conducted by the University of Texas (UT) personnel in March of 2000 with a survey-grade GPS, collecting point data on ground-control features such as roads, soccer fields, bridges, and buildings. The other set of surveys was made by USGS personnel during field surveys of the bridges with a total station tied into benchmarks. The benchmarks were established by UT personnel. Results of the point surveys by UT personnel shows vertical errors ranging between 0.03-0.30 m on the soccer field and 0.10-0.45 m on building roofs, and the standard deviation of errors are within 0.097 m (Table 3-3).The mean absolute error were within the reported accuracy of 0.15 m. To assess horizontal accuracies, GPS ground points on ground-control features were overlaid on a 1- to 2 m^2 LIDAR-derived DSM with a 1m cell resolution. UT compared the positions of ground control features with the DSM for any discrepancies in horizontal positions. In all the LIDAR surveys, horizontal agreement between the GPS-derived points and the LIDAR data was within the 1-meter cell resolution of the DSM. More details can be found in *Mastin (2002).*

Table 3-3: Statistical analysis of elevation differences obtained from GPS ground surveys and LIDAR airborne survey, adapted from (Mastin, 2002)

Mean difference (ground - LIDAR) (m)	Std elev. differences (m)	Range of elev. differences (m)	Ground feature	No. of elev. differences
-0.134	0.097	0.10 to 0.45	Building roof	89
-0.152	0.071	0.03 to -0.30	Soccer field	142

3.3.3 Creation of the bare Earth surface model

To detect urban topological objects such as buildings and trees, a digital terrain model (DTM), which represents the bare Earth surface, is derived from a gridded laser DSM. The process of extraction of a DTM from laser scan data is known as filtering *(Vosselman et al., 2004)*. Many filtering algorithms exist in literature *(e.g. Kraus and Pfeifer, 1998; Vögtle, 2000; Vosselman, 2000). Sithole and Vosselman (2004)* gave an experimental comparison of several filtering algorithms and their findings were that generally all filters perform well in smooth rural landscapes, but have problems in complex urban and rough terrain with vegetation.

This study employed the surfacing growing algorithm described by *Vosselman et al. (2004)*. Firstly, a seed surface is identified and then it grows based on proximity of points to this surface. The method for seed selection is to fit many planes and analyse residuals. For each point, a plane is fit to points within some distance of that point. The points in the plane with the lowest square sum of residuals compose a seed surface if the square sum is below a defined threshold. This method is based on the assumption that there is a part in the dataset where all points within some distance belong to the same surface. The growing of the surface is based on proximity of points, such that only points that are near one of the surface points can be added to the surface *(*details can be found in *Vosselman et al., 2004)*. The whole process determines a low smooth terrain surface locally and then all surfaces that belong to that surface are manually identified and connected ending up with a smooth approximation of the terrain (Fig. 3-2 b). This DTM is subtracted from the original DSM to obtain a normalised DSM (nDSM) which is used for segmentation of 3D urban objects.

$$nDSM = DSM - DTM \quad (1)$$

Fig. 3-2 shows the original gridded DSM, with the real earth surface including topographic objects such as buildings and trees (Fig. 3-2 A), the created DTM, which an approximation of the bare Earth surface without topographic objects (Fig 3-2 B), and the nDSM depicting only the topographic objects with real terrain surface removed, a closer look reveals that the roads and bare surface become darker and only the buildings are brighter, indicating removal of elevation information in darker parts (Fig. 3-2 C). The nDSM is going to be used for extraction of urban objects for the rest of study.

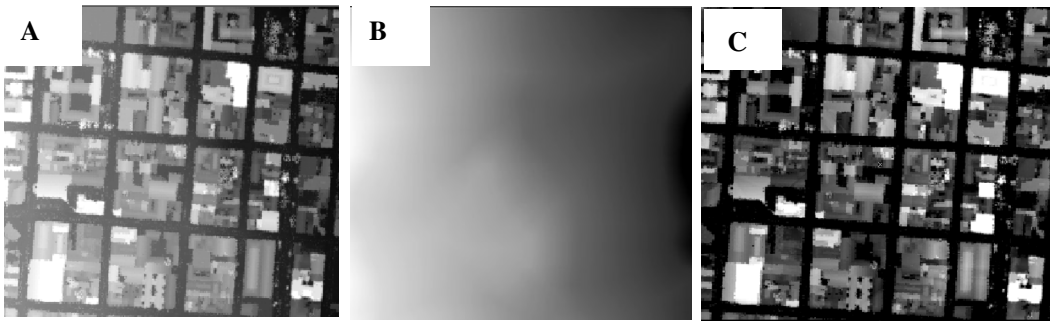

Fig. 3-2: showing (A) original DSM, (B) created DTM, and (C) nDSM, with terrain surface removed

3.3.4 Landsat ETM image

The Landsat programme is the oldest Earth observation programme, which started with the launch of Landsat-1 satellite carrying the multispectral scanner subsystem (MSS) sensor, in 1972 *(Huurneman and Jansen, 2001).* In 1984, Landsat-5 carrying the Thematic Mapper (TM) was launched and it replaced the MSS scanner. The latest successful launch was Landsat-7 carrying ETM scanner. Although only Landsat-5 and Landsat-7 are operational today, an archive of images from Landsats 1, 2, 3 are available as baseline reference for land use changes throughout the world. Some of the common application for Landsat imagery include: geological mapping, land use mapping, soil mapping, environmental monitoring, natural hazards and agriculture. A summary of characteristics of Landsat Enhanced Thematic Mapper (ETM) image used in this study are given in Table 3-4 below.

Table 3-4 : Landsat-7 ETM+ Characteristics

Launch	1999	
Resolution	15 m PAN	30 m MS
PAN band (μm)	0.52 –0.9	
MS bands (μm)	0.45-0.52(1), 0.52-0.60(2), 0.63-0.69(3) 0.76-0.90(4), 1.55-1.75(5), 10.4-12.50(6) 2.08-2.34(7)	
Swath width	185 km (FOV =15^o)	
Revisit time	16 days	
Altitude	705 km	
Altitude	450 km	
Inclination	98.2^o	
Dynamic range	8 bits	
Orbit type	sun-synchronous	

Source: ***(Huurneman and Jansen, 2001)***

3.4 Pre-processing

Image pre-processing refers to the operations that are performed to improve geometric and radiometric quality prior of the image to main image analysis. Typical pre-processing operations include: (i) feature selection, which is the isolation of components within multispectral data that are most useful in portraying the essential elements of the image; (ii) radiometric corrections, which involves correction of visible noise and errors in image data, and atmospheric correction to compensate for effects of atmospheric illumination parameters such as haze, sun angle and skylight on the image data *(Huurneman and Jansen, 2001)*; and (iii) geometric correction, that is bringing an image into registration with a map or another image.

For this case all the data sets but the Landsat ETM, were already corrected and referenced to UTM (Zone16), NAD27 (Central America) ellipsoid. The Landsat ETM scene was in UTM WGS84 system. It was co-registered to the other images using image to image registration and using the QUICKBIRD as the reference image. Twelve tie points were used and the root mean square error (RMSE) was 0.37. The nearest neighbour interpolation method was used for resampling the image because unlike other methods that average the neighbourhood pixels, the pixel value in the transformed image is assigned to the nearest value in the original image. It has the advantage that it preserves the original pixels which is useful for subsequent image classification.

3.5 Image fusion

The purpose of image fusion is to make the best use of the complementary information acquired in different imagery data sets about the same terrain features. A popular image fusion approach is the fusion of panchromatic (PAN) and multispectral images. The purpose of this approach is to have an image with both the advantage of high spatial resolution of panchromatic and high spectral resolution in the multispectral bands.

Several image fusion methods have been proposed in the literature. Examples include IHS (Intensity-Hue-Saturation), PCS (Principal Component Substitution), HPF (High-Pass Filter), RVS (Regression Variable Substitution), and SVR (Synthetic Variable Ratio). In this study, the IHS and PCS methods available in ERDAS IMAGINE software were used to fuse the PAN and multispectral data

IHS is one of the most often used methods for merging multisensor imagery data examples include: fusing Landsat TM and SPOT PAN data *(Welch and Ehlers, 1987),* and SPOT multispectral and PAN data *(Thormodsgrad and Feuguay, 1987).* The IHS transformation process is illustrated in Fig. 3-2. It is assumed that the intensity component is spectrally equivalent to the PAN image, and that all the spectral information is contained in H and S components. The implementation of IHS involved: (i) the multispectral bands 4, 3 and 2 of the QUICKBIRD image were displayed in RGB system, resampled from 2.44 m resolution to 0.61 m resolution for PAN and transformed into IHS space as intensity, hue and saturation (IHS) image; (ii) the 'I' component was replaced by the high resolution PAN image, and the (PAN, H, S) was converted back to (RGB). The result was a high resolution 0.61 m colour composite, which is suitable for discerning small urban features like shacks and cars, while having the colour for discerning features like vegetation (see Fig. 3-3).

The procedure for the merging of the multispectral and PAN data using the PCS method is similar to that of the IHS method. The justification used for replacing the first principal component image with the stretched PAN image is that the PAN image is approximately equal to the first principal component image. This assumption is made because the first principal component image will have the information that is common to all the bands used as input to PCA, while spectral information unique to any of the bands is mapped to the other components. In this approach, first the principal components of the multispectral image are computed and then PC-1 is replaced with high resolution PAN image, and finally an inverse principal components is performed *(for details see Jensen, 1996).*

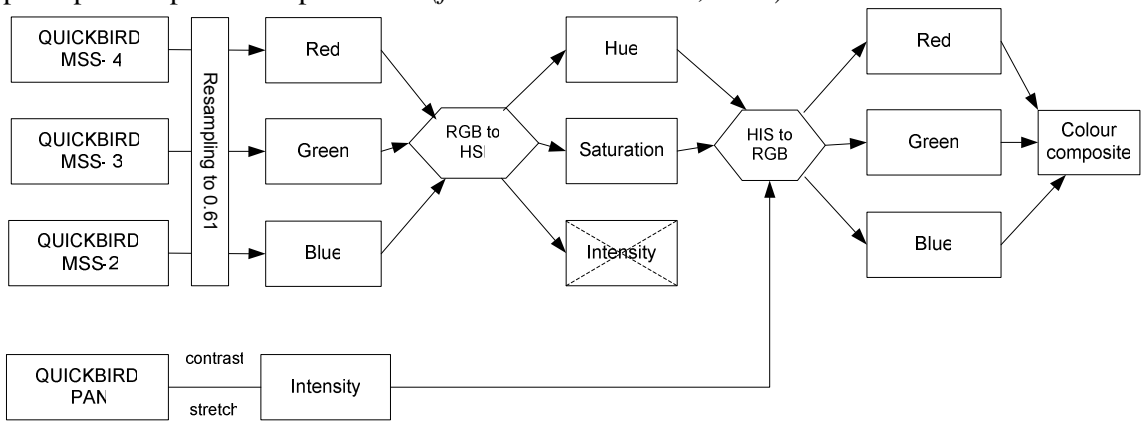

Fig. 3-3: Fusion of QUICKBIRD MS and QUICKBIRD panchromatic into 0.61 m resolution colour composite *(modified from Huurneman and Jansen, 2001)*.

Fig. 3-4 shows the results of IHS and PCS fusion operations. A visual comparison of the resultant fused images shows that the IHS method produced a shaper image. However, the IHS technique is limited to three bands but this is an advantage in our case since more memory is required for extra bands. eCognition, the software used for segmentation-based image (see section 4.5) analysis in this study has a limitation of size of image that can be processed efficiently. Considering the

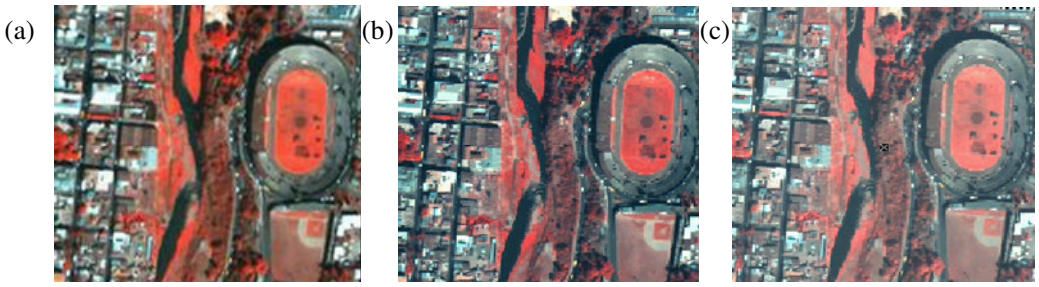

Fig. 3-4: results of image fusion, (a) is the original image, (b) is an IHS fused image, and (c) is a PCS fused image

two factors, IHS was chosen for implementation in the subsequent image analysis. However, for the low resolution Landsat ETM image, which does not require extensive memory the PCS fused image was adopted for subsequent classification because it gives more bands for discerning different features.

4 Review of information extraction techniques from imagery

4.1 Introduction

Information extraction from satellite is an active research field, which has yielded numerous techniques. The techniques range from visual interpretation and manual digitizing from high resolution RS imagery by a human analyst *(Richards and Jia, 1999)*, to complex automatic pattern recognition techniques and automatic extraction of real world objects *(Heipke et al., 1999; Holfman, 2001; Marangoza et al., 2004; Rottenstein and Jansa, 2002; van der Sande et al., 2003; Zhang et al., 2002d)*. The choice of information extraction techniques varies depending on the: (i) complexity, resolution, information content and structure of the imagery; (ii) target objects to be extracted (e.g. buildings, roads, trees, forest or entire city foot print); (iii) required accuracy and the intended application; and (iv) the type of sensor used.

Image interpretation is the general term for information extraction from remotely sensed data *(Guindon, 1997)*. It is a process in which such image elements as tone, color, shape, size, texture, pattern, shadows, site, and association are used to achieve the goal of detection, identification, delineation, and enumeration purposes *(Huurneman and Jansen, 2001; Lillesand et al., 2004)*. The goal of image interpretation is to extract information from remotely sensed data using a combination of some or all of the above elements. This is particularly true for human based image interpretation. In some recent literature relating automatic extraction of buildings and roads, the term, “object modelling”, has been used as a replacement for information extraction *(e.g Baltsavias, 2004; Heipke et al., 1999; Zhang et al., 2002b)*. This means geometric description and, where possible, additional attributes (radiometric, spectral, textural) and semantic or functional properties or topological relations of natural and man-made objects.

While image interpretation techniques based on human brains have been well developed (*Guindon, 1997)*, image interpretation by computers in an automated or semi-automated manner is still under intensive investigation. However, two obvious restrictions exist limiting the wide use of human interpretation of remotely sensed imagery. Firstly, it is hard to achieve consistent results even though the same procedure is followed by different human interpreters due to human subjectivity. Secondly, the human brain cannot detect subtle changes and cannot handle large volumes of data. Moreover, human interpretation is usually labour extensive and cost ineffective. For over four decades, a large number of efforts have been devoted towards automating human image interpretation by digital computers *(Strat, 1995)*.

The aim of the extraction process is to generalise the information into meaningful real world objects classes that can be easily understood by policy makers and managers in various fields of geo-information application. Among various base-data, this research focuses on detecting different settlement patterns, buildings footprints, and general land cover maps, which constitute very important geo-spatial data inputs layers for flood risk modeling that, and are extractable from RS imagery available for this study. Other topographic objects of equal importance to flood risk modeling that can be extracted from RS imagery include: forests and agriculture fields. The latter objects will not be considered in detail because the study area is in the heart of the city where such objects are not found, or are of insignificant contribution.

4.2 Automatic information extraction techniques

A large variety of remote sensing imagery from a wide range of sensors provides a multitude of information about the earth surface, which caters for both global and localised analysis of both natural and man made objects as well as events. These sensors provide information at resolutions ranging from a few centimetres to hundreds of metres. A number of automatic information extraction algorithms have been developed over the years to retrieve the hidden information from imagery. Some of the commonly used information extraction techniques from RS imagery are: (i) image classification, which is the partitioning of image pixels into classes according to their similarity in spectral and/or spatial aspects *(*see *Campbell, 1996; Lillesand et al., 2004* for details*);* (ii) linear feature extraction, which refers to a group of algorithms that uses spatial contrast in an image to derive linear features such as building edges, roads, rivers and geological faults *(e.g. Heipke et al., 1999; Steger et al., 1995);* (iii) statistical regression, where the dependent variable is the parameter to be estimated from remote sensing imagery such as population density *(e.g. Lo, 2001),* soil organic matter *(e.g. Aynekulu, 2003),* and the independent variables can be brightness data from a single spectral band, a combination of bands, or transformed brightness such as various texture measures; (iv) mathematical morphology, which is a method for analysing digital images based on geometrical shape, using mathematical set operations such as union, intersection, complementation as well as dilation, erosion and other derived operations *(Soille, 1999; Soille, 2002);* and (v) change detection, which is analysis of differences in land cover and land use on images of the same area acquired at different times. Information extraction in this study will be mainly done using item (i), and therefore it is treated in detail below.

4.3 Image classification

Image classification is the most commonly used thematic information extraction approach. It is a mapping process that groups image pixels into categories of information that are more general than the data, e.g., land cover or land use. It requires a classification scheme specifically designed according to an application purpose, a proper classification algorithm optimal for deriving the desired land categories, and a minimum mapping unit smaller than patches of classified pixels which will be merged into neighbouring larger patches. As in cartography, image classification is a generalization and abstraction process that simplifies original image data to a level that can be better used in decision making or to improve our understanding of an area of interest. It converts radiometric data at the ratio measurement scale down to thematic classes at the nominal measurement scale *(*see *de By, 2001* for a discussion on scale of measurement*)*. In this process, remotely sensed data is converted into various classes according to their similarity in spectral and spatial aspects. Particularly, land cover and land use types are mapped with image classification techniques. Land cover is the physical material on earth surface while land use is a cultural concept related to human activities on the land. Because the radiometric properties of earth surface materials are directly recorded by remotely sensed data, it is relatively easy to classify land cover classes such as various vegetation, paved surface, and water bodies *(Zhang, 2003).* However, it is more difficult to map land use types because they appear spatially heterogeneous in physical properties (e.g., a residential area is characterized by a mixture of roof tops, paved surfaces, and gardens and trees). Because land use classes such as residential, commercial, and industrial lands are important in urban area remote sensing, and need high resolution imagery *(Guindon, 1997; Steinnocher and Bauer, 2001),* which cannot be sufficiently handled by standard classification methods such as minimum distance and maximum likelihood classifiers, many studies *(e.g. Herold et al., 2003; Scott et al., 2003; Shackelford and Davis,*

2003; van der Sande et al., 2003) have employed advanced classification algorithms that uses not only the spectral information in the image, but also spatial information indirectly characterized by spatial measures that can be calculated from pixel neighbourhoods.

Typically, image classification involves two stages *(Gong and Howarth, 1990a).* The first stage is designing a classification scheme; these are usually information classes such as built-up, forest, agriculture at the highest level to individual houses, tree species, crops, pools at the lowest level (see *Anderson et al., 1976* for details). The second stage is the implementation of the classification scheme and the general steps followed are:

- Data pre-processing, including radiometric and geometric corrections, feature selection and noise reduction and sometimes initial clustering results.
- Selecting representative areas on the image, analyse initial clustering results, or generate training signatures *(ERDAS field guide, 2003).*
- Conducting image classification using either supervised mode, which involves using training signature and clustering algorithm to classify an image into initial information classes or, unsupervised mode, which involves image clustering, cluster grouping, and analysis of clusters for information labels. Supervised classification is the most used approach.
- Post-processing classification for improving the appearance of the image by filtering
- Accuracy assessment by comparing the classification results with ground truth data or data of higher accuracy. Details can be found in *Richards and Jia (1999), Lillesand et al. (2004) and Campbell (1996).*

Richards and Jia (1999) distinguish two types of classes that can be derived from RS data: (i) information class, which is a class defined by an image analyst referred to as information to be extracted and these can be associated to land use classes, and (ii) spectral class, a class of similar grey-levels in the multispectral space and this can be directly associated to land cover classes. It follows that in supervised classification; an image analyst first specifies an information class on the image and then uses a supervised training algorithm to summarise the specified areas on an image to form class signatures. The unsupervised case, a clustering algorithm is first applied to an image to form spectral classes (clusters). After which an image analyst, assigns spectral classes to appropriate information classes.

4.3.1 Conventional multi-spectral classifiers

Conventional multispectral classification methods make use of spectral response of ground objects. The spectral response of ground objects within one pixel is a set of n radiance measurements obtained in the various wavelength bands. This set of radiance measurements is referred to as a spectral vector in the measurement space. The classifier or the decision maker assigns the measurement vector to one of a set of classes according to an appropriate decision rule *(Lillesand et al., 2004).*

The fundamental basis for multispectral satellite image classification is the electromagnetic reflectance properties of earth surface features. Because ground objects have their own characteristic spectral response in different spectral bands of the electromagnetic spectrum, they can be identified and delineated in a multispectral image. The spectral reflectance characteristics of ground objects are described by spectral reflectance curves, which are graphs of the spectral reflectance of objects as a function of wavelength. Because spectral responses measured by remote sensors over various features of ground objects often permit an assessment of the type and condition of the features, these responses are also referred to as

spectral signatures. By analyzing a scene in several spectral bands, different terrain features can be discriminated. For example, water and vegetation might reflect nearly equally in visible wavelengths, yet these features can be clearly discriminated in near-infrared wavelengths.

There are many pixel-based multispectral classification algorithms *(Gascuel et al., 1993; Lillesand et al., 2004; Richards and Jia, 1999)*, and they are split into two main categorise: parametric classifiers, if they assume the existence of underlying probability distribution and non-parametric if they do not assume anything about the probability distribution of the data *(Cortijo and Perez de la blanca, 1997; Kloer, 1994)*. Examples of parametric classifiers are maximum likelihood and Mahalanobis distance classifiers *(see ERDAS field guide, 2003),* and of non-parametric classifiers are nearest neighbours and classification trees classifiers *(Cortijo and Perez de la blanca, 1997).*

However, multispectral pixel-based parametric classifiers are the mostly commonly used and are available in most commercial image analysis software packages. The most versatile and widely used is the maximum likelihood classifier. This classifier assumes normal distribution of data in each input band and uses only spectral information.

4.3.2 Limitations of conventional multispectral classifiers

Conventional spectral classifiers have been widely used for image classification and have given good results for a wide variety of low to medium resolution images. Usually conventional spectral classifiers perform well over limited areas where spectral signatures do not vary greatly from those captured in the training data. However, as the size of area to be classified increases, the classification accuracy typically decreases *(Carlotto, 1998)*. In many real applications, the thematic (class) maps generated by conventional spectral classifiers are often found to be very "noisy", with a considerable portion of image pixels being misclassified. Some of the problems that lead to misclassification are *(Benz et al., 2003; Campbell, 1996)*:

(i.) Limited sensor radiometric and spatial resolution. Limitations in radiometric resolution reduce the distances of classes in the feature space making it difficult to discriminate between classes. The limitation in geometric resolution leads to class mixture with one cell (mixed pixel) and since the cell boundaries in the image does not correspond with the boundaries of terrain features, this more eminent on the transition zones between land covers. A detailed discussion on causes of mixed pixels can be found in *Fisher (1997).*

(ii.) The definition of information or land use classes is vague; there is no distinct boundary between different land uses (for example urban/rural, forest/grassland). Therefore, the boundaries that are set by image analysts are just limited idealisations of the real world which makes it difficult for automatic classification results to replicate.

(iii.) The relationship between land cover and land use is based on vague knowledge and is therefore only modelled, which limits the performance of algorithms based on it.

(iv.) The diverse composition of urban scenes (different objects with similar spectral values and same objects with different spectral values e.g building and roads) coupled with high resolution RS imagery (less than 10 m) cannot be sufficiently handled by conventional multispectral classifiers that rely on spectral information only.

In conventional multispectral classifiers a particular pixel can only be assigned to one class irrespective of the proportion of spatial and spectral similarity of a pixel to several classes. Therefore, such classifiers are known as hard classifiers. This type of decision rule results in areas of categories with spatial extents smaller than a pixel being overestimated or

underestimated. Some application like extraction of urban features require information at sub-pixel level for clear definition of boundaries *(Zhang, 2003).*

4.3.3 Fuzzy logic and spectral unmixing

In order to deal with problem (i) (section 4.3.2), several algorithms have been developed to estimate partial membership of a pixel to several classes. These algorithms come in two major groups: those based on statistical similarity and those based spectral similarity. Fuzzy classification algorithms are an example of methods based on statistical similarity *(Zedeh, 1965).* The other algorithms which estimate the partial membership of classes based on spectral similarity are called spectral unmixing.

Fuzzy logic is a mathematical approach to quantifying uncertain statements. The basic idea is to replace the two strictly logical statements "yes" and "no" by the continuous range of [0…1], where 0 means "exactly no" and 1 means "exactly yes." All values between 0 and 1 represent a more or less certain state of "yes" and "no." Thus, fuzzy logic is able to emulate human thinking and take into account even linguistic rules. Fuzzy classification systems are well suited to handling most vagueness in remote sensing information extraction. Fuzzy classification assigns each pixel the degree of membership to different land covers or land uses. The maximum membership degree determines the final classification to build an interface to crisp (boolean) systems. Unlike classifiers that assign a pixel to a class based on the probability to belong to that class, fuzzy classification assigns a pixel to a class based on its possibility that it belongs to that class. The difference is that while the probability of all possible events adds up to one, this is not necessarily true for possibilities *(Lillesand et al., 2004)*. For applications relating to urban land cover classification and/or roads and buildings extraction see *Shackelford and Davis (2003)* and *Zhang (2003).*

Spectral unimixing is an extension of image classification where instead of one class being stored or mapped for each pixel, the proportions, $f = (f_1, f_2, \ldots, f_n)$ of different surface cover types or components are stored and where:

$$f_i \geq 0 \ldots and \ldots \sum_{i=1}^{n} f_i = 1 \qquad (2)$$

This type of analysis is also called "unmixing", or "pixel decomposition". '*f*' can be estimated using a number of methods *(*for example see *Zhang, 2003).*

4.4 Improvement trends on classifiers

The limitations in multispectral classifiers has stirred active research on classification algorithms, which attempt to achieve results of higher integrity and these can be found in recent literature *(Baltsavias, 2004; Carlotto, 1998; Cortijo and Perez de la blanca, 1997; Gascuel et al., 1993; Mena, 2003; Pal and Pal, 1993; Pal and Wang, 1996; Zhang, 2003). Sun et al (2003)* identifies four major trends for improving classification results:

4.4.1 Better use of spectral information

The first is making better use of spectral information based alternative spectral representation. *Carlotto (1998)* proposed a multispectral classifier that is based on an alternative spectral representation. In his approach, spectral classes are represented by their spectral shape, i.e. is vector of binary features that describes the relative values between spectral bands. The classification accuracy of the full-scene spectral shape classifier was shown to be superior to that of a stratified Maximum likelihood classifier.

Other studies use characteristic spectral relationships as expert knowledge in an expert system designed for image classifications. An example of such studies was *Wharton (1987),* who developed a prototype expert system to classify multispectral remotely sensed data on the basis of spectral knowledge. In this approach, a knowledge base was developed that describes the target categories in terms of characteristic spectral relationships. Classification decisions are made on the basis of convergent evidence as derived from applying the spectral rules to a multiple spatial resolution representation of the image.

4.4.2 Contextual classifiers

The second group are contextual classifiers that make use of not only the label at a single pixel but also the information from neighbouring pixels to determine the appropriate class for a pixel. Many algorithms that use contextual information have been developed and can be summarised into two major categories namely: pre-processing and post processing approaches.

Using filters before classification is the simplest method to exploit and enhance the spatial context of image data. For example, a median filter will reduce salt and pepper noise that would lead to inconsistent class labels. Simple averaging filters (possibly with edge preserving thresholds) can be used to impose a degree of homogeneity among the brightness values of adjacent pixels, thereby increasing the chance that neighbouring pixels may be given the same label *(Richards and Jia, 1999)*. Generating a separate channel of data is another pre-processing contextual method. In an attempt to improve the accuracy of classification of image data containing urban segments, *Gong and Howarth (1990b)* set up a "structural information" channel to bias a classification according to the density of high spatial frequency data, and it significantly improved the classification results compared to conventional classifiers.

Other pre-processing steps take the approach of first segmenting the image into homogeneous regions, followed by classification on the image segments *(Herold et al., 2003; Holfmann, 2001; 2004; Steinnocher and Bauer, 2001; van der Sande et al., 2003)*. Segmentation techniques can be divided into three categories *(Ballard and Brown, 1982)*:

- Edge finding: in these methods discontinuities in the spectral domain of the image, strong enough to be detected, are searched for. These discontinuities are detected as edges, which are then composed by edge linking methods into a more elaborate structure representing a boundary of a homogeneous image class. Many types of edge finding operators have been developed *(e.g Canny, 1986; Lacroix, 1988; Robinson, 1977).*
- Region growing: in these methods an attempt is made to group pixels with similar characteristics into contiguous regions. The similarity property may be defined in terms of radiometric closeness or by some other criterion such as conformity with a local texture measure. Details about region based segmentation techniques can be found in *Haralick and Shapiro (1992)* and *Zucker (1976).*
- Map or knowledge based: these methods use ancillary information to guide the segmentation procedure. This can be, for example, a digital map providing a background reference indicating where segment boundaries can occur *(Corr et al., 1989).* Much research has been devoted to segmentation and this indicates that existing methods provide with difficulty the performance that image analysts require *(Lucieer, 2004; Wilson and Spann, 1988).*

Another type of contextual classification approach is post processing of results obtained using a multi-spectral classifier. This can be done by applying a simple majority filter *(*e.g *Townsand, 1986).* Some algorithms are based on the modification of the probability of each pixel based on the probability compatibility among pixels in the local neighbourhood. This technique is known as probability relaxation *(*for details, see *Richards and Jia, 1999). Gong and Howarth (1989)* applied probability relaxation to urban land cover classification and found that it improves classification accuracy, though at the expense of more computation time. Other approaches are based on rough classification or clustering results leaving the post processing analysis to regroup the clusters into a final map *(Gong and Howarth, 1992).*

4.4.3 Information fusion techniques

Information fusion technique is another basic strategy for improving image classification accuracy. Broadly, two types of data are used in information fusion techniques. The first is image information; for example fusing high resolution panchromatic band with low resolution multispectral information *(Bauer and Steinnocher, 2001; Marangoza et al., 2004; Scott et al., 2003; Sun et al., 2003).* The second approach involves use of ancillary data. Ancillary data are information used in the classification process that is not directly obtainable from either spatial or spectral characteristics of the remote sensor (e.g soil data, DTM, vector GIS data, social economic data etc.) Examples of applications can be found in *Haala and Brenner (1999), Heipke et al. (1999; 2000) and Balstavis (2004).*

4.4.4 Knowledge based techniques

The value of knowledge-based techniques for land-use classification in remotely sensed imagery is widely recognized. Knowledge-based image recognition systems have two features in common: (i) a database of computed image features is matched with antecedents of production rules (rules are represented as logical statements of the form "if…, then…"). (ii) there is a control system that supervises rule activation. *Ton el al. (1991)* demonstrated a knowledge-based segmentation and interpretation methodology for the interpretation of Landsat images. The image interpretation system establishes a coarse segmentation of the imagery using spectral features alone during a stage denoted by category-oriented segmentation, with simple, application independent spatial constraints. The identified terrain regions are transferred to a second stage, denoted by image-oriented segmentation, where a hierarchical implementation of various image processing operations establishes an accurate segmentation of the image. A comprehensive review of knowledge based information extraction techniques can be found in *Balstavis (2004).*

4.4.5 Neural networks

A new type of classification came into use during the past decade, which is called neural networks. It differs significantly from the above explained approaches, because the decision boundaries are not fixed by a deterministic rule applied to the prototype training signatures, but are determined in an iterative fashion by minimising an error criterion on the labelling of the training data. A basic network consists of three layers of nodes and weights. The first layer contains the input layer nodes, and these are the multi-spectral vectors of the training pixels used for classification. The second layer contains the processing nodes, where summation and transformation operations are executed. The results are then expressed in the third layer in the output nodes. The discrimination capability of a neural network is contained in its weights. These weights are given fuzzy values between 0 and 1. During training, they are iteratively adjusted toward a configuration that allows the network to distinguish the prototype patterns

of interest. Examples of land use classification studies that used artificial neural networks are *Cortijo and Perez de la blanca (1997), King et al. (1999) and Kontoes et al. (2000).*

Common remote sensing software packages like Erdas Imagine, ILWIS and ENVI support some of the above mentioned context classification techniques, such as filtering operations. ENVI even has the possibility to build neural networks. However, pre-processing such as segmentation techniques or the inclusion of other data is either not possible or very limited. In general, contextual classification techniques, even where they are available still need detailed user knowledge to achieve good results. User friendly automatic information extraction techniques in generic commercial software packages are mostly suitable for medium to low spatial resolution (10 m – 1000 m) images.

4.5 Proposed approach for this study

Extraction of urban objects from high resolution RS imagery is a challenging task that requires proper pre-processing (geometric/radiometric correction and image enhancement), advanced image analysis techniques and credible accuracy assessment to assure certainty of the generated results for application in decision making. As already discussed above, most generic image processing software lack powerful image analysis tools, that are suitable for analysing high resolution imagery. On the contrary, powerful contextual classification algorithms are mainly stand alone, specifically for image analysis or feature extraction and generally lack tools for pre-processing and post-processing operations for proper integration with other data in a GIS environment. In order to bridge the operational gaps, the best approach is to integrate the available software tools, which enable powerful analysis that is beyond the capacity of single software.

In line with the above, this study integrates the following software tools (see Figure 4-1) at different levels of image analysis:

- ERDAS imagine for pre-processing operations and accuracy assessment
- eCognition for information extraction and image analysis
- ArcGIS for generation of reference data and post classification analysis

Since the extraction of information is the major focus of this study, the main image analysis features in eCognition are briefly described below.

4.5.1 Basic concepts of eCognition

As outlined in section 4.4.2, segmentation is one of the necessary pre-processing steps carried out before classification in some contextual classifiers *(Schowengerdt, 1983; Sun et al., 2003).* Moreover, the advent of high resolution RS imagery are making object-oriented image analysis increasingly popular *(Herold and Scepan, 2002; van der Sande et al., 2003; Zhang, 2003)* . However, advanced segmentation algorithms are not implemented in most commercial image analysis software packages. eCognition was the first commercial tool for segmentation and object-oriented classification for RS imagery *(eCognition, 2004).* It is based on the concept that important semantic information necessary to interpret an image is not represented in single pixels but in meaningful image objects and their mutual relations, i.e. the context. The analysis is performed at three general levels: (i) segmentation, where the image is portioned into contiguous homogeneous image segments or objects, (ii) classification of image objects based on their physical properties (e.g. spectral values, form and texture) and

their neighbourhood relations and (iii) accuracy assessment of the generated results and exporting of generated results for further analysis with other data in advanced GIS software.

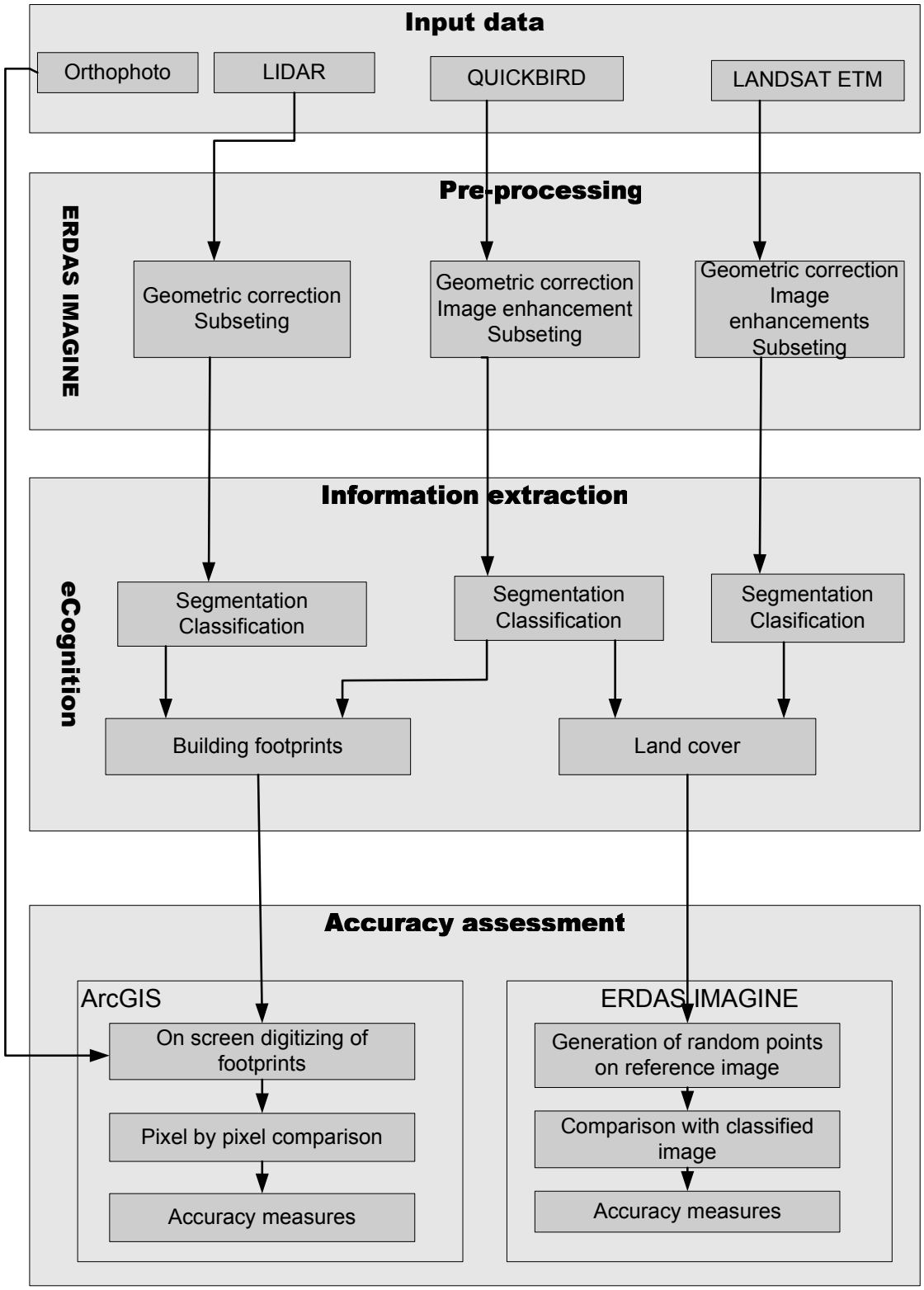

Fig. 4-1: proposed integrated approach

4.5.2 Image segmentation

eCognition's multi-resolution segmentation is a bottom up region-merging technique starting with one-pixel objects. In subsequent steps, smaller objects are merged into bigger ones by taking criteria of homogeneity in shape and colour into account. The objects' size is adjusted by the *scale parameter,* which determines the maximum allowed heterogeneity of the objects *(for details see Baatz and Schape, 2000).* Image objects are generated at different sizes in a network of hierarchical levels, and are logically linked such that each object knows its neighbours and sub- and super-objects. The image objects at the lowest level target fine objects such as building footprints and trees, and the highest level show large objects such as different settlement types, thus applying the classification scheme as in *Anderson et al. (1976).* The shape of the derived image objects is determined by the following parameters *(Hofmann, 2001b):*

- Weight of image channels: this parameter can be used to more or less weight one or more image channels' influence on the object generation. When working with image data of comparable channels in size and content such as QUICKBIRD, each channel should be weighted equally (see Fig. 4-2).

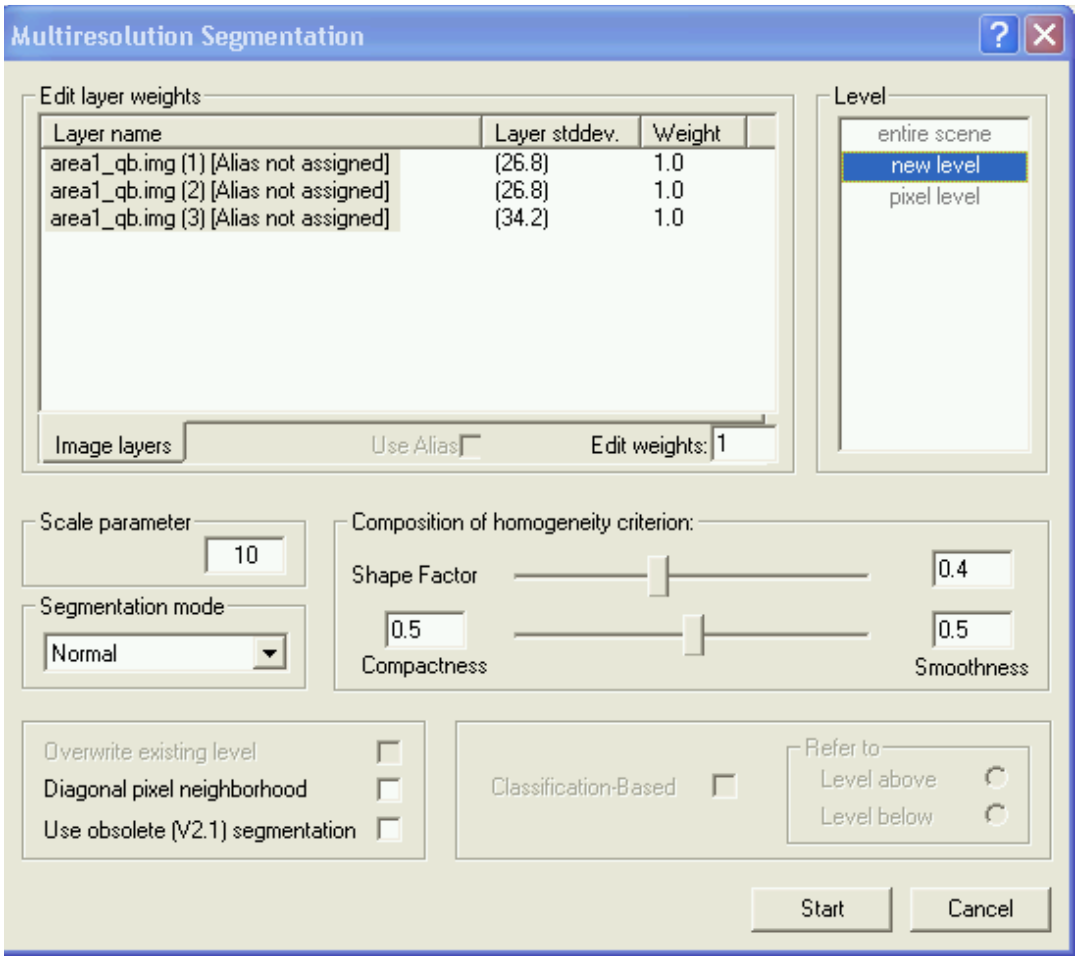

Fig. 4-2:segmentation parameters

- Scale parameter: this parameter indirectly influences the average object size. In fact this parameter determines the maximal allowed heterogeneity of the objects. The larger the scale parameter the larger the objects become. For example, image objects produced using a scale parameter of 10, will include at least ten pixels with different values that are grouped to form an object.
- Colour/Shape: with these parameters the influence of colour vs. shape homogeneity on the object generation can be adjusted. The higher the shape criterion the less spectral homogeneity influences the object generation.
- Smoothness/Compactness: when the shape criterion is larger than 0 the user can determine whether the objects shall become more compact (fringed) or more smooth.
- Level: determines whether a new generated image level will either overwrite a current level or whether the generated objects shall become sub- or super-objects of a still existing level. The order of generating the levels affects the objects' shape (top-down vs. bottom-up segmentation).

However, it should be noted that there is no rule on what scale parameters are suitable for extracting which land cover, the suitable parameters are normally arrived at through a trial and error process. Though giving more shape weighting for extracting urban man made features works well and more colour weighting for vegetation and water gives better results. Moreover, other data sources like DSMs are entirely dependant on colour since elevation is represented in intensity of grey levels. Therefore, in case of DSMs, the rule of thumb is that all the weight is given to colour. The software also offers a possibility of generating image objects based on the classification using classification-based segmentation.

4.5.3 Classification

Typically, there are two classification techniques available in eCognition: (i) the Nearest Neighbour (NN) classifier, which performs class assignment based on minimum distance measures, and (ii) fuzzy classification, in which classes are precisely described, using fuzzy membership functions (see section 4.33). The former requires training samples before the actual classification, while the latter requires good knowledge about the characteristic of the objects and the attribute used to define membership classes should give a reasonable separation between the of objects of interest. Depending on the on preference and image complexity, either one or both methods can be employed to extract features of interest.

The classification approach can either be by elimination or selective strategy *(Lillesand et al., 2004)*. In the first case, beginning with a coarse and mostly spectral classification, further classes are added to the class hierarchy which are described by additional criteria of form, size, texture or context and by inheritance, until a refined classification is achieved. This classification technique leads to more complete classification but also describes classes that are not the main focus of the classification. In the latter case only the classes of interest are described, while others that do not meet the criteria of described classes remain unclassified. To avoid misclassifications this technique needs the classes of interest to be described very precisely and normally the fuzzy membership functions are used to perform this classification.

The final step is to aggregate the classes into semantic groups, which are used for classification based segmentation. The derived contiguous segments are used for further neighbourhood analysis to derive a more meaningful classification and the final result can be exported to a GIS for further analysis.

4.5.4 Features used for classification

The software has a number feature that can be use by means of fuzzy logic to build class descriptions. The commonly used features are:

- Object features: -layer spectral values (e.g. mean, ratio, standard deviation)
  -form features (e.g. area, main direction, length /width ratio)
  -texture feature (e.g. standard deviation of spectral values, GLCM statistical measures)
- Class related features: -relations to neighbour objects
  -relations to super-objects
  -relations to sub-objects
- Feature distance: -distance between objects on different levels
  -distance between objects on the same level
- Operators: -logical terms to combine and evaluate two or more expressions (e.g. and, or, not)

Layer values are features concerning the pixel channel values of an image object and feature, and are very useful when discerning different features based on their spectral values, some of the layer values used widely in this study are given below.

(i.) The mean value $\overline{C}$, which is calculated from the layer value C_{Li} of all n pixels forming the image object.

$$\overline{C} = \frac{1}{n}\sum_{i=1}^{n} C_{Li} \tag{3}$$

(ii.) Brightness, the sum of mean values of layers containing spectral information '$\overline{C}$'divided by their quantity computed for an image object n_L (mean value of an image object).

$$b = \frac{1}{n_L} = \sum_{i=1}^{n_L} \overline{Ci} \tag{4}$$

(iii.) Ratio of layer, $r_{L,}$ is the mean value of an image '$\overline{C_{L,Object}}$' object divided by the sum of all spectral layer mean values $\overline{C_{L,SO}}$.

$$r_L = \frac{\overline{C_{L,object}}}{\overline{C_{L,sumobject}}} \tag{5}$$

Another important feature for image object classification is texture, and in this case it is calculated using the grey level co-occurrence matrix (GLCM) after *Harallic (1973).* The GLCM is a tabulation of how often different combinations of pixel grey levels occur in an image. Every GLCM is normalized according to the following operation:

$$P_{i,j} = \frac{V_{i,j}}{\sum_{i,j}^{N-1} V_{i,j}} \tag{6}$$

Where *i* is the row number and *j* is the column number, *Vi, j* is the value in the cell *i, j* of the matrix, *Pi, j* is the normalized value in the cell *i, j,* and *N* is the number of rows and columns.

The normalized GLCM is symmetrical. The diagonal elements represent pixel pairs with no grey level difference. cells, which are one cell away from the diagonal, represent pixel pairs with a difference of only one grey level. Similarly, values in cells, which are two pixels away from the diagonal, show how many pixels have a 2 grey levels and so forth. The more distant to the diagonal, the greater the difference between the pixels grey levels is. Summing-up the values of these parallel diagonals, gives the probability for each pixel to be 0, 1, 2 or 3 etc. different to its neighbour pixels. The statistical definition of these measures together with a brief description of their meaning is given below. more details can be found in *Haralick et al (1973).* From the several statistical texture descriptors derived from this matrix, this study uses the homogeneity, contrast and dissimilarity.

(i.) Homogeneity, which measures the closeness of the distribution of elements in the GLCM to the GLCM diagonal.

$$Homogeneity = \sum_{i,j=0}^{N-1} \frac{Pi,j}{1+(i-j)^2} \tag{7}$$

(ii.) GLCM: Contrast, is the opposite of Homogeneity, it is measure of the amount of local variation in the image. It increases exponentially as (*i-j)* increases.

$$Contrast = \sum_{i=0}^{N-1} P_{i,j}(i-j)^2 \tag{8}$$

(iii.) GLCM: Dissimilarity, which is similar to contrast but increases linearly and it high if the local region in the image has high contrast.

$$Dissimilarity = \sum_{i=0}^{N-1} Pi,j|i-j| \tag{9}$$

The texture is very important for discerning buildings from non-building objects especially vegetation in the height data and it was used widely in section 5.1 and 5.2

4.5.5 Accuracy assessment

The accuracy assessment in eCognition is performed based on an error matrix. It compares on a class-by-class basis the relationship between known reference data and the corresponding results of the classification *(for a detailed explanation see Campbell, 1996; eCognition, 2004).* The accuracy assessment tools available in eCognition were not used in this study since a reference thematic layer with the same classes as the classified image is required. Such a reference map was not available in this study and, therefore, the evaluation was done in ArcGIS for building footprints and in ERDAS IMAGINE for land cover maps. Application and interpretation of an error matrix have been dealt with in section 5.2.

4.6 Previous works on extraction of urban objects

Extraction of urban objects is a challenging task that has been the subject of extensive research. An extensive collection of papers on extraction of man-made objects can be found in *Baltsavias, (2004), Baltsavias et al. (2001), Gruen et al. (1997; 1995)* and *(Guindon, 1997),* while a thorough review on automatic road extraction is presented in *Mena (2003).* Generally, many studies have reported successes, in efficiency and cost effectiveness of these systems especially when applied in smooth terrain at small to medium scale and when using small and medium resolution imagery. However, the performance decreases rapidly for complex scenes in dense urban areas and when using large-scale imagery. Some of the cited causes of degradation in performance of automatic systems are: (i) poor image contrast, (ii) occlusions, (iii) similarity in spectral characteristics of urban objects of different classes, (iii) shadows, (iv) poor or repeated textures, (v) poor image quality, (vi) foreshortening and motion artefacts, (vii) heterogeneity of urban objects of same class, (viii) problems in defining rules for extracting target objects (e.g. height, size, shape and colour of buildings; width and length of roads etc.) and the lack of models of man-made objects. To offset these problems, most of the extraction of urban objects is still being done by human-guided interactive operations, such as stereo compilation from a screen *(Zhou et al., 2004).* This process is still costly and time consuming. Over the past years active research in the fields of photogrammetry and computer vision has been striving to develop a comprehensive, high success rate and reliable systems with either full automation or semi-automation to ease human–computer interactive operations. Examples can be found in *Baltsavias (2004)* and *Mena*, *(2003).* However, automatically extracting building information is still an unsolved problem. Efforts for overcoming the problems mentioned above are still needed.

In an effort to solve the problems encountered many methods have been proposed. some focused on automation of extraction of urban features using RS images and existing knowledge from a vector database *(e.g. Gerke et al., 2003; Haala and Brenner, 1999; Vosselman and Suveg, 2001),* some on fusing LIDAR data and multi-spectral imagery *(e.g. Rottenstein and Jansa, 2002; Vögtle and Steinle, 2000; Zhou et al., 2004),* and others on combining pixel-based and object-oriented approaches to extract urban objects *(e.g. Shackelford and Davis, 2003). Baltsavias et al. (1995)* discuss three different approaches for extracting buildings from LIDAR for the 3D data analysis namely: using an edge operator, mathematical morphology, and height bins for detection of objects higher than the surrounding topographic surface. These approaches have been used by other authors *(e.g. Eckstein and Munkelt, 1995; Haala and Brenner, 1999).*

Although success has been reported in automatic or semi-automatic extraction of urban objects most of these are experimental works or stand alone systems that are not available on the market. eCognition is the first commercial object-oriented software, and is used widely to extract urban objects. Examples of works related to this can be found in *Herold et al. (2003; 2002), Marangoza et al. (2004)* and *van der Sande et al. (2003).* In the next chapter this study will explore the use of this software to extract risk-related urban objects from multi-source remote sensing imagery.

5 Image analysis and results

5.1 Extraction of building foot prints

The advent of high resolution multi-spectral imagery remote sensing imagery such as IKONOS, EROS and QUICKBIRD and recent advances in Laser Scanning technology have provided a new window of opportunity for the extraction of urban topological features *(Meitnel et al., 2001; Scott et al., 2003).* Several studies have used high resolution multi-spectral remote sensing imagery for urban modelling, and examples of recent works on this subject can be found in, *De Kok et al. (2003), Herold and Scepan (2002) and Schiewe (2003).* Other studies have used Airborne Laser Scanning (ALS) data to extract buildings for the construction of building city models*(Fujii and Arikwa, 2002; Vosselman and Suveg, 2001)* Some have used a combination of aerial images and ALS data to extract buildings for building city models *(Haala and Brenner, 1999a; Vögtle, 2000).*

Many methods follow a step-wise approach in eliminating objects other than buildings, during automatic extraction of buildings from remote sensing imagery. Some studies start with a pixel-based classification followed by segmentation and refined classification *(Scott et al., 2003).* Others start with segmentation followed by step-wise classification on generated image objects to extract buildings and other urban topographic features *(Holfmann, 2001; Marangoza et al., 2004; van der Sande et al., 2003).* Those that use laser scan data mainly start with creation of a DTM from the laser raster DSM, followed by creation of a nDSM (see section 3.3.3), from which buildings are extracted using a step-wise process *(Kraus and Pfeifer, 1998; Rottenstein and Jansa, 2002; Vögtle, 2000).*

In this study, a segmentation-based classification is employed (see section 4.5). In contrast to classical pixel-based image processing, the building blocks of object-oriented image analysis are contiguous homogeneous image segments. The basic image object is a single pixel. Ideally, the image segments should outline pictured real world objects that are to be extracted from the image. Two data sets are used to extract buildings on the same area: (i) a gridded LIDAR DSM, and (ii) a QUICKBIRD image.

The rest of the section is arranged as follows: section 5.1.1 describes the test site, section 5.1.2 describes the segmentation process, section 5.1.3 details the classification process, section 5.1.4 details the extraction of building footprints from LIDAR nDSM, section 5.1.5 descusses the extraction of building footprints from QUICKBIRD imagery and section 5.1.6 gives the quality assessment of the extracted results.

5.1.1 Site description

The test site for this study is about 270 x 370 m. It contains a well defined urban area with scattered vegetated areas, well shaped buildings, and roads crowded with cars. The vegetation stands out of other objects for its high reflectance in the infra-red band, appearing red in Fig 5-1. Buildings vary in tone from light grey to brown, roads and car parks vary in tone from light grey to dark grey, and cars mostly stand out in light grey against the dark grey road back ground.

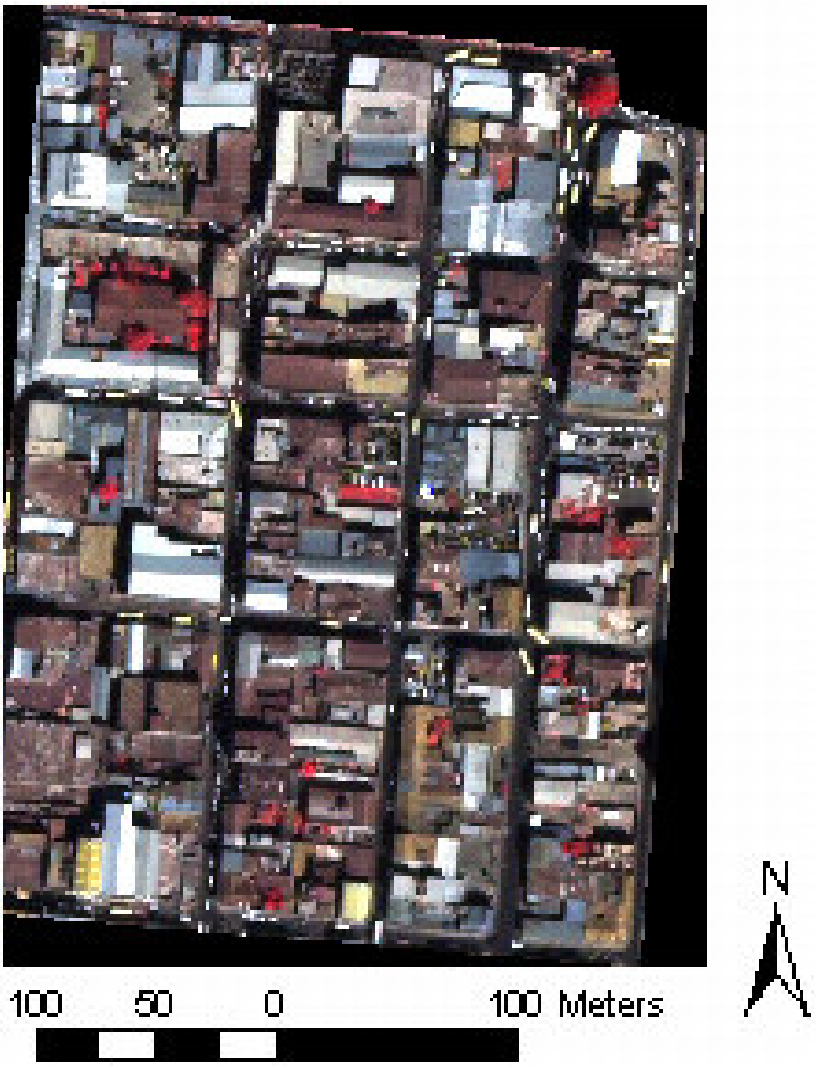

Fig. 5-1: Test site for building footprints

5.1.2 Segmentation

The first stage in the object extraction from the QUICKBIRD imagery was segmentation and it was performed by equally weighting all the three bands of the pan-sharpened QUICKBIRD imagery. The segmentation was carried out in three hierarchical levels and the parameters used are summarised in the Table 5-1.

At level 1 the scale parameter of 8 was found suitable to discriminate small objects like cars from other objects. Level 2 was suitable for classification of all other features (buildings, vegetation and roads). Level 3 was achieved using semantic grouping of buildings and non building objects at level 2 through a classification based segmentation, and the result was two groups of image objects: *building* and *non-building*.

For the classification of the nDSM (see section 3.3.3 for a description of nDSM) only two segmentation levels were sufficient, since features are well separated by their heights and there is limited heterogeneity in features of the same class. At level 1 a scale parameter of 15

was used and the heterogeneity criterion was 90% based on colour, which in this case are grey levels indicating elevation. Level 2 was based on classification based segmentation as above.

Table 5-1 Segmentation parameters

	Segmentation and classification level	Land cover types	Segmentation parameters				
			Scale parameter	Homogeneity criterion			
				Colour	Shape	Shape settings	
						Smoothness	Compactness
QUICKBIRD IMAGERY	Level 1	Cars	8	0.4	0.6	0.5	0.5
	Level 2	Buildings, vegetation roads, shadows	25	0.4	0.6	0.5	0.5
	Level 3	Roads and built-up	Classification -based				
nDSM	Level 1	Background and building blocks	15	0.9	0.1	0.5	0.5
	Level 2		Classification based				

5.1.3 Classification

Different attributes and approaches were applied to classify the nDSM LIDAR and the QUICKBIRD imagery, since the data sets have different properties. The QUICKBIRD imagery uses spectral values to separate different features, while the nDSM uses height differences to discriminate the different urban features.

Urban features such as roads, building roofs and bare land sometimes have similar spectral values, which makes it difficult to separate them using spectral information alone. In addition, there is heterogeneity even within the same objects; for example caused by, cracks, shadows and use of slightly different materials, which results in the same object falling in different classes. Though the QUICKBIRD imagery has a high spatial resolution of 61 cm, it is still limited in spectral resolution to separate features with slight variation in spectral values and features that are occluded by high objects are difficult to extract using the approach used in this study. However, the high spatial resolution provides high texture differences among objects and proper definition of object shapes which are important attributes for extracting urban features. Furthermore, knowledge about the neighbourhood relations and size of urban objects can also be explored to help in the extraction of urban objects. With a logical combination of spectral, spatial, textural, contextual and semantic information, complex urban features can be extracted from the QUICKBIRD imagery. Details on steps used to extract information from QUICKBIRD imagery are shown in the next section with illustrations.

On the contrary, separating urban objects on height values alone is also not straight forward as there are other raised features such as trees, flyover bridges, raised roads and small hills that are difficult to separate from buildings. Again, knowledge about the size, neighbourhood relation, orientation, shape *(Zhang, 2000),* and texture of the objects of interest is helpful to discriminating different urban scenes. Detailed steps about how building footprints were extracted from the nDSM in this study are shown in the next section.

5.1.4 Extraction of building footprints from nDSM

The extraction of buildings was done in four steps:

- First the segments were classified as building and not-building using the criteria used by *van Westen and Montoya (2004)* in the same area that buildings roofs should be at least 2.7 m higher than the ground level. But this threshold also includes trees and other raised objects which have to be removed (see the result in Fig. 5-2a).
- In the second step (Fig 5-2 b) the building segments are further subdivided according to the number of floors (see table below in relation to Figure). The building blocks are segmented into different floor levels because lower buildings are more mixed with other terrain objects and different rules should be applied at different levels to clean the errors.
- At step 3, (Fig. 5-2c), a length/width ratio was applied to elongated objects to three storey buildings and texture measures, a GLCM homogeneity or dissimilarity criteria *(*see section 4.5.4. or *Haralick et al., 1973)* is used to remove non-buildings objects and trees from one-three storey buildings. This is from knowledge that building roofs have more homogeneous roof heights as compared to other terrain objects at all levels. In 'c' some trees and a fly-over bridge are removed using this operation (in light green*)*.
- Finally, all classified image objects are merged into two semantic groups namely, *building* and *non-building,* by running a classification-based segmentation to generate image objects for level 3. At level 3, a final classification is performed with only two classes; *building* and *background*, which is exported is exported to ArcGIS for evaluation of results as described in section 5.1.6.

Table 5-2 Threshold for floor levels

Height range	No. of floor	Colour
2.75 – 5.50	1	yellow
5.50 – 8.25	2	dark gren
8.25 - 11	3	red
11 – 13.75	4	red
> 13.75	5	orange

Adopted from (van Westen and Montoya, 2004)

Fig. 5-2 nDSM classification steps, (a) after separating ground level and raised objects, (b) the buildings are separated into different levels according to number of floors, (c) some non building objects like fly-over bridges are removed (light green), and finally (d) all the elongated and small non building objects are removed.

5.1.5 Extraction of building footprints from QUICKBIRD

The extraction of building from the QUICKBIRD is more complex than from the nDSM since objects belonging to different classes share the same spectral characteristics. To simplify the extraction process, the classification is broken down into three levels using image objects generated in the segmentation described above and levels are interlinked. At level 3, with largest image objects or segments, two general classes are defined; buildings and non-buildings. At level 2 image objects are relatively smaller, and most objects of interest are classified at this stage. The classes identified at this stage are: brown roofs, grey roofs, cars, vegetation, bare land, and shadows streets car parks and roads. At level 1, the image objects are very small and only cars can be identified and vegetation can be clearly discerned. This is mainly formed for further analysis, since attributes of lower level objects can also be used to classify higher level objects they belong to. The typical steps followed to achieve the final results at level 2 are:

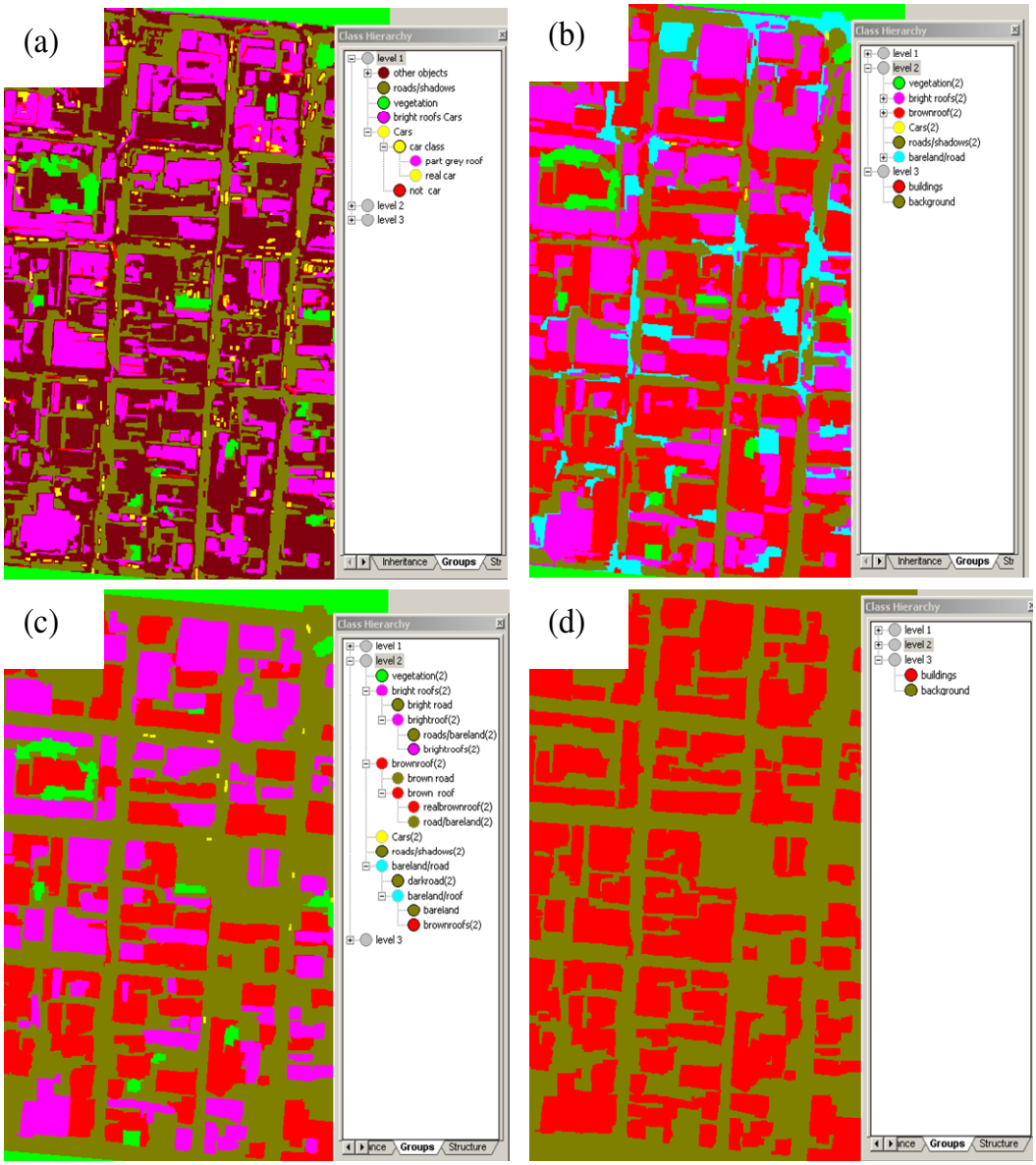

Fig. 5-3 Classification steps for the QUICKBIRD imagery: (a) separates vegetation from other classes and eliminates most cars, (b) first classification step at level 2, most cars are eliminated from roads, (c) final classification at level 2, showing bright roofs (pink), brown roofs (red), vegetation (light green), and other non-building objects (dark green), and (d) level three classification building (red) and background (dark green)

- At level1, vegetation was separated from other objects using a fuzzy membership function for its high reflectance in the infrared channel. The other objects are mixed and could not be entirely separated using spectral information alone, and were therefore divided into three general classes using the using their brightness value and size as follows: (i) *cars* were discerned using brightness value greater than 50, and a size restriction of not more than 25 m^2 (yellow, Fig. 5-3 a); (ii) all objects with brightness value greater than 50, and lager than 25 m^2 were assigned to *bright roof* class (pink, Fig. 5-3 a); (iii) all objects with brightness value less than 25 were assigned to the *roads/shadow* class since roads are predominantly dark in the image; (iv) all image objects that do not satisfy any of the above conditions are assigned to the

brown roof class; (v) there are some other small bright objects on roof tops which are wrongly assigned to the *cars* class and are, therefore, assigned to the bright roof class if they are at least 70% surrounded by *bright roofs*; and (vi) *cars* that are 50% surrounded by *roads/shadows* class are assigned to that class. The purpose of this level was to eliminate cars and assign them to roads in the next level.

- At level 2, (see Fig 5-4 for generalised steps) a more refined classification of all classes is carried out as follows: (i) *vegetation* is separated from the other classes as at level 1 above; (ii) *roads/shadows* are separated from other classes using existence of *roads/shadows* in the lower class or brightness as above, or brown and grey objects with high length width/ratio; (iii) *bright roofs* are discerned from *non-building* using a high average length of polygon edges since buildings should have well defined geometry as compared to other objects, or brightness and size as in the lower level; the remaining small bright objects are assigned to *cars* class (yellow, Fig. 5-3 c); (iv) objects with brightness value between 25 and 30 were assigned to *bare land or roads* (cyan, Fig. 5-3 b), and *buildings* within this range were separated using their high average length of edges and low length /width ratio; and (v) all the objects not satisfying any of the above conditions were assigned to *brown buildings* and were separated from *non-buildings* using size and geometry as above. The next step was to make structural semantic groupings of all *building* parts and *non-building* parts and use classification based segmentation to generate image objects for final classification at level 3,
- At level 3 only two classes are generated: using existence of building parts in the lower level, and the rest were *non-building*. The results were exported to ArcGIS for accuracy evaluation as explained in the next section.

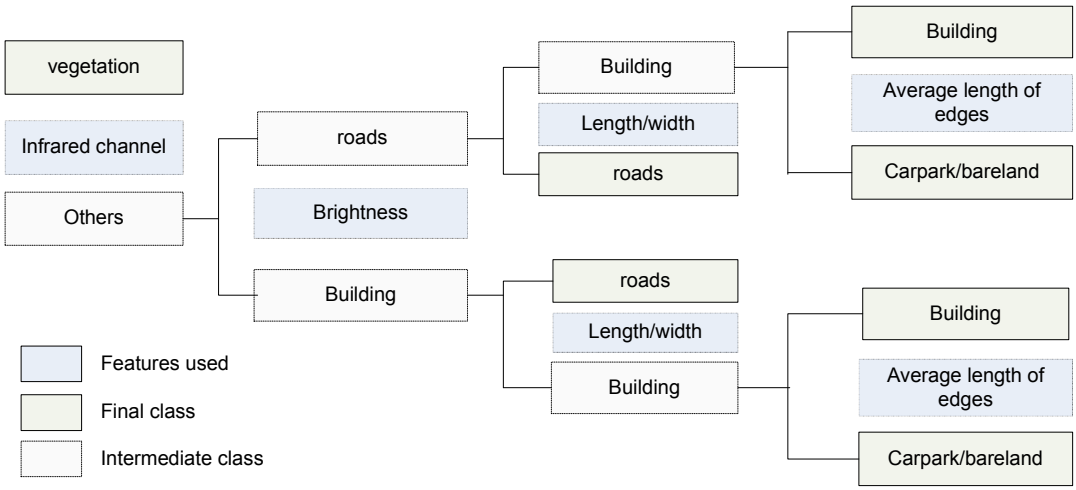

Fig. 5-4: General class hierarch and features used to separate classes at level 2 for QUICKBIRD image

5.1.6 Quality assessment

In order evaluate the accuracy of the entire building footprints extraction result; the building blocks were manually digitized from the imagery. The polygon building footprints layer formed by digitising served as reference with which to compare the automatically extracted results. But before generating the reference data, some important observations were made on the results and in relation to the source data.

- The results obtained from the LIDAR nDSM were mainly solid block with less or no inner spaces inside the building blocks. This resulted from the fact that the data used was gridded format at original cell resolution of 1.5 m (see section 3.3.2) and the narrow inner spaces and streets (average width less than 6 m) surrounded by tall buildings were averaged out during interpolation, since at the edges the average is taken between the roof and the ground points.
- On the contrary, the QUICKBIRD imagery at 0.61 m resolution was fine enough to characterise inner streets.
- The third data set, an aerial photo mosaic at 1 m cell resolution has less detail as compared to high resolution QUICKBIRD imagery.
- Apart from that the QUICKBIRD imagery has the problem of perspective errors and could therefore not be used as the single source for generating reference data for evaluating the extraction of both data sets.
- There was a large time gap between the acquisition dates of the two data sets (33 months) and being an active city area under reconstruction from a disaster many changes and adjustments to building outlines could have taken place as evident in the missing buildings in the LIDAR data.

Considering the above observations, it was imperative to generate two independent data sets. One based on QUICKBIRD and the other on LIDAR, with the orthophoto serving as a complimentary image for interpretation. After digitizing, the polygon building layers was converted to raster and compared pixel-by-pixel with the automatically extracted results. Two approaches were used. First the two maps were subtracted to make an error map for visual comparison (see Fig 5-5), which gives a quick visual overview of the quality of the extraction results.

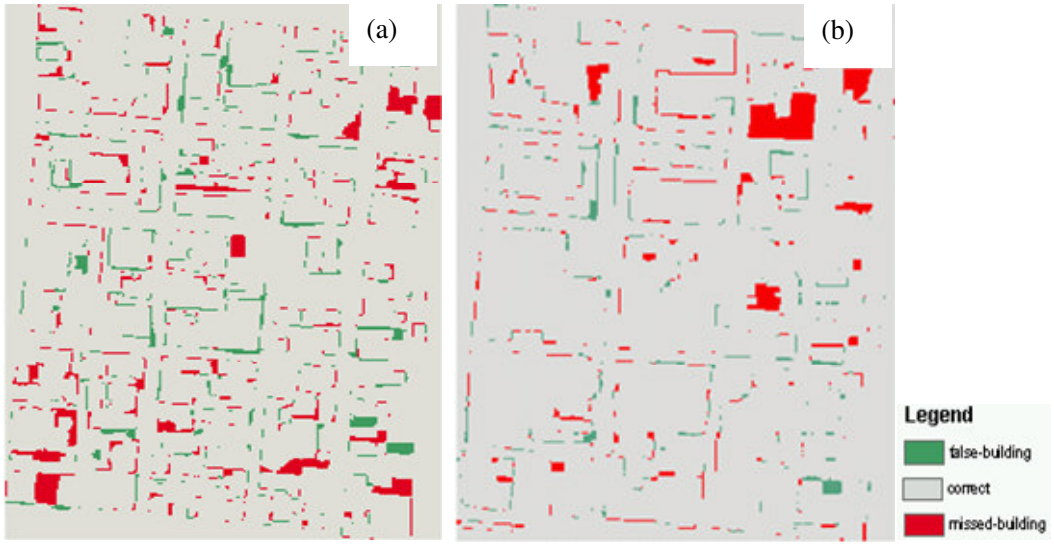

Fig. 5-5: showing classification error maps, (a) for QUICKBIRD and (b) for LIDAR nDSM

For a comprehensive quantitative assessment, a number of quality metrics described by *Shufelt* (*1999)* were used. These metrics can be defined as follows:

True Positive (TP): Both automated and manual methods label a pixel as building.

True Negative (TN): Both automated and manual methods label a pixel as background

False Positive (FP): only automated methods label a pixel as building.

False Negative (FN): only manual methods label a pixel as building.

Using these four categories, the following statistical measures are computed to evaluate the performance of automated building extraction process:

$$Branching\ Factor: \frac{FP}{TP} \tag{10}$$

$$Miss\ Factor: \frac{FN}{TP} \tag{11}$$

$$Building\ Detection\ Percentage: \frac{TP*100}{(TP+FN)} \tag{12}$$

$$Quality\ Percentage: \frac{TP*100}{(TP+FN+FP)} \tag{13}$$

Table 5-3: Pixel classification

Pixel classification	Number of Pixels	
	QUICKBIRD	nDSM
True Positive (TP)	119756	136258
True Negative (TN)	152233	146070
False Positive (FP)	9127	5133
False Negative (FN)	14480	11289

Table 5-4 Building extraction measures

Building extraction metric	Evaluation of result	
	QUICKBIRD	nDSM
Building detection percentage	89.21%	92.35%
Branching factor	0.08	0.04
Miss factor	0.12	0.08
Quality percentage	83.53%	89.24%

Table 5-3 shows the pixel classification result, while the evaluation of the automatically generated results is shown in Table 5-4. The interpretation of the above calculation is as follows:

- The branching factor indicates the degree to which the automatic system has over-classified background pixels as building pixels (FP), while the miss factor indicates the

degree to which the automatic system has under-classified building pixels as background pixels (FN). If a system never over-classifies the extent of any building, its branching factor would be zero, the best possible branching factor, and likewise if the system never under-classifies, its miss factor would be zero. These two measures give the delineation performance of the automatic system.

- The building extraction percentage indicates the percentage of building pixels correctly labelled by the automatic process, and it is a measure of building detection performance.
- The quality percentage describes how likely the building pixel produced by the automatic process is true, and is the most stringent measure of the overall result, because it combines aspects of all measure to summarise the automatic extraction performance.

5.1.7 Discussion

The results in Table 5-4, with the overall accuracy of 84% and 89% for QUICKBIRD and LIDAR, respectively, show a good potential for interchangeability of these data sets to extract buildings. However, there are errors in the automatically generated results (*FN* and *FP*, also see Fig. 5-4) which should be minimised to produce more optimal results and we categorise them as follows:

- Boundary errors: most of the '*FPs*' and *FNs* are lying at the edges of the buildings because of the planimetric accuracy of the input data (reference data, QUICKBIRD, LIDAR nDSM), which show that boundaries are not well defined in both the manual and automatic process. From the reference data it is difficult to define exact boundary of the buildings due to limited contrast and resolution in the imagery, and lack of ground truth knowledge for the test area. Unlike the automatic process that follows pixel by pixel, in delineating, from the human point it was necessary to generalise small bends. For the LIDAR data, the interpolation caused poor definition of boundaries and sometimes its influence caused deviation of two-three pixels along the boundaries, which resulted in the increase of '*FPs'* and '*FNs*'. The QUICKBIRD imagery had problems in places where there were shadows, which caused parts of buildings, been eliminated.
- Detection errors, these were mainly caused by the fact the reasoning or conditions set to automatically extract the buildings could not satisfy all buildings, and in trying to eliminate non-building objects some building were also eliminated. Likewise, some non-building objects were added. The problem with QUICKIRD imagery is that smooth non-building parts like a concrete slab are extracted as buildings and it is difficult to separate them from real buildings, while in the LIDAR lower buildings below the set threshold are eliminated.

The overall good performance of automatic system in this test area can be attributed to low vegetation cover. In areas with extensive tree coverage especially at building edges, the automatic extraction of the buildings becomes more difficult and extraction accuracy from both data sets will reduce dramatically. The likely effect of errors on modelling results is discussed in section 6.3.

5.2 Extraction of land covers from QUICKBIRD imagery

Land cover and land use maps are important input to flood risk modelling since many important parameters related to hydrological modelling can be derived from these maps e.g.

permeability, interceptions to flood water flow, surface roughness etc. *(Alkema, 2004)*. The coefficient of roughness also known as Manning roughness coefficient represents hydraulic roughness, which develops resistance to water flow through a retarding force. The roughness controls overland velocity and flood plain flow rates *(De Roo, 1999)*. Different land cover types have different roughness values. Consequently, a land cover map from which

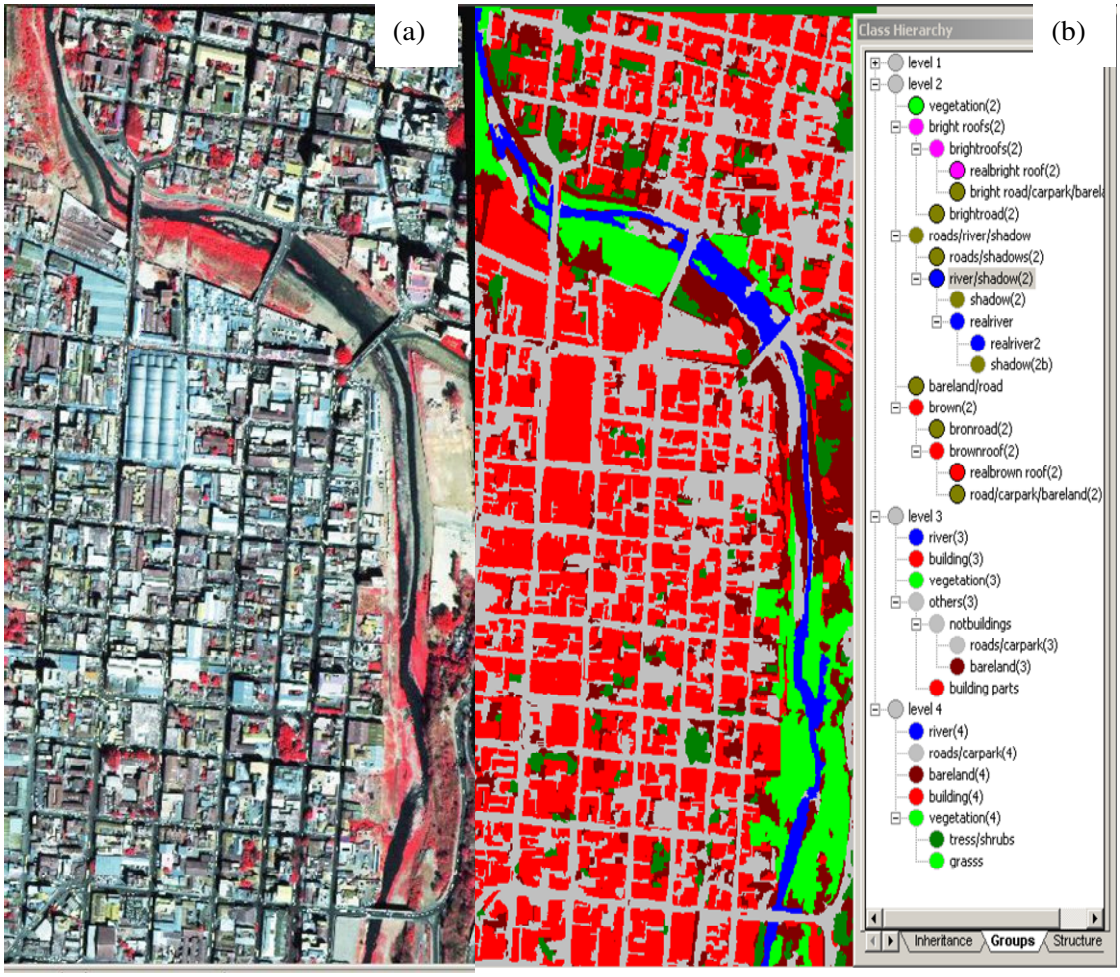

Fig. 5-6: QUICKBIRD false colour composite (a) , and (b) classification result

these roughness values are derived, is an important attribute for flood hazard modelling. The accuracy and resolution of these land covers is more crucial in urban areas where land cover is more heterogeneous as compared to rural areas. This study used QUICKBIRD imagery to derive a land cover map detailing, roads, buildings, trees, river line, grassland and bare land, which are important attributes for deriving surface roughness values. The procedure used to extract building footprints in section 5.1.3 was adopted with little modifications for extracting this land cover map. Consequently, the extraction steps for buildings will not be repeated. Only a few modifications to accommodate new land covers will be briefly highlighted.

The classification was implemented at four hierarchical levels with level 1 and 2 classes using the procedure described in section 5.1.5. At level 2, the *rivers* and *roads* were found to be in the same class since they both have low brightness values and high length/width ratio. A GLCM homogeneity criterion, a texture measure was use to discern *roads* from the *rivers,*

since rivers have a smooth homogenous surface as compared to roads. *Shadows* also have a smooth texture and were therefore mixed with *river*. But most shadows were eliminated using their neighbourhood relation with buildings, since most *shadows* bordered buildings while the *river* did not. The remainder of the *shadows* were eliminated at level 3, because after running the classification-based segmentation *river* was a connected single segment while shadows were isolated small patches. Therefore, a size restriction was used to eliminate them. *Bare land* was separated from *paved roads* using the relatively high reflectance in the infrared band for *bare land.*

The grassland could not be separated from the trees using spectral information because they had the same spectral characteristics. However, grassland was lying on the banks of the river while trees were inside the built-up areas. So the topological relation to the river was used to separate them. Fig. 5-6 shows the final classification, result compared to the false colour composite of QUICKBIRD image. The overall cover patterns of buildings, roads, bare land, grass, trees and river are represented in the classified map, though there were a few instances were roads and smooth bare land were mixed with buildings, and paved roads with bare land.

However, the neighbourhood relationships used to separate roads from shadows and grass from trees are not applicable to all situations. The strategy in this approach is to study the characteristics of the image and objects of interest, and then identify the classification attributes to employ. eCognition software offers many options as illustrated in section 4.5. For example, in this case grass could not be separated from trees using spectral information due to spectral distortion caused by image fusion. Alternatively, grass and trees can be separated using a pure infrared channel or using a normalised difference vegetation index (NDVI). As for the case of separating roads from shadows, other attributes such as shape could be explored.

The reference data used for classifying this map were the QUICKBIRD imagery and the orthophoto. The classified map was tested with the reference data and the accuracy assessment is explained in the section below.

5.2.1 Accuracy assessment

Before using the land cover map derived from the satellite image for any application it is important to test it against reference data until the results are satisfactory; otherwise the classification process has to be repeated. The other reason for assessing accuracy of the generated map is to assure its fitness for use for the intended application. The most common way to represent the classification accuracy of remotely sensed data is in the form of an error matrix. It compares on a class-by-class basis the relationship between known reference data and the corresponding results of the classification *(Campbell, 1996)*. From this error matrix the producer's accuracy was derived, which is the number of correctly classified pixels in each class divided by the number of pixels used for that class. This is a measure of omission error, which refers to the points in the reference map that were assigned to a class other than their known class. The commission error is measured with the user's accuracy and this is computed by dividing the number of correctly classified pixels in each class, by the total number of pixels that were classified as that class. This is indicative of the probability that a pixel classified on the map actually represents that category on the ground. The overall accuracy is then the number correctly classified pixels divided by the total number of pixels checked (see equation 14).

$$Overall\ accuracy = \frac{1}{n}\sum_{k=1}^{m} n_{kk}\ , \tag{14}$$

where: n is the total number of checked pixels, m is the number of end-member classes, n_{kk} is the number of correctly classified pixels.

According to *Campbell (1996)* the overall accuracy strongly overestimates the accuracy, because it only incorporates the major diagonal and excludes omission and commission errors. In the case of an error matrix it is not simply a matter of correct and incorrect, but a matter of which categories are being confused. Therefore, a full picture of variations in accuracies of specific classes, which might be of importance to a particular application, can only be obtained by examining the full error matrix.

Another quality measure that can be derived from error matrix is the kappa coefficient, defined as an estimate of a measure of overall agreement between image data and the reference data *(Campbell, 1996).* According to *Congalton (1991),* the kappa coefficient expresses the proportionate reduction in error generated by a classification process compared with completely random classification. This is a widely used technique and it considers within class correlation as well as overall image correlation. The kappa coefficient indirectly incorporates the off-diagonal elements as a product of the row and column marginals:

$$Kappa\ coefficient = \frac{n\sum_{k=1}^{m} n_{kk} - \sum_{k=1}^{m} n_{k+}n_{+k}}{n^2 - \sum_{k=1}^{m} n_{k+}n_{+k}}, \tag{15}$$

where m is the number of end-member classes, n_{kk} is the number of correctly classified pixels, n_{k+} is number of pixels classified into class k, n_{k+1} is number of pixels classified into classified into class k in the reference data set and n is the total number of checked pixels.

In eCognition accuracy assessment is possible using an error matrix, but only if a thematic map of higher accuracy with an exact number of classes is available. Since there was no reference thematic map, the obtained results were exported to ERDAS IMAGINE where the above mentioned reference images were used to assess the accuracy. This was done by generating 200 random points and comparing the classification result and land cover in the reference images. The summary of the classification is shown below in the error matrix below.

Reading from the road/car park classified data we can see that 13 points are wrongly classified as building, and 4 points are wrongly classified as bare land, while from the buildings classified data 3 points are wrongly classified as road/ car park and 6 as bare land, which shows that roads and buildings were confused during classification due to spectral similarity. The other observation is that most of the samples fell in the buildings and road/car park classes, while only 4 samples fell in the river class. This is because these classes cover most part of the scene and only a small portion is covered by the river. Consequently, the error matrix shows an overestimated producer's and user's accuracy for the river class. However, the users' and producer's accuracy for buildings and roads classes, which are the main land covers in this image, can still be considered as valid since they have not been corrupted by small number of pixels falling in other classes.

Table 5-5: Error matrix for the classification results derived from QUICKBIRD imagery

Classified Data	**Reference data**						
	Buildings	River	Road/Car park	Bare land	Grass	Trees	Sum
Buildings	**76**	0	3	6	0	0	**85**
River	0	**4**	0	0	0	0	**4**
Road/car park	13	0	**56**	4	0	0	**73**
Bare land	1	0	0	**19**	0	1	**21**
Grass	0	0	0	0	**11**	0	**11**
Trees	0	0	1	0	1	**4**	**6**
Sum	**90**	**4**	**60**	**29**	**12**	**5**	**200**
Accuracy							
Producer	**84%**	**100%**	**93%**	**66%**	**91%**	**80%**	
User	**89%**	**100%**	**77%**	**90%**	**100%**	**67%**	

Overall accuracy: 85%, overall kappa coefficient: 78%

Moreover, the kappa coefficient gives a more objective quality measure since it takes into account the agreement contributed by chance and considers that the frequency of a sample appearing in a class is proportional to the percentage of number of pixels that this class covers in the whole image. Therefore, the combination of these measures assures the quality of the extracted results. The likely effects of these errors on modelling results are discussed in section 6.3

5.3 Estimation of building heights from LIDAR nDSM

Building height is an important attribute for urban land use classification as high-rise buildings are mainly found in central business district (CBD). Moreover it can also be used to subdivide residential areas into single and multi-storey building *(Zhang, 2003).* With respect to disaster risk assessment, especially earthquakes building height is an important input as buildings of different heights respond differently to ground motion. For floods ground floor area, building material, and total number of floors are import attributes for building damage assessment *(van Westen and Montoya, 2004)* But high rise buildings are normally constructed using strong material as compared to lower buildings and are therefore more likely to be more resistant to flood damage.

This section explores the use of LIDAR data to estimate building height. The average height of each building is obtained by extracting buildings with height information as explained in section 5.1.4. The crucial part here is to remove vegetation and other non building objects, which might be mistaken to be buildings, and this is done using texture measures of homogeneity and dissimilarity (see section 4.5.4), since building are supposed to have a more homogeneous surface at all levels as compared to trees. Fig. 5-6 shows a colour composite of QUICKBIRD image and the corresponding to the classified image showing filtered non building parts in light green. After filtering out the vegetation and other non-building objects, the final map is Fig. 5-8, depicting the extracted buildings with their estimated heights, which depending on the building regulations of the country, can be translated into number of floors. The number of floor plus the footprint area can be used to estimate the total floor area of building per flood scenario, the flood scenario maps were adopted from USGS, *Smith et al. (2000).* Since there is no ground data for verification for the purpose of this study we are going to conceptualise that the first range of height corresponds to single story, and then use

this information to compute the total floor area which is vulnerable to each flood scenario. The extracted buildings footprints/heights were exported to ArcGIS and converted to vector format. The base area for each building was multiplied by the number of floors to give the total floor area. All the areas were summarised according to building's number of floors. Using the topological relationship of inside each flood scenario boundary, the generated results were plotted as show in Fig 5-9. The flood scenarios are depicted as total exposed areas (left) and annual exposed area (right). These are one of the inputs for risk reduction programmes. The charts illustrate the danger of providing decision makers with absolute figures (total exposed area), as decisions could be made to target a 50 year return period, which has a lower cost benefit index *(van Westen and Montoya, 2004).* In this case, priority should be given to the 5 year return floods as shown in the annual exposed area chart. Such graphs can be used in combination with damage curves and cost information for quantitative risk assessment.

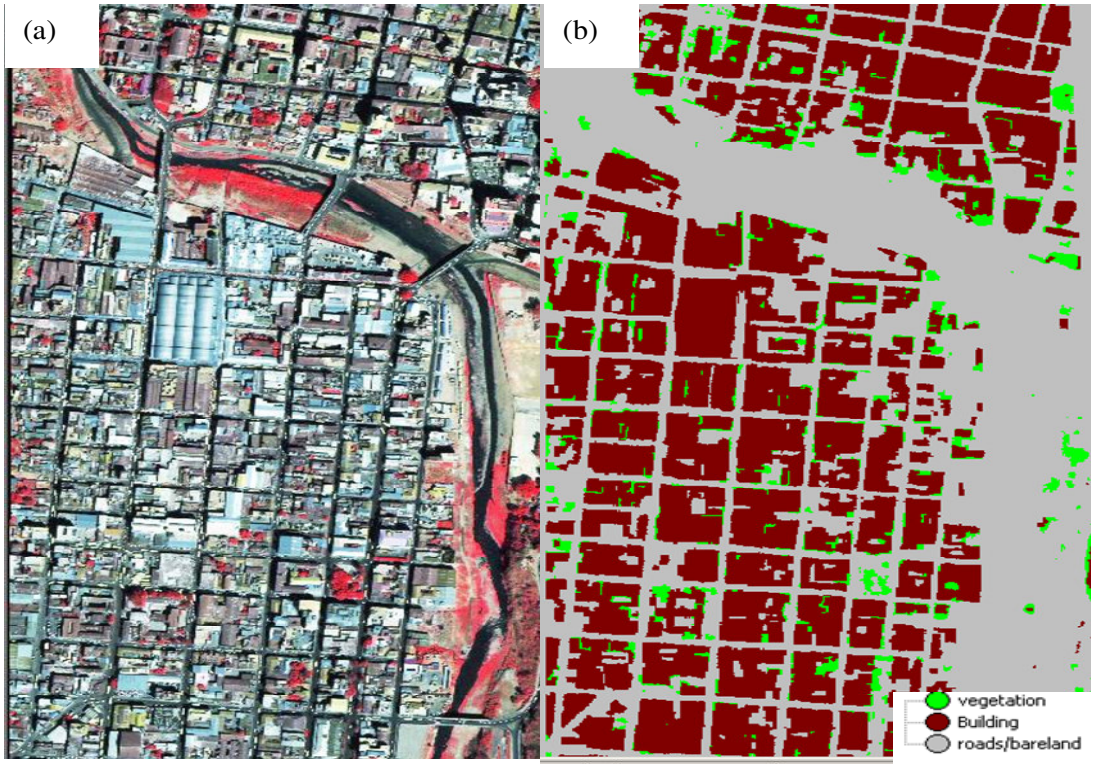

Fig. 5-7: (a), is a colour composite of the QUICKBIRD imagery and (b), is a classified LIDAR nDSM showing removed vegetation and non building parts using texture analysis

The other danger these graphs exposes is the way scientist report modeling results to lay persons or decision makers. For example communicating a flood event of 1/50 annual probability of occurrence as a 50 hundred year return period flood, decision makers will not take it as priority since they would think it would never during their tenure of office or lifetime. Yet the same probability applies to every year including the one immediately after the disaster. Perhaps the better way to put it, is that there a 50-1 chance against such a flood occurring in any year. The risk of misinterpreting such useful information can be reduced and better migration strategies can be developed from them.

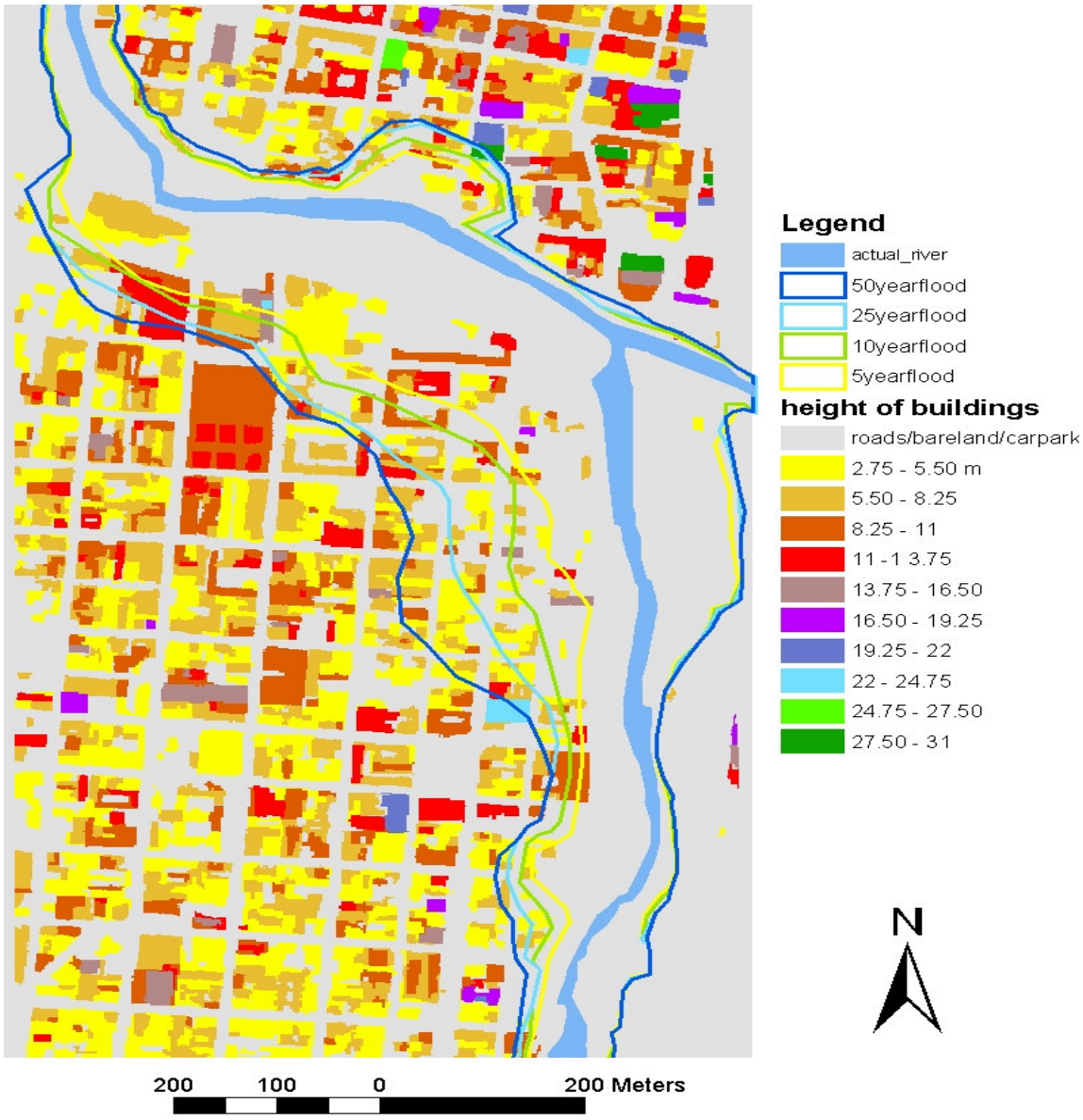

Fig. 5-8: Map showing flood return periods and extracted buildings with estimated heights

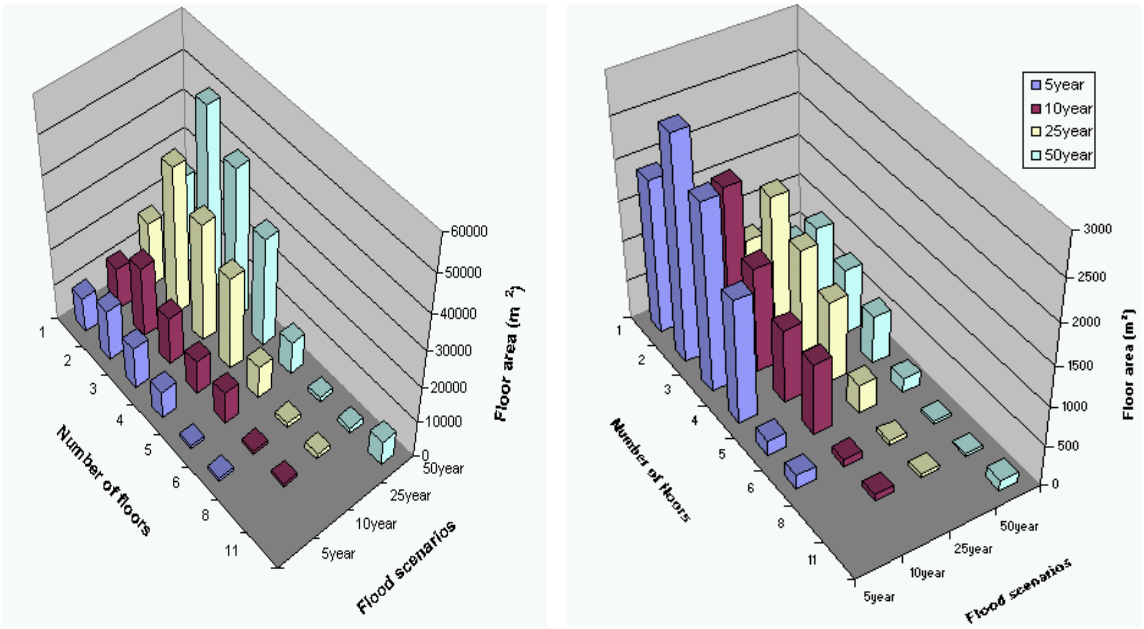

Fig. 5-9 Total vulnerable area (left), and annual vulnerable area (right)

5.4 Detecting informal settlement areas

Demographic factors such as settlement patterns and migration are fundamental to nature and gravity of natural disasters impacts. According to *Martine and Guzman (2002)*, the capacity to recover from the effects of a natural disaster is a result of the physical magnitude of the disaster, and socioeconomic conditions of individuals or social grouping living in the affected area. Vulnerability is differentiated by social groups in almost all natural disasters. There is an important relationship between the settlement patterns, population density and socioeconomic status of the people who live there *(Hardoy and Satterthwaite, 1989; Herold and Scepan, 2002)*. *Annan (1999)* cites poverty and population pressure as factors that force growing numbers of poor people to live on flood plains, in earthquake-prone zones and on unstable hillsides, which increases the vulnerability of the urban poor. Most settlements that are built in these hazard-prone areas take the form of informal settlements.

Informal settlements (often called as squatter settlements or shanty towns) are defined as dense settlements comprising communities housed in self-constructed shelters or shacks under conditions of informal or traditional land tenure. They are a common feature of developing countries and are typically the product of an urgent need for shelter by the urban poor. As such they are characterised by a dense proliferation of small, makeshift shelters built from diverse materials (such as plastic, tin sheeting and wooden planks), by degradation of the local ecosystem (for example, erosion and poor water quality and sanitation) and by severe social problems *(Mason and Fraser, 1998)*. *Ruther et al. (2002)* defined informal settlements as unplanned settlements, typically with no maps indicating the positions and patterns of buildings or shacks. *Martine and Guzman (2002)* describe them as precarious houses or shacks made of flimsy, nondurable materials, on the least-valued plots such as steep hillsides, on floodplains, in fragile ecosystems and watersheds, and on contaminated land, right-of-ways, and other inappropriate areas. Common to all definitions is that they are settlements comprising substandard shelters largely unsuitable for human habitation. Such location

patterns contribute enormously to the vulnerability of poor people, while also endangering the overall population (see discussion in section 5.4.3). The key words in all definitions are the type of material and social status of the people who live their and, moreover, these areas are in most cases unmapped. Therefore, informal settlements are an integral part for flood risk management and the need for finding methods that can be used to detect and map them in a cost effective manner cannot be overemphasised.

5.4.1 Informal settlements and floods disasters

Typically, due to high demand for land in urban areas, the only land that is available for the poor rural-urban migrants is in hazard prone areas previously identified as unsuitable for residential occupation. Detailed information about the characteristics of the settlements in terms of infrastructure (e.g. roads, water and sanitation, health and education etc.) and socioeconomic status of the communities living there, are essential at all phases of a flood disaster management. By definition, with regard to the socioeconomic status of the inhabitants and their interaction with the environment, informal settlements stand out to be of critical importance in managing a flood disaster. Their influence on flood risk management is twofold: (i) their physical impact on the environment and flooding dynamics and, (ii) the vulnerability of the inhabitants to the floods. Each of these dimensions will be discussed briefly.

5.4.2 Effects of informal settlements on the flooding situation

A closer look at informal settlements reveals serious physical impacts on the flooding situation. Settling on river banks, flood plains, unstable hills and steep slopes has effects on the sediment load into the river network and some permeable surfaces in the flood plain are converted to impermeable, which all together increases the flood extent during flooding events, making a relatively larger community vulnerable. The interference with forests and water catchments also causes an increase in erosion and impermeability, which has great influence on the magnitude of the flooding. A good example of the effects on deforestation is Haiti, where the impact of flooding was more severe as compared to neighbouring Dominican Republic due to rapid urbanization, lack of land management, the over exploitation of charcoal and consequent deforestation making Haitians more vulnerable to mudslides *(Inter.-Agency Secretariat of the International Strategy for Disaster Reduction (UN/ISDR), 2004).* Another look at the first definition “use of poor construction materials such as plastic, tin sheeting and wooden planks “: When the flood water comes and these densely built shacks collapse, the floating debris from these shacks, particularly timber and plastic will interfere with smooth flow of water and flood water will divert to adjacent settlements that would otherwise have been out of danger.

5.4.3 Vulnerability of inhabitants to floods

By definition, the socioeconomic status of the inhabitants of informal settlements is mainly low, coupled with poor housing and sanitation. With these attributes, their resilience and coping capacity to a flood hazard is extremely low, making them very vulnerable. Related to vulnerability of informal settlements to floods, *Martine and Guzman (2002)* carried out a study on impact of Hurricane Mitch in relation to population, poverty and vulnerability of inhabitants of different settlements and revealed the following findings:

- The highest number of the missing and dead were found to be from informal settlements.
- The informal settlements housed the least educated and their relative risk of being affected by the Mitch was 80 times higher than those with higher education. This was compounded by lack of information and difficulty in interpreting the available information.
- The population per household was higher in informal settlements because women in these areas were found to have twice as many children as they would like to have due to limited information and resources for birth control.

From these findings, we can conclude that the composition of the population in informal settlements is a valid indicator of vulnerability to flood disasters. Coming back to the definition of informal settlements and the nature of their construction materials, these structures are at risk of being washed away or completely submerged during flooding, rendering the inhabitants homeless. The debris of submerged tin sheeting and floating timber will cause serious injuries to people attempting to escape to higher ground. Moreover, large quantities of floating debris will hamper boat rescue efforts. Again, from the definition of poor sanitation conditions will cause a serious health hazard when sewage material mixes with flood waters. Above all, the general lack of transportation infrastructure within these settlements will hamper rescue and relief efforts.

5.4.4 Imagery as data source

Given the dynamics of informal settlements, their unplanned nature, density and size of the individual shacks, coupled with uncontrolled expansion, mapping of shacks is one of the most challenging tasks. RS imagery is a promising data source for mapping informal settlements, and several studies have been carried out at various levels of abstraction and for different applications, with some focusing on mapping of individual shacks *(e.g. Mason and Fraser, 1998; Ruther et al., 2002)*, others on mapping their extent *(e.g. Hofmann, 2001a; Weber and Puissant, 2003)* and using RS techniques to estimate the population of the people living in informal settlements for evacuation purposes during flooding events *(e.g. Ramala, 2001).* The roles of RS imagery and image analysis in supporting floodplain management in relation to mapping of informal settlements are many and include: (i) beginning with the regional application, the imagery can be used to monitor and control the expansion of informal settlements and their impact on the environment and land cover changes (e.g. deforestation, which, has a big impact on flooding) using relatively coarse resolution imagery like SPOT4; (ii) at the local level, high resolution imagery can be used for actual shack detection and counting to support social services and estimate population of the inhabitants. Moreover, detailed information like quality of housing and accessibility to roads, health facilities, water and sanitation, which are essential attributes for assessing vulnerability can be extracted from imagery of 0.50 m resolution or better and video imagery; and (iii) the imagery can also be used for reconnaissance and response planning during the disaster.

Mason and Fraser (1998) carried out a comprehensive study on image sources for automatic mapping of informal settlements, and one of their principal findings was that the suitable resolution of RS imagery for automatic extraction of individual dwellings in these areas is 0.5 m or better. This study uses QUICKBIRD imagery at 0.61 cm cell resolution, which is just out of the recommended threshold and, therefore, suitable detecting a good percentage of some individual units which are later used as attributes for mapping out the extent of the informal settlements in object oriented image analysis. The other data set used for the same purpose is a

gridded LIDAR DSM at 1.5 m cell resolution. Although it is not suitable for extracting individual shacks, it is sufficient for mapping out the extent of different settlements.

5.4.5 Description of settlement types

Successful automatic extraction of different settlement forms is largely dependant on recognising the characteristics that make them discernable from each other *(Hofmann, 2001a)*. Therefore, the first step is to visually identify the characteristics of different settlement types. From the image (Fig 5-10) the following forms can be seen:

- Well structured big buildings with roofs varying in colour from dark brown to grey and very little vegetation can be seen in the eastern part of the image. The road network in this area is very regular and mainly orthogonal, crowded with cars in many places and has some car parks near the buildings. The buildings are very densely spaced; these characteristics are common to business areas. In this study we call this area *DC*
- In the central part of the image, small crowded buildings with very bright buildings materials can be seen. The average size of the buildings is about 6 m^2 to 15 m^2 and there are no visible access roads inside the built-up area. This area exhibits the characteristics of unplanned settlement and will therefore, be called *DI.*
- Buildings of sizes between 70 m^2 and 200 m^2, built close to each in an orderly manner with good access to the roads, can be seen in the western part of the image. The buildings have very short shadows and there is a good percentage of vegetation cover. There are few or no cars visible on roads. This exhibits the characteristics of a dens residential area and will therefore, be called *DFR*.
- In the southern central part, there is an area dominated by good vegetation cover with very few small bright buildings similar to those found in *dense informal* described above. These characteristics are also found to the immediate south western part of the *dense informal* settlements. Indications are that it is the expansion of informal settlements and for the purpose of this study we call these areas *NI.*
- And in the far north of the image most of the land is bare with scattered grass, this will called *bare land.*

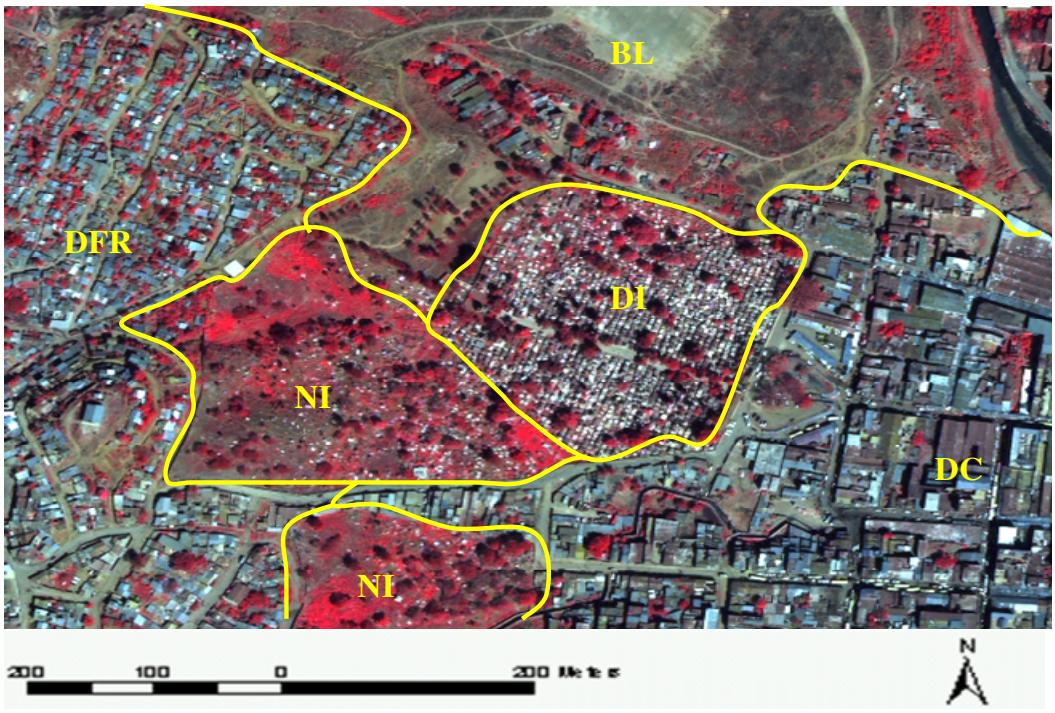

Fig. 5-10 QUICKBIRD false colour composite showing different settlement types: DFR is dense formal residential, NI is new informal, DI is dense informal, DC is dense commercial and is BL is bare land (see section 5.4.5 for description)

5.4.6 Segmentation

Urban settlements are difficult to separate spectrally due to high heterogeneity within settlements and similar characteristics are exhibited across different settlements. Different settlement patterns can be distinguished by the size, form and height texture of the buildings within the settlement. The ratio of vegetation cover is also another important attribute for classifying urban land use. In this study, residential areas have more vegetation cover compared to commercial areas, this attribute will be important for separating commercial areas from residential areas.

Since texture is important for discerning different settlement types, the lowermost level should have very fine segments that would target single shacks, and the highest level should outline the different settlement types. In this case, a scale parameter of 8 was used at the first level and more weighting of 0.6 was assigned to the shape criteria to give a good outlines of single shacks. At the intermediate level, a scale parameter of 25 with same weighing of colour and shape was used to target slightly lager buildings and roads. Then a classification-based segmentation was performed to generate image objects for classification of different settlement types (see Table 5-6) one for all segmentation parameters. For the DSM, only two hierarchical levels were adequate for this type of application. The first level is for extracting roads and building blocks.

5.4.7 QUICKBIRD Classification

In identifying different settlements, the general approach is to extract the general land cover, just like in the extraction of building foot prints (see section 5.2). In this case the first two levels were used for land cover classification. The land cover extracted in the first level is used as an attribute for discerning different settlements types.

Table 5-6: Segmentation parameters

	Segmentation and classification Level	Land cover types	Segmentation parameters				
			Scale Parameter	Homogeneity criterion			
				Colour	Shape	Shape settings	
						Smoothness	Compactness
QUICKBIRD IMAGERY	Level 1	Cars/shacks	8	0.4	0.6	0.5	0.5
	Level 2	Buildings, vegetation roads, shadows / bare land	25	0.4	0.6	0.5	0.5
	Level 3	settlements	Classification based				
DSM	Level 1	Building blocks roads vegetation, bare land	10	1	0	0.5	0.5
	Level2	Settlements	Classification based				

A selective classification approach was used to extract the land cover at levels 1 and 2, using the fuzzy membership function and applying the following conditions:

- Vegetation was separated from other objects using its high reflectance in the infrared channel.
- Roads were separated using their high length/width ratio (in pink, Fig. 5-9a).
- Shacks were separated using their high brightness values and size of not more than $30m^2$. To separate shacks from cars all objects in the group shack that are at least 60% surrounded by roads or bare land class are assigned to cars (in yellow, Fig. 5-9 a).
- All bright roofed objects greater than $30m^2$ with high average length of polygon edges are assigned to grey roofs class. This is done taking into consideration that buildings have a well defined geometry compared non-building objects (in orange, Fig. 5-9 a).
- The conditions for size and geometry used to extract grey roofs and bright shack were also applied to extract brown roofs and shacks (in brown, Fig. 5-9 a).
- All features that did not satisfy the above conditions were assigned to the bare land class (in grey, Fig. 5-9 a).
- The final step is to group the land covers into semantic grouping, and then a classification-based segmentation is performed to generate image objects for the higher level.
- At level 3 (see Fig. 5-11)the first step is to extract roads, since these in most cases serve as boundaries for different settlement types. This is simply done by using the existence of roads in the lower level and this should be more than 200 m^2 to eliminate short irrelevant road segments (in pink, Fig. 5-12b). The bare land and informal settlements are separated from formal settlements by the relative area of road networks. *Dense residential formal* are separated from *dense commercial* using the

size and type of buildings at level 2. *Bare land* (grey Fig 5-12 b), *new informal* (dark red, Fig 5-12), and *dense informal* (red, Fig. 5-12) are separated using the average mean difference to neighbours of sub-objects in the infrared channel, and number of shacks at level 2.

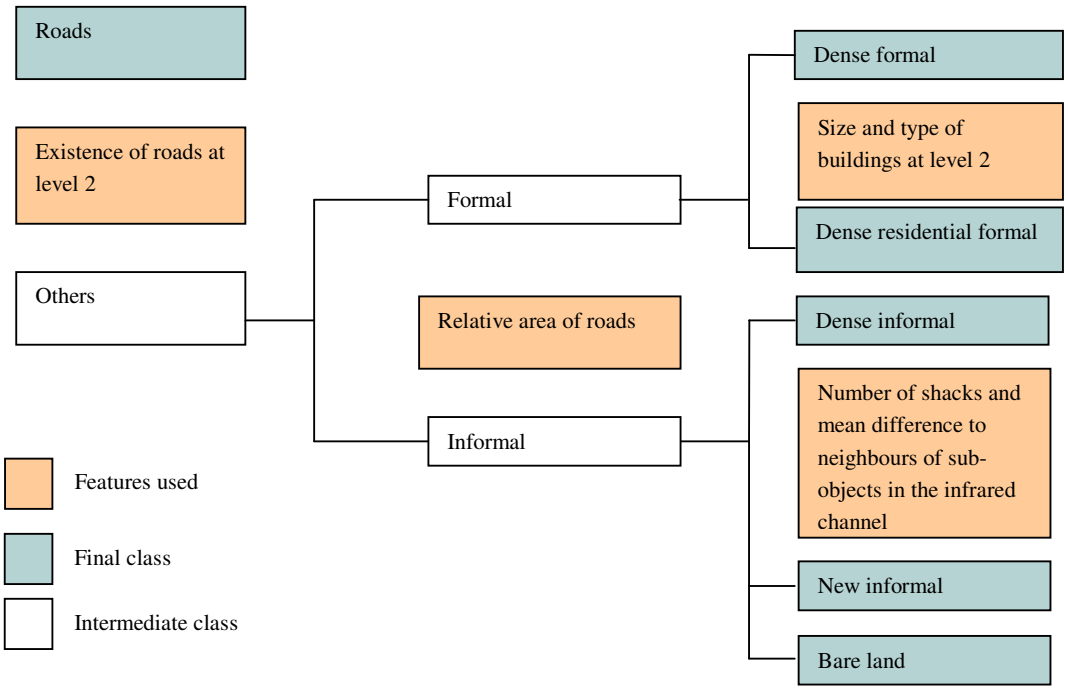

Fig. 5-11: Generalised class hierarch and features used to separate classes at level 3 for QUICKBIRD

In general when discerning settlement patterns, it is important to study the land cover characteristics of each settlement which are later used to for classification of different settlement types at the higher level. For example commercial areas normally have a high average area of buildings as compared to residential areas and therefore, this one of the general attributes that can be used to discern these areas. Moreover, by definition informal settlements normally have few access roads due to their unplanned nature, and therefore, the relative area of roads in these settlements is another general attribute that can be used to discriminate them from each other. Another useful attribute for discerning settlement patterns is the layer value texture based on sub-objects. It describes the typical texture of settlement areas by using *mean of sub-objects standard deviation in the near infrared channel* and the *average mean difference to neighbours of sub-objects in the near infrared channel (*for details see *eCognition, 2004).* This is because the infrared channel is suitable for discriminating the built-up areas from non built-up areas as compared the bands in the visible party of the spectrum.

The above features and conditions worked well to separate different settlement types but there are several other features that can be used within eCognition *(see eCognition, 2004)* and this may vary depending on the area under consideration and image characteristics as you will see that when using the DSM, a different strategy is applied to discern different settlement types. The best way to go about it is to first study the characteristics of target settlements and identify features that are suitable for extracting them.

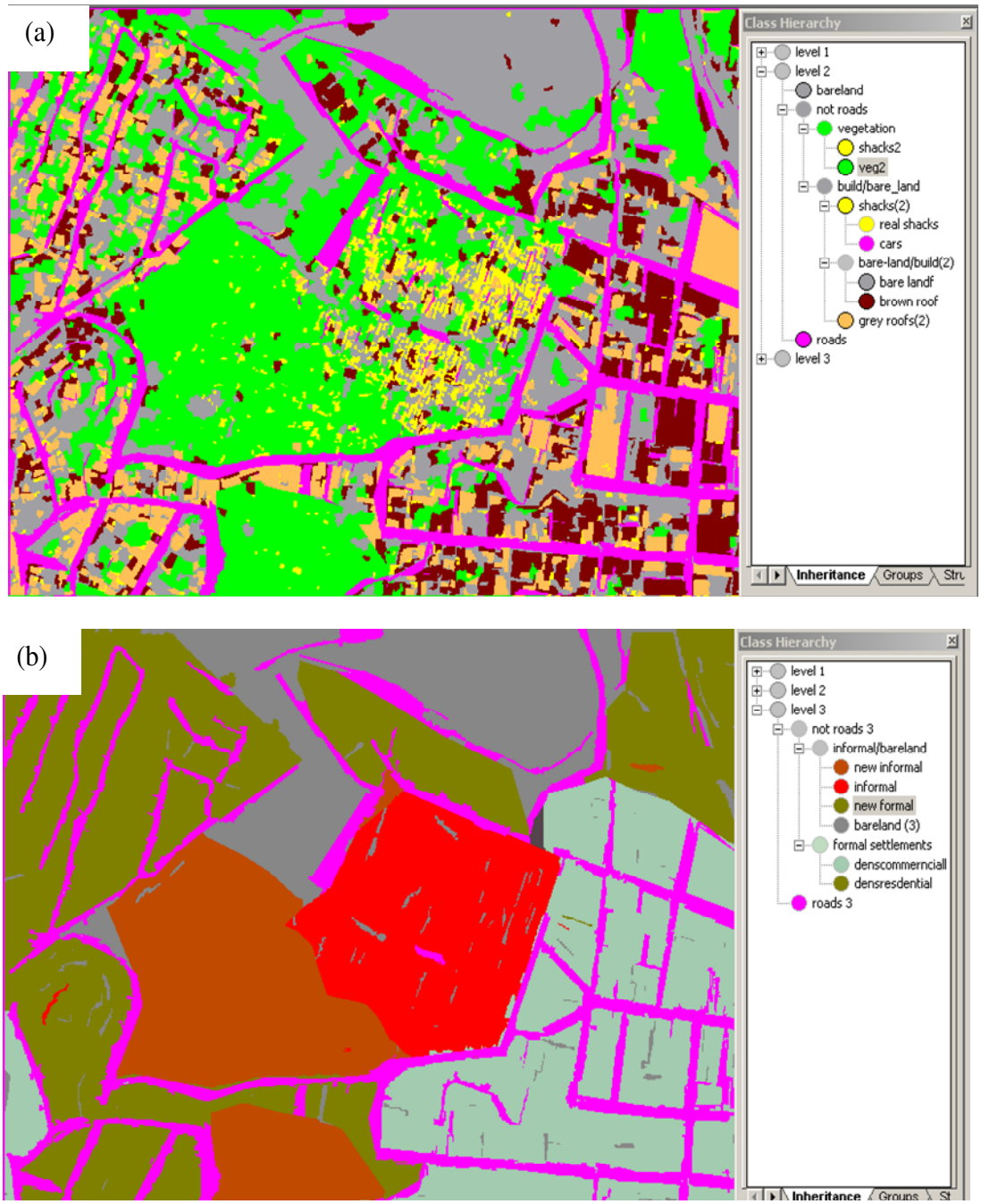

Fig. 5-12: (a) QUICKBIRD classification at level 1&2, and (b) classification result of different settlement types at level 3

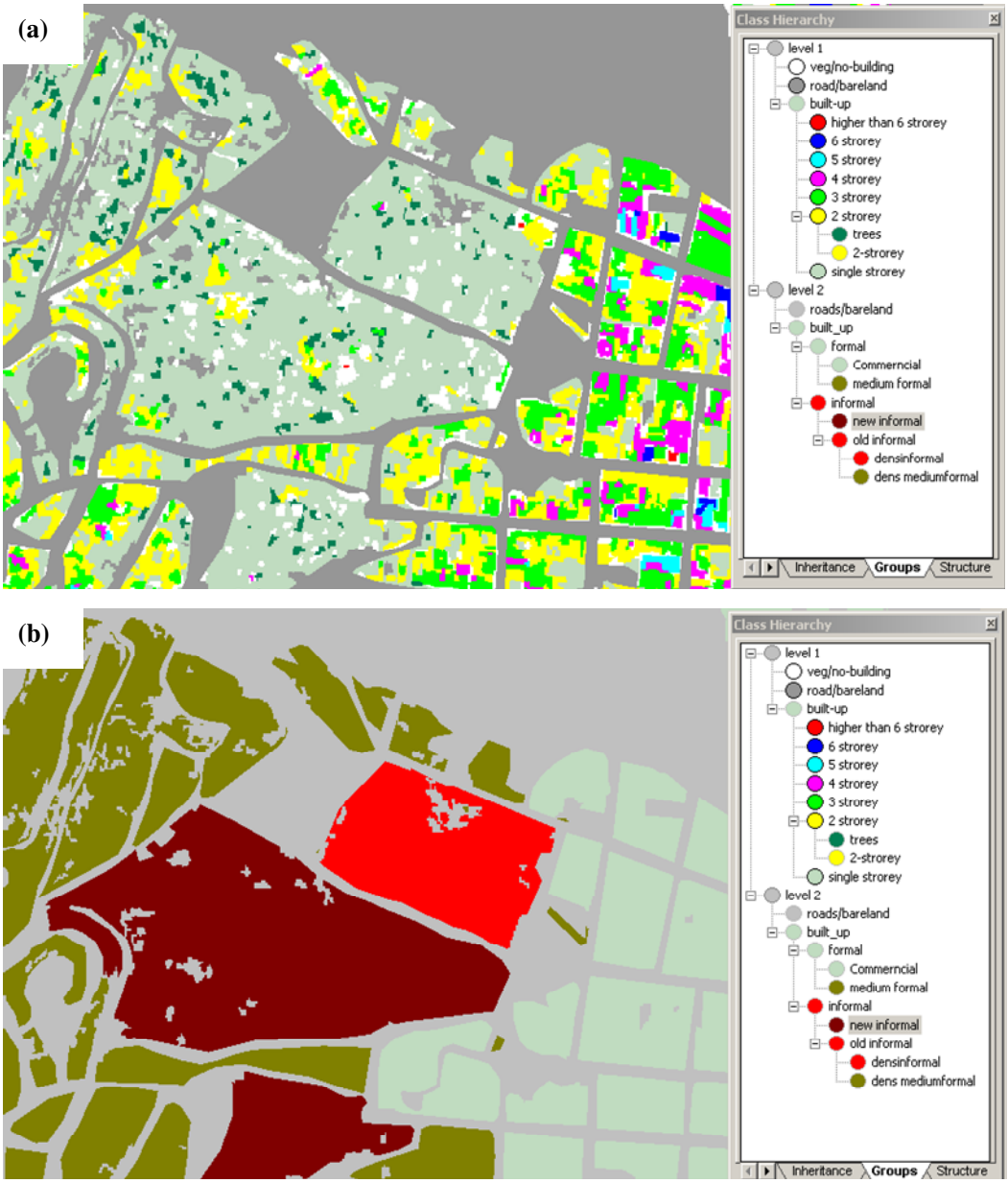

Fig. 5-13 (a) nDSM classification at level 1&2 and (b) classification result of different settlement types

5.4.8 nDSM classification

With a gridded nDSM of 1.5 m resolution, it was not possible to extract individual building foot prints and shacks in level 1 due to high building density and low height, coupled with averaging effects during interpolation (see section 3.3.3). Since our interest is not single buildings but settlement patterns, these data still provided adequate information for extracting roads and subsequently building blocks which are later used for discerning different settlement patterns.

The following approach was used in extracting building blocks and land cover at level l:

- The first step was to separate roads and bare land from built-up areas using height threshold of 2 m (grey Fig 5-13 a).
- Then the built-up candidate regions are classified into meaningful thresholds of 3 m height corresponding to the number of floors. This strategy was also used to estimate number of floors by *Zhang (2003)* where he used 1 m thresholds to eliminate non-building segments. The idea in this case is to identify non building objects like trees that are expected to be heterogeneous at different levels. This is helpful in distinguishing trees from actual shacks in informal settlements since in this case trees were higher than the surrounding shacks.
- The non-building parts were eliminated using the heterogeneity criteria, a texture measure described in section 4.5.4 (for details about texture measures for image classification see *Haralic et al., 1973*). This was applied to likely single-3 storey buildings, which is a range for most tree heights (tree green Fig 5-13a).
- In the informal settlements all those regions that are more than single store buildings and are at least 80% surrounded by their single storey neighbour are assigned to trees class, (see white clusters Fig.5-13 a).

The final step is to perform a classification based segmentation to generate image objects for the higher level.

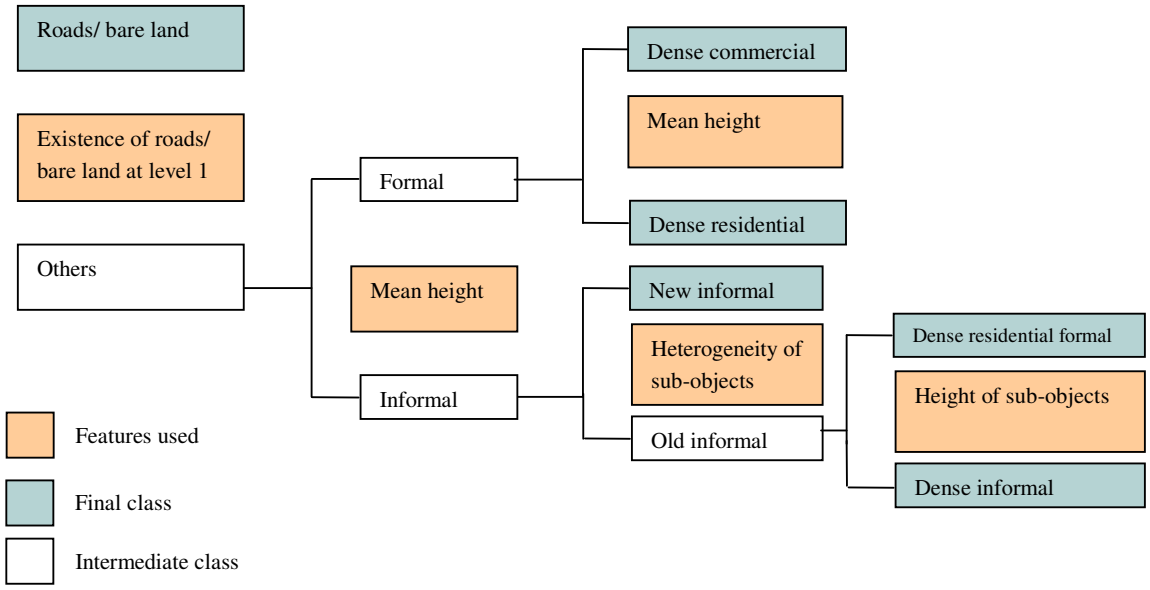

Fig. 5-14 Generalised class hierarch and features used to separate classes at level 2 for LIDAR DSM

At level 2, (see Fig 5-14) just like in the QUICKBIRD classification, the first step is to extract roads/bare land using the existence of roads/bare land in the lower class. The built-up area is split into *formal* and *informal* using the mean height threshold of image objects. But this resulted in part of the *dense residential formal,* and *new informal* and *dense informal* lying in the same class these were separated as follows: the *new informal* was separated using the high existence of vegetation in the lower level, the *dense residential formal* was separated from *dense informal* using its high mean height of sub-objects, since in most cases and by definition of informal settlements, the average height of buildings in the formal settlements is expected to be higher than in the informal settlements. The other part of the *dense residential formal*

area went to formal settlements class due to the presence of high rise apartment buildings in that section. However, the height of sub-objects in the commercial areas is generally more homogenous than in residential areas and therefore this attribute was used to separate *dense commercial* from *dense residential formal.*

The results from the two data sets are correlated, which is a good indicator for interchangeability for the two data sets to extract different settlement types (difference image in (Fig 5-12). Apart from *A, B*, and *C,* which were classified differently in the two image due to use of different classification attributes, the rest of the green patches are bare land patches which were well handled in the nDSM classification. In the QUICKBIRD classification bare-land classes within the settlements blocks were eliminated using neighbourhood relations. The size and density of shacks, with average size between 6 m^2 and 15 m^2, limited the ability of the available data sources to extract individual foot prints. With the gridded LIDAR nDSM with 1.5 m resolution it was not possible to extract individual foot prints due to the low height and high density of the building in residential areas, as a result the interpolation in producing the gridded averaged out the narrow spaces between buildings, making it difficult to separate individual buildings. On the contrary, the high vegetation coverage also brought difficulties in extracting these individual shacks from the QUICKBIRD imagery. However visual inspection shows good potential for the imagery to extract these features, as a good percentage of the individual shacks are extracted (see Fig 5-10a), though we cannot evaluate this quantitatively because it is very difficult to digitize individual shacks from the imagery of limited resolution.

The other indications are that the methods would perform better using the QUICKBIRD in most cities because generally informal settlements have an average shack size varying between 15 m^2 and 30 m^2 *(see Mason and Fraser, 1998; Weber and Puissant, 2003).* From the LIDAR the better alternative would be the multi-return pulse data, not the gridded data used in this case, in which case it would be possible to identify individual shacks

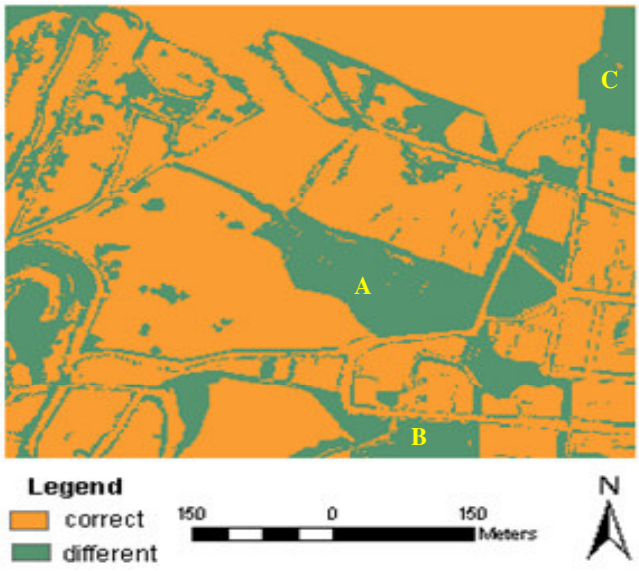

Fig. 5-15: Difference image of the classification results from the the two images, A, was classified as *DI* in QUICKBIRD in image, and *NI* in LIDAR nDSM, B was classified as *DC in* QUICKBIRD while in LIDAR it was classified as *DR,* and *C* is classified *DRF* in the QUICKBIRD and as *BL* in LIDAR.

5.5 Extraction of land covers from medium resolution imagery

High resolution imagery provide fine details that are ideal for generating inputs to flood risk models *(Smith et al., 2004; van der Sande et al., 2003).* However, the cost of acquiring high resolution imagery is very high, especially for developing countries with remitted financial resources. Consequently, it is difficult to produce regular updates of land cover changes that are essential for modelling the dynamics of flood hazard dynamics. Moreover, flooding is not just monitored at a local level, but requires information about the upper and lower catchments of the river network, which would require a number of scenes to cover with high resolution imagery. Flood related studies that are carried out at a more regional or national level mainly employ medium to low resolution RS imagery(e.g. Landsat, ASTER or Modis) to take advantage of extensive coverage and low cost provided by these imagery *(e.g. du Plessis et al., 1999; Nirupama and Simonovic, 2002; Zhang et al., 2002a)* as compared to high resolution IKONOS or QUICKBIRD.

In order to explore the amount of information that can be extracted from readily available medium resolution imagery, this study used a degraded QUICKBIRD imagery at 15 m resolution, Landsat ETM imagery enhanced with PAN band at 15 m resolution, and Landsat ETM imagery at 28.50 m resolution to extract land covers (health trees/grass, trees/shrubs, heavily built-up, and lightly built-up/bare land and river). The 15 m resolution imagery was classified at two hierarchical levels while the 30 m resolution imagery was processed only at one level. More details are given in the subsequent sections.

5.5.1 Land cover classification

The first step was to segment the image into homogeneous objects, and in this case more weight was given to spectral information (0.7) than shape (0.3) in the segmentation parameter setting (see section 4.5 on segmentation parameters). This was done to clearly discern the vegetated areas. The classification for the three images was carried out as follows:

At level 1 of the degraded QUICKBIRD imagery, vegetation was separated using its high reflectance in the near infrared channel, and trees/shrubs were separated from grass and very healthy trees by using high reflectance in the near infrared channel for grass as compared to un-health trees. The river was discerned using the high standard deviation in the infrared channel, or high length/width ratio. The heavily built-up areas had the lowest reflectance in the near infrared channel and the rest was lightly built-up and bare land, which had medium reflectance in the near infrared channel. The information in other bands could not be used to clearly discriminate different classes. Then classification-based segmentation was carried out to generate image objects for level 2, where size, form and context was used to refine the classification.

The classification approach of the enhanced Landsat ETM image is more or less similar to the one explained above. The major difference was that in this case there was additional channel near infrared channel 5, which was used for discerning the river. Then, as above, a classification-based segmentation was used to create image objects for level 2 and then form and context was to refine the classification.

5.5.2 Accuracy assessment

For the 30 m resolution Landsat imagery, the river could not be extracted since it has a limited width of about 14 m, which cannot be extracted at this resolution. The other classes were extracted using the near infrared channels as above but using only a single level. The classified images are shown in Fig. 5-15. The accuracy assessment was conducted based on 256 randomly generated points in ERDAS IMAGINE and the original QUICKBIRD image. These random points were used to assess the accuracy all the three images and the summary of accuracy from an error matrix given in Table 5-7. Both visual comparison and the accuracy report of the classified images indicate that the degraded QUICKBIRD imagery had the highest accuracy compared to the other two images. Some of the contributing reasons to this discrepancy even with the enhanced Landsat ETM of the same resolution are:

- The degraded QUICKBIRD image used pure pixels from the higher resolution imagery. Since the nearest neighbour interpolation method was used during down sampling of the image, the degraded image still had stable pixel values which closely approximate the extent of land covers depicted in the original high resolution image. While in the enhanced image the PCS fusion method distorts the multi-spectral information contained in the original image, which reduces the spectral separation of the land cover to be classified. The spectral distortion can be seen on the grass and trees (Fig 5-13), where the original multi-spectral image at 28.50 m resolution has more correlated results to the degraded QUICKBIRD image as compared to the enhanced image. Moreover, the original ground sampling of the multi-spectral Landsat image is 28.50 m and it cannot be recreated even if the spatial resolution is enhanced. Also the georeferencing errors affect the classification result.

Table 5-7: Summary of the accuracy assessment results for the three images

Class name	**Degraded QUICKBIRD**		**Enhanced Landsat**		**30 m resln. Landsat**	
	Prod. Acc.	User Acc.	Prod. Acc.	User Acc.	Prod. Acc.	User Acc.
Heavily built-up	92.24%	95.54%	73.96%	93.42%	67.06%	96.61%
Built-up /bare land	86.36%	87.69%	92.11%	77.78%	97.62%	71.30%
Grass/health-veg.	90.48%	82.61%	93.75%	68.18%	50.00%	83.33%
Trees	87.76%	87.76%	58.33%	87.50%	80.00%	84.21%
River	100.00%	66.67%	60.00%	75.00%		
Overall accuracy	**90%**		**82%**		**80%**	
Kappa statistics	**0.85**		**0.71**		**0.68**	

- The other reason is that the 33 month gap between the acquisition dates of the two images is quite large for an active urban area, because changes could have taken place to the landscape, which has an influence on the classification results. In addition, the Landsat image was acquired on 31st March 2000, one month before the rainy season, while the QUICKBIRD image was acquired on 31st December 2002, two months after the rainy season. These seasonal variations have an influence especially on vegetation cover, which translates into differences in classification results.
- As for the multi-spectral 28.50 m resolution Landsat ETM image, the spatial resolution was too low, which resulted in small isolated land covers being generalised due to mixed

land covers within one pixel. The effect of low resolution was more evident on the river which was completely eliminated due to limited average width of about 14 m.

However the overall land cover pattern in all the classified images was well depicted and indicates good potential for use to generate roughness values required for input to flood hazard models at a more regional level. Moreover, low resolution images such ASTER and MODIS are already widely used for this purpose in many studies *(e.g. Zhang et al., 2002a).*

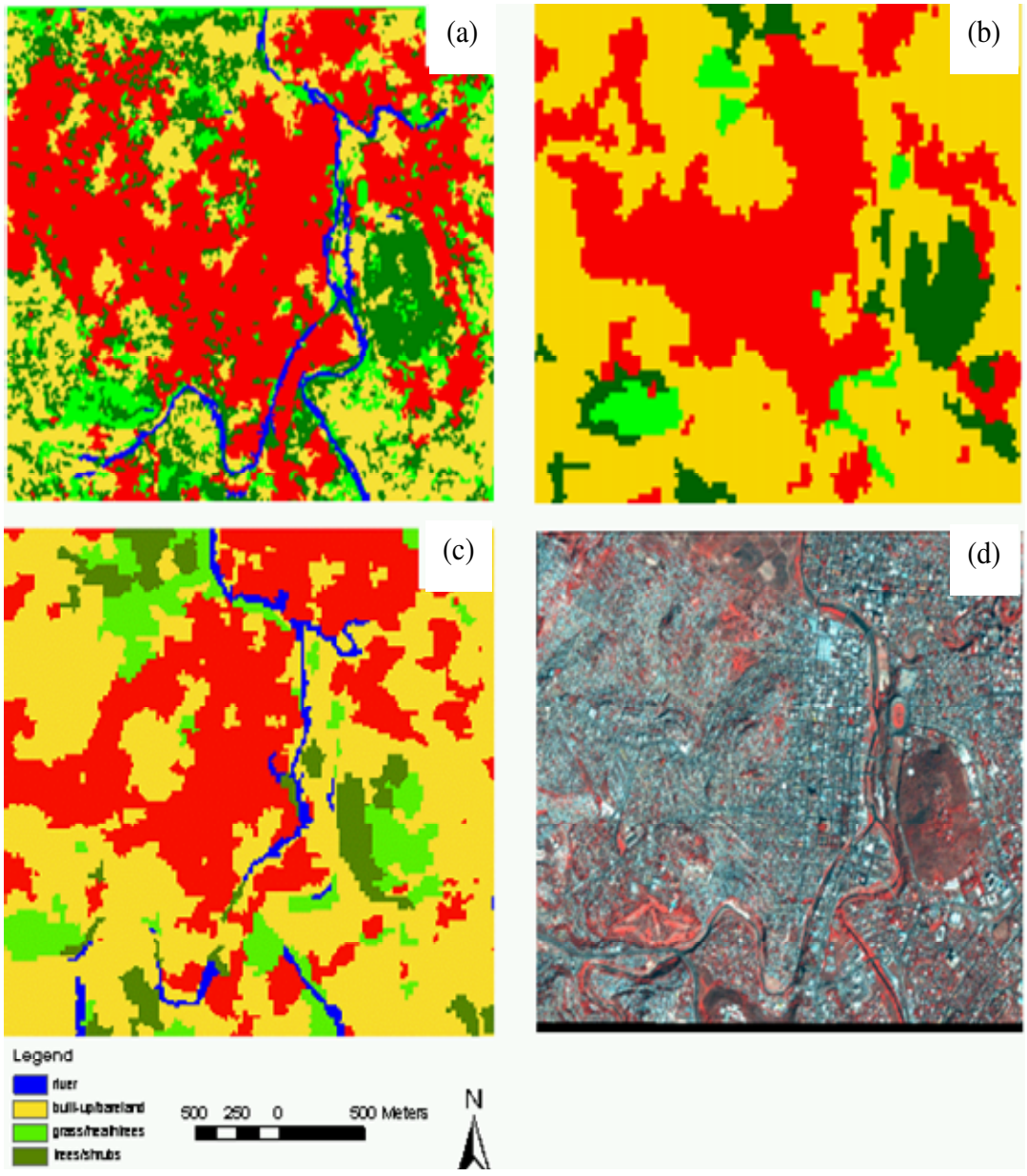

Fig. 5-16: showing the classified results, (a) is from the degraded QUICKBIRD imagery, (b) the Landsat image at 30 m resolution, (c) is the is from enhanced Landsat imagery, and (d) in the original QUICKBIRD imagery

6 Discussion

6.1 Introduction

The main objective of this study was to extract flood risk-related base-data from multi-source remote sensing imagery and investigate the interchangeability of the data sets for the purpose. Chapter 2 described the flood risk model input requirements, and in chapter 5 a series of base-data sets were extracted from the available imagery. In this chapter the methodological approach and results obtained will be discussed in relation to: (i) flood hazard models input requirements, (ii) vulnerability model input requirements, and (iii) applicability to developing countries in relation to cost implications.

6.2 Methodological approach

Three generic software tools have been integrated at various stages of image analysis to a form a powerful tool as proposed in the first objective. ERDAS imagine was mainly used for pre-processing (co-registering, sub-setting, image fusion, etc.) and post classification quality assessment of land cover maps.

eCognition was used for segmenting the image to form image objects for use in the subsequent classification (see section 4.5). During classification several tools available within eCognition were used to incorporate attributes such as spectral values, form, size, context, and texture and class hierarch to handle complex classification tasks. Even after using a combination of different tools to perform the classification it still remains difficult to separate homogeneous urban objects such as paved roads, roofs and car parks. Although accuracy assessment operations are available in eCognition, they were not used in this case because they require a thematic reference map with similar classes, which was not available for this study.

The major limitation in eCognition version 3.0 software was that it could not handle large images due to memory problems. The problems were experienced during the segmentation process because the created image objects are stored in the internal memory. Therefore, when segmenting large image, the computations took much time and in many instances terminated without a result due to memory problems. The same problem was experienced when incorporating texture measures in the classification. In this case classification tasks could take as long as 60 minutes and sometimes terminated pre-maturely without a result. Then it was decided to process only small representative portions of the image. However, the software vendor promises that the new software version has proper handling of this memory problem.

ArcGIS was mainly used for digitizing reference data accuracy assessment for building footprints (section 5.1.6), generating post classification maps (e.g Fig 5-8), and performing computations like floor space area as to generate useful summary graphs (Fig 5-9).

The integration of the softwares worked well for this study, but this may be very costly and beyond reach of most developing countries. The idea was to demonstrate some useful tools that are scattered in various software packages, which when integrated can produce products beyond the capabilities of single software. The other reason for such an approach is to expose possibilities that are available in other software packages, so that some operations that are not

available locally can be outsourced to specialised companies, which is usually cheaper. The current geoinformation market trend encourages out sourcing of services that are not core to the organisation rather than a centralised approach where an organisation has all the software including those that are not used frequently, which is very costly.

The other alternative to deal with the cost issue is manual on screen digitising from imagery, which could be useful for extracting most of the base-data discussed in this study in a single software like ERDAS, which has capabilities for: pre-processing, digitising, producing basic maps, accuracy assessment, and automatic classification operations but mainly suitable for low to medium resolution imagery.

6.3 Flood hazard model input requirements

6.3.1 Digital elevation model

An accurate representation of the terrain is the principal requirement for all flood hazard models, since the model results are primarily dependant on it. When we talk of interchangeability of QUICKBIRD imagery (non- stereo) and LIDAR DSM, in this respect LIDAR DSM has an advantage, since it gives an accurate representation of the terrain and topographic objects. The modellers have a choice of whether to represent the buildings as solid blocks with their true heights or filter out the buildings and represent them as partial solids by assigning high roughness values. In both cases it is expected to give more accurate results since it gives a better representation of terrain as compared to combining data sets from different sources, at different levels of accuracy, and probably referenced to different datums. However, LIDAR data are rarely available and the cost involved in acquiring them, is too high for most municipalities in developing countries. On the contrary, most municipalities do have topographic maps and aerial photographs from which DTMs can be derived.

Considering the fact that DTMs are one of the most stable data sets over time, with changes typically confined to human construction activities (e.g. dams, quarries, roads, buildings, etc.) and natural process such as surface erosion and landslides *(Tempfli, 2004)*, combining such DTMs with updated land covers from other high resolution imagery such QUICKBIRD can provide very useful updated information required for modelling. The elevation information on the constructed facilities is normally available at the departments responsible for construction, regulation or maintenance of such facilities. These data sets can be combined to create high resolution DSMs *(e.g. Tennakoo, 2004)*. The other areas affected by natural processes could be filled in by spot heights using field methods, which can turn out to be cheaper than a LIDAR survey or complete field survey. To illustrate this, a DSM created from a contour map (Table 3-1) was combined with a land cover map and buildings were given an assumed constant height value (Fig 6-1). In a typical case where sufficient ground knowledge about land use is available or where elevation information is available at the municipality, more appropriate heights could be assigned to give a more reliable DSM. For other modelling cases where buildings are represented by high roughness values, only the planimetric position of the buildings would be more important.

However, care must be taken when assembling different data to form a DSM. The accuracy of the data sets (e.g. land cover) is very crucial, for example in this case, where there is confusion between roads and building foot prints (section 5.2) during classification.

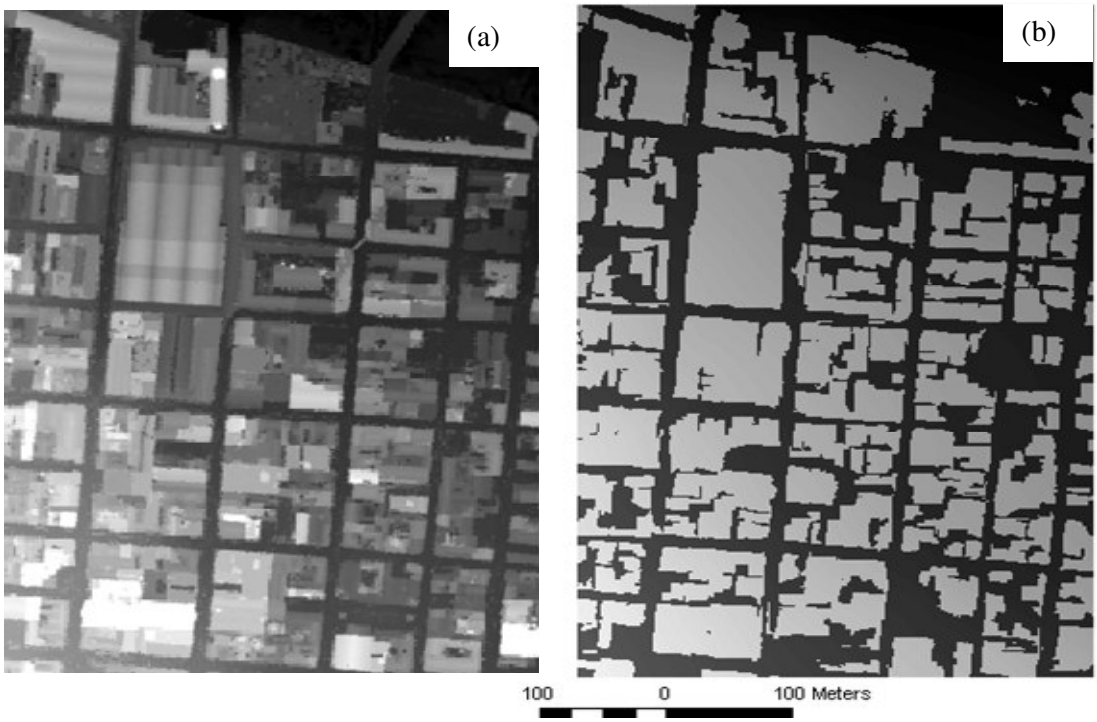

Fig. 6-1: Original LIDAR DSM (a) and contour DEM with simulated building heights from a QUICKBIRD derived land cover map (b)

These two classes have very different effects on the flow of water. Normally flood water conveys along the roadways and buildings act as constriction to flow, so if part of the road is misclassified as building, then water flow will be blocked at that portion of the road while in reality it is supposed to flow at high velocity and vice versa. Such classification errors can cause very serious implications on the modeling results and the best approach is to carefully study the accuracy of the different data sets. In this case a detailed analysis of the error matrix to identify confused classes is a requirement, and then misclassified portions should be corrected by manual methods if not possible by automatic methods. The same applies to data sets that may be collected from different sources. It is imperative that they are checked for consistency and correctness to assure the integrity of the assembled DSM for application to flood modeling.

If applied correctly, then DSM assembled using a land cover or land use map from QUICKBIRD imagery, and a large scale contour map can give a more reliable representation of terrain close to what we have from LIDAR DSM, which would satisfy the objective of the interchangeability of the two data sets to offer such a product.

The major limitation of all DSMs created from RS methods is that they give a representation of the terrain as seen from the sky, while what is important for water flow is the terrain as seen on the earth surface. For example areas covered by fly-over bridges and tress will show high elevation values, that can block water flow in the model, while in reality water will still flow under those objects. Therefore, in order to have terrain representation that can simulate real water flow, modelers should correct for such structures in their data sets. Field survey methods are ideal for producing a DSM that can accurately represent the terrain on the surface as required by water flow. However, these methods require more time and skilled manpower

to collect data over extensive areas required for flood modeling. Consequently, the cost of producing such a DSM is beyond the budget allocation for such project in developing countries. Moreover, due to extensive memory and computation time required for processing high resolution DSMs in flood models most modeling projects are performed at 5 m resolution or higher, which degrade the accuracy of the expensively generated DSM. Therefore, even with the aforementioned limitations RS methods offer better cost effective option that can satisfy modeling requirements with little correction and ground truthing in critical areas.

6.3.2 Land cover

Apart from the DSM which gives the topography of the area, there are other factors that control the flow of water such as the cross section area of the water boundary area, the wetted perimeter boundary layer and coefficient of roughness *(Smith et al., 2004)*. The coefficient of roughness also known as Manning roughness coefficient represents hydraulic roughness, which develops resistance to water flow through a retarding force. The roughness controls overland velocity and flood plain flow rates *(De Roo, 1999)*. Different land cover types have different roughness values. Consequently, a land cover map, from which these roughness values are derived, is an important attribute for flood hazard modelling. The accuracy and resolution of these land covers is more crucial in urban areas where land cover is more heterogeneous as compared to rural areas. To illustrate this, two sets of land cover maps were generated, one for detailed urban modelling (section 5.2) and the other for coarse modelling (section 5.5).

In urban areas a detailed land cover map like the one generated in section 5.2 is ideal. For proper representation of heterogeneous land covers, other than QUICKBIRD, imagery of at least 5 m resolution or better could be used. A resolution coarser than this will increase the problem of mixed pixels, which can lead to confusion in assigning roughness values. Just like in the case of assembling DSMs above, misclassification errors can have serious consequences on the modelling results. For example the confusion of bare land for building foot prints will result in assigning wrong roughness values for these classes, which will lead to underestimation or overestimation of overland flow velocity. Again, careful interpretation of quality measures like the error matrix is critical to be aware of the certainty of the assigned roughness values.

Just like in the case of DSMs, land cover maps generated from RS imagery also have a limitation of presenting information as seen from the sky as opposed to what exist on the surface where the water flows. Therefore, when assigning roughness values in difficult areas such as forests and recreational parks, modellers should always bear in mind that the situation on the ground is different. Such areas needs field verification and detailed ground sampling. The ideal method is to map the entire areas using field survey methods but it can be very costly to cover extensive areas required for flood modelling. The RS generated land cover maps offer a cost effective option since most land cover types can be extracted quickly and critical areas can identified from these maps for more refined field verification.

As regards interchangeability of LIDAR DSM and QUICKBIRD imagery to extract urban land cover maps, QUICKBIRD imagery has an advantage over a LIDAR DSM, since a proper land cover classification is partly dependant on the proper interpretation of the image by the operator. But it is difficult to interpret a LIDAR DSM without additional multi-spectral information, which might lead to misinterpretation of trees for buildings or canals for roads.

However, texture analysis of the nDSM enables reasonable discrimination of trees from buildings as demonstrated in section 5.3 (Fig. 5-7), but these are not the only covers of importance. It would be still difficult to distinguish grass loans from bare land or car parks which have very different roughness values. Nevertheless, some modern laser scan systems incorporate capabilities for capturing multi-spectral information, which will in future increase the potential for interchangeability of the two data sets to extract land covers.

Urban areas are not modelled in isolation; for complete modelling it is important to have a synoptic view of the lower and upper catchments area which requires extraction of land covers on very extensive areas. In such cases use of high resolution imagery such as QUICKBIRD is not feasible due to high cost involved in acquiring them. Section 5.5 illustrated this, by extracting lower resolution land covers from degraded QUICKBIRD at 15 m resolution, Landsat ETM image enhanced with panchromatic band to 15 m resolution and a multi-spectral landsat ETM image at 28.50 m resolution. The results obtained showed a good impression of the overall land cover pattern. Typically, land covers in rural areas are more homogenous than in urban areas, which make it relatively easier to extract them. But for more reliable modelling results the classification results should be treated with caution just as in the urban case, as classification errors will result in wrong assignment of roughness values which will affect model flow results.

Apart from extracting regional land covers, readily available lower resolution imagery is useful for frequent monitoring of land use changes in urban areas, such as the expansion of built up areas. If a significant change is discovered as to affect flood flow pattern, then results from lower resolution imagery can be used as basis for another updating cycle using high resolution imagery.

The extracted land covers showed a good potential of interchangeability of different image sources at that lower resolution. Even the land cover 28.50 m resolution, which had the river missing due to limited narrow width still had good representation of other land covers comparable to imagery at 15 m resolution. The importance of investigating the interchangeability of different image sources was even made stronger during this part of the research. A search for ASTER imagery of the area of interest from the NASA website revealed that there was no cloud free image from the year 2000 to date. Since these images are acquired by satellites that follow different orbital paths with different repeat cycles, it is important to investigate the interchangeabilty of the data sets to provide the required base-data in case the other satellite passes the area of interest during unfavourable conditions.

6.3.3 Informal settlements

Typically many of the settlements on the floodplains of developing countries take the form of informal settlements, which have a strong influence on flood overland flow. Settling on river banks, flood plains, unstable hills and steep slopes has effects on the sediment load into the river network and some permeable surfaces in the flood plain are converted to impermeable, which all together increases the flood extent during flooding events, making a relatively larger community vulnerable. The interference with forests and water catchments also causes an increase in erosion and impermeability, which has great influence on the magnitude of the flooding. Another look at the first definition “use of poor construction materials such as plastic, tin sheeting and wooden planks “: When the flood water comes and these densely built shacks collapse, the floating debris from these shacks, particularly timber and plastic will

interfere with smooth flow of water and flood water will divert to adjacent settlements that would otherwise have been out of danger. Subsequently, mapping of informal settlement is indeed an integral part of flood risk management. This is one of the necessary input base-data sets for flood hazard modelling. While there is usually information about construction plans about other settlement types, detailing the location of settlements and roads, available in municipalities, the informal settlements are always largely unmapped, making it more difficult to manage them. Information gathered by remote sensing regarding the extent and impact of informal settlements on the environment can be useful flood hazard management. Their characteristic of quick expansion is of great importance considering the dynamics they bring to the flooding situation by transforming the flow regimes. Though we used very high resolution imagery to map their extent in this research, it is possible to map their coarse extent from medium resolution imagery such as SPOT and ASTER due to their unique texture of dense small shacks. However, mapping the individual shacks is still difficult even from high resolution imagery. Even to map them using field survey methods is still a difficult task due to their unplanned nature and the ever changing structures of individual shacks and overall extent. The best approach is to combine high resolution RS imagery with field methods.

Investigating the interchangeabilty of different data sources to map them other than the ones used in this study is a topic which needs further exploration. Just like in any other land cover or land use mapping the level of accuracy and captured detail will reduce with a decrease in resolution. The summary of interchangeabilty of inputs is given in Table 6-1.

Table 6-1: Summary of LIDAR DSM/QUICKBIRD interchangeability

Inputs	Imagery	
	LIDAR DSM	QUICKBIRD
Building footprints	Good	Good
Building heights	Good	Fair
Settlements	Good	Good
Land cover	Fair	Good
River networks	Good	Good

6.4 Vulnerability modelling input requirements

6.4.1 Building footprints

In sections 5.1.4 and 5.1.5 building foot prints were extracted from LIDAR DSM and QUICKBIRD imagery at accuracies of 89% and 84%, respectively. When estimating losses to building infrastructure and the economic losses in terms of business disruption, it is important to have accurate maps of building foot prints in terms of position and area. When using building footprints data for damage assessment, the global accuracy values as stated above should be treated with caution. It is more important to critically analyse accuracy measures like the miss factor or the number of false negatives (section 5.1.6), and the branching factor or the degree to which the automatic extraction system has over-classified building background pixels as building pixels. These quality measures can give an indication of the degree of overestimating or underestimating of the damage.

If we consider an area where there are no high-rise buildings, the interchangeability of the two imagery sources is very good. But if there are high-rise buildings, a DSM has an advantage since a more accurate estimation of number of floors and total loss can be calculated (see section 5.3). However, some studies have estimated heights of building from single optical high resolution RS imagery using the geometric relationship of the shadow length, building height and sun angle at the date and time of image acquisition *(e.g. Hui et al., 2004; RSCC, 2005).* The studies reported successful height estimates with approximately 2 m accuracy. However, methods based on shadow analysis to estimate height can only be employed successfully if at least the buildings are well separated from each other so that their shadows are clearly visible without much overlapping. Such a method can have limited success in a crowded city like Tegucigalpa. Consequently, the interchangeabilty LIDAR DSM and QUICKBIRD in terms of height in Table 6-1 only refers to a situation were buildings are well separated from each other.

Even using a LIDAR nDSM data alone for building height and foot prints has been found to not be sufficient due to difficulties encountered in removing trees that can be mistaken for buildings and result in overestimation. Other studies have incorporated high resolution imagery such as IKONOS and QUICKBIRD to calculate NDVI and filter to out vegetation from LIDAR data *(van Westen and Montoya, 2004; Zhang, 2003).* These high resolution images are difficult to have at the same time especially for developing countries with limited resources. In section 5.3 this study has demonstrated that texture measures can significantly aid in discerning vegetation from buildings. This can reduce the need to fuse high resolution multi-spectral imagery and LIDAR data.

6.4.2 Building use

Building use is another important attribute for risk assessment. Considering the mixed nature of building use patterns common to most urban areas and the level of detail required for risk assessment, it is not possible to extract all the required information from RS imagery alone. However, many municipalities maintain cadastres, which also incorporate information on building use for revenue collection purposes. To be more versatile, such cadastres could also include information on the number of floors. The combination of cadastral base-data and RS derived data could generate more complete products useful for comprehensive risk assessment. Moreover detailed building use information could assist in estimating day time population for facilities such as schools, hospitals, workplaces and industries, especially when assessing flash flood risk. Such information is also important in estimating disruption to social services and business losses.

Therefore, RS imagery should not be treated as the source of information related to risk, but also as complimentary information, which should be combined with existing data. This also calls for transformation of the available data, such as cadastral information system to common coordinate systems, so that they can easily be integrated with new data collection methods such GPS and RS, and GIS for analysis.

6.4.3 Building materials

The major limitation of RS imagery used in this study was that it was not possible to explicitly extract information on building materials that are very important for vulnerability analysis. However, where sufficient ground data is available, it is possible to infer information on building material from their spectral properties. Since urban residential areas are normally built in homogeneous blocks, the blocks, and area and position of individual buildings within the blocks can be mapped using high resolution imagery, and field data on a few buildings

within the block can be used to generalise the whole block with a minimum loss of accuracy on overall results. For example buildings of a certain roof pattern or colour can be related to their use or the year in which they were constructed if ground knowledge is available. The height of the building can also be used to indirectly derive information on the strength of the building materials since high-rise buildings are likely to have stronger construction material as compared to single storey buildings making them more resistant to floods.

6.4.4 Informal settlements

A good example of the inputs derived in this study, from which information on construction materials and the social status of the people who live there can be derived, are settlement types (section 5.4). By definition, the socioeconomic status of the inhabitants of informal settlements is mainly low, coupled with poor housing and sanitation. With these attributes, their resilience and coping capacity to a flood hazard is extremely low, making them very vulnerable. A more detailed discussion of vulnerability of these settlements to flooding was given in section 5.4.3. By the nature of their construction materials, these structures are at risk of being washed away or completely submerged during flooding, rendering the inhabitants homeless. The debris of submerged tin sheeting and floating timber will cause serious injuries to people attempting to escape to higher ground. Moreover, large quantities of floating debris will hamper boat rescue efforts. Again, from the definition of poor sanitation conditions will cause a serious health hazard when sewage material mixes with flood waters. Above all, the general lack of transportation infrastructure within these settlements will hamper rescue and relief efforts.

Several studies have suggested provision of alternative shelter and a culture of prevention as a solution to this problem (e.g. IDNDR, 1999; Martine and Guzman, 2002). But this problem presents both technical and political difficulties. As Annan (1999) puts it, the problem of relocation has high short term costs, while the benefits lie in the distant future, which makes it difficult to convince decision makers to invest in such a venture. From this background it is eminent that this will continue to haunt disaster managers and planners alike in developing countries. With difficulties it presents in data collection, the RS methods enriched with newly launched high resolution satellite imagery presents the solution to provide the much needed information at a variety of scales. One promising RS technique for capturing information on building materials are video imagery, either from low flying aircraft or moving vehicle and geo-referenced using GPS *(du Plessis et al., 1999; Montoya, 2002).* These images if combined with high resolution imagery can significantly reduce the need for field methods and in turn lead to substantial cost serving and improve the speed of data collection.

6.5 Cost and applicability to developing countries

Risk assessment for the purpose of disaster mitigation is an expensive venture, which requires a detailed survey on the elements at risk. For an objective quantitative risk assessment, detailed information on population (age, heath status, etc.), building inventory (height, materials, size, use, contents, age, etc.), and other infrastructure should be gathered. In addition, these data must be geo-referenced for them to be used together. The traditional method of collecting these data is by ground survey methods, which are labour intensive and cost ineffective. With high resolutions of up to a few centimetres that allow analysis of elements at risk at a local scale, aerial photographs have been used as a compliment for field methods. Recently, high resolution satellite imagery such as QUICKBIRD and IKONOS, which can capture spatial detail close to aerial photography, has come on the market.

Comparing the cost effectiveness of high resolution RS imagery against aerial photography especially in developing countries, where specialised aircraft needed to acquire aerial photos are not available, is a difficult task as it depends on: the product (e.g. panchromatic, multi-spectral), scale/resolution, area of interest, time frame within which images are required, aerial traffic restrictions etc. *(Bauer, 2002)*. However, after all considerations the following aspects can make high resolution RS imagery more cost effective for developing countries as compared to aerial photographs:

(i.) Film processing and aircraft related cost are avoided with satellite imagery
(ii.) Time saving in terms of hiring aircraft and processing air traffic clearance permit, which are not needed for RS imagery
(iii.) Aerial photographs are often expensive in digital, mosaiced and orthorectified formats that are useful for GIS applications, while RS imagery are usually available in digital georeferenced formats.
(iv.) RS imagery covers large geographical areas in one scene compared to aerial photographs, for example a nadir QUICKBIRD scene covers an area of 272 Km^2, which reduces the need for mosaicing and edge matching and saves many hours of image processing, and
(v.) RS imagery can be ordered and acquired at relatively short notice.

Nevertheless, all the mentioned data collection methods are still too expensive for an average municipality in developing countries. Though, it should be realised that disaster mitigation has high initial investment, but has long term cost saving measures to both life and property. Moreover, disaster mitigation projects cuts across municipal, regional and international boundaries. Many risk assessment projects are carried out as regional effort and with combined resources Areas that are in critical need of high resolution data can be identified and the cost of acquiring imagery can be shared since if one area is severely affected, it has spill over effects across the region. Moreover, even the cost for acquiring image analysis software can be reduced since most software vendors do offer special prices for non-profit making organisations such as regional disaster mitigation and early warning system centres. The other alternative for extracting building footprints were advanced image processing software are unavailable is on-screen digitising which can be done in most commonly available image processing software. The other alternative is to make existing databases such as cadastral information systems more detailed as mentioned above, then that way less information will be required from imagery and alternative cheaper images could be used. Other alternative high resolution RS imagery can found in Table 7-2.

6.6 Limitation of the research

The major limitation of this research was that the generated inputs were not implemented in the actual flood modelling. However a thorough literature review and consultation with experienced flood modellers enabled us to theoretically validate the usefulness of the results. The other limitation was that there was no reference data for the study area and no fieldwork, which are crucial when undertaking a research of such a magnitude. This presented some difficulties in interpreting some features in the image and defining the classification rules since we do not know the construction regulations of that city, which are important for extracting urban features such buildings and roads. For more conclusive results reference data and field work are very important. Nevertheless, the high resolution imagery available for the study was sufficient for interpreting most of the details in the study area.

7 Conclusions and recommendations

7.1 Conclusions

The research proposed to extract flood-risk related base-data from multi-source RS imagery with a focus on (i) integrating existing tools to extract base-data from multi-source remote sensing imagery, (ii) investigating the interchangeabilty of different image data sources to provide those data, (iii) and extracting quantitative information from various imagery sources. Seven research questions were put up to address these objectives. The first three required studying the characteristics of the data and study area, identifying the data to be extracted in this study, and identifying the suitable methods to extract those data from the available imagery. The model input requirements were identified based on the literature review in chapter 2, consultations with flood modellers and characteristics of the study area and data in chapter 3. The analysis of flood-risk model input requirements revealed that there is a significant variation in base-data requirements according to the level and place at which, the flood modelling is done. At a local level and in an urban environment, more accurate base-data are required due to the complexity of urban scenes, while in rural areas; relatively coarse data can suffice in most cases. Moreover, urban areas require more frequent update of base-data and modelling due rapid changes in developments and the consequent dynamics to hydraulic regimes and flood risk, as compared to rural areas where landscapes are more stable. After a review of information extraction techniques from imagery, and considering the high information content in the available imagery, object-oriented classification techniques were found suitable for the extraction base-data from high resolution imagery, which took the major part of the study. The major finding here was that the higher the information content in the image, the more complex are the classification rules required to extract the required base-data. The hierarchical classification structures available within eCognition software were employed to simplify the classification process. In this approach, image objects of different sizes were generated at each hierarchical level and interlinked. For example at the lower level, small objects where generated to represent houses, which were linked to large objects representing a settlement they belong to at the higher level.

Question four examined the role of lower resolution imagery (and this was treated in section 5.5). It was found relevant for large scale regional modelling that includes the upper and lower catchments. In addition, lower resolution imagery (15-30 m) was found suitable for depicting the general land cover patterns for monitoring of changes that can transform the hydraulic regimes and risk, before employing detailed high resolution imagery. The fifth question focused on evaluating the accuracy of automatically extracted base-data from imagery for correct application to flood risk modelling. Analysis of the results against flood risk model input requirements revealed that for flood risk modelling global accuracy values such as overall accuracy have little meaning especially when dealing with heterogeneous urban landscapes. Errors in specific classes are more important as confusion of classes can have serious implications on flood modelling results. It is more important to analyse the whole error matrix in order to identify the confused classes and apply appropriate remedial measures before applying the results to flood modelling.

The sixth question examined the importance of RS techniques in dealing with dynamic nature of flooding. After reviewing the factors that influence flooding (e.g. land cover/use changes, environmental degradation and climate change), it was found that RS techniques are suitable

for monitoring all these phenomena due to advantages of extensive coverage per scene, wide availability at various resolutions and speed of processing results. Question seven looked at the importance of high resolution RS images in extracting quantitative information for flood risk modelling, and this was demonstrated by various inputs that were generated in chapter 5.

7.1.1 Interchageability of the different image source

The major problem identified in this research, which results in most developing countries not having adequate flood-related early warning systems, is lack of flood risk models, which is in turn largely due to scarcity and cost of image sources from which most of the base-data needed to run them are derived. This study investigated the potential of interchangeabilty of QUICKBIRD and LIDAR DSM to provide some of the required base-data. In sections 5.1.4 and 5.1.5 building footprints were extracted from these two data sets for the same area and accuracies of 84% and 89% for QUICKBIRD and LIDAR DSM, respectively showed, a good potential for interchangeabilty of these data sets. The investigations were extended to discerning the boundaries of different settlements in section 5.4, and the results obtained also showed a good potential for interchangeabilty of the two data sets. The promising results obtained in this part of the research is good step towards handling the problem of scarcity and cost of image sources, since this study has demonstrated that different data sources can provide similar results. This is a cost saving measure especially for developing countries with limited budget allocation to projects of such a nature, because single images can be used instead of the usual trend of fusing image sources, which can provide the same base-data. In section 5.5, the interchangeabilty of medium resolution imagery was also investigated and different images showed good interchangeabilty to extract land covers for the area under investigation. In this case, the lack of an cloud free ASTER image from the NASA website, where these images are downloaded, strengthened the need for investigating the interchangeabilty of different data sets since satellites follow different orbital paths with different repeat cycles and one satellite may pass over the area of interest during unfavourable conditions.

However, QUICKBIRD are not 100% interchangeable with LIDAR DSM for providing all the base-data required for flood risk modelling in urban areas. In the case of representation of terrain, which is crucial for modelling the flow of flood water, the LIDAR DSM is superior. This study proposed combining results extracted from QUICKBIRD imagery with large scale contours maps generated DEMs and elevation information for man-made topographic objects that can be obtained from construction companies and maintenance organisations. These data sets can be supplemented by field methods in areas that are not sufficiently covered to assemble DSMs that can be useful for flow modelling in urban areas. This approach has significant cost saving benefits since high cost involved in acquiring DSM by either LIDAR or field methods can be avoided. Nevertheless, the successful implementation of this approach is dependant on a good archiving system of the height data for urban man-made objects as well as using the same reference datum. Therefore, municipalities interested in implementing such an approach should begin with developing a database for archiving such data.

7.1.2 Methods used

Automatic segmentation and classification of QUICKBIRD imagery and LIDAR nDSM for extracting building footprints based on eCognition software was studied and gave promising

results. However comparison with manually generated results revealed some errors that required human correction, as automatic methods were only partially applicable. If not properly addressed, errors such as false positives and false negatives can have serious implications on modelling results as they may lead to over or underestimating of the area covered by buildings.

The same methods were also used to extract a detailed land cover map in a crowded urban environment from a QUICKBIRD image as well as estimating building heights using LIDAR nDSM. An accuracy of 85% was achieved for the Land cover map. However, there was still confusion among urban land covers with similar spectral characteristics such as roads, buildings, and bare land.

The accuracy of the estimated of building heights could not be assed quantitatively due to lack of reference data. However, the results obtained corroborated an earlier study by *van Westen and Montoy (2004)* on the same area, though they used a different approach. Overall, the software proved useful as it gives possibilities to classify different types of images and meets different image analysis tasks.

Classification of high resolution imagery with eCognition proved advantageous because it considers features such as size, shape, texture, and topological relations that simplify the extraction of urban objects. In addition the possibility for class hierarchy allows for discrimination of mixed features in a logical stepwise approach. However, version 3.0 of the software, which was used in this study, has a limitation in that it was built to store all image information in its internal memory. Therefore, there is a limitation of the size of the image it can process at a time.

7.1.3 Final remarks

It would be stating the obvious to highlight the usefulness of RS imagery for generating input to flood-risk modelling, as various examples given in this study already demonstrated this. However, it is important to note that until now, RS imagery cannot give all the information that is required for flood risk assessment. For complete results on building materials, population, and socioeconomic data, integration with field methods and other techniques is not an option but a must. Moreover, existing framework data such as cadastral databases, river networks, road networks and topographic should be transformed to systems that can be easily integrated with new data collection methods such as GPS, GIS and RS. RS techniques can be useful in implementing a cost effective strategy for collecting base-data for flood risk modelling. For example land cover/use maps derived from medium resolution landsat imagery can be used for decision making and generating inputs to flood modelling at the regional level as well as a guide for identifying strategic areas to be covered by high resolution imagery such QUICKBIRD and IKONOS. High resolution imagery can be used to generate inputs for detailed analysis and modelling at the local level as well as a guide for identifying areas to be covered by aerial photos or field methods. Finally field methods can only be employed in areas that are not sufficiently covered by other methods and need more detailed analysis.

The present study shows a great potential for various remote image sources to extract base-data for input to flood risk models, which are used to generate useful information for decision makers to reduce the impacts of flood disasters through sustainable and safe land use planning. Most importantly, they are useful for providing effective early warning and in the

long run reduce the currently high number of fatalities caused by flooding in developing countries.

7.2 Recommendations

- Future research projects should be done in combination, for example one topic could look at aspects of extracting base-data, the other hazard modelling, and another handling the social aspects of vulnerability. That way more optimal methods and data needs can be identified since the projects would be carried out in a real life scenario.
- One aspect that still needs further research in flood hazard modelling is the effect and uncertainties brought about by misclassification errors. While the effects of DSM resolution have been well handled, very little effort has been put to studying the effect of resolution of land use/land cover on modelling results. Furthermore, for effective assessment, a detailed study on effects of assigning wrong roughness values due to misclassification should be carried out.
- The topic of using video imagery for collecting data for damage estimates should be explored further.
- At the municipality level building regulations should be strengthened and enforced to prevent people from building sub stand shelters and developing in the floodplains.
- Disaster mitigation, especially in developing countries, should be handled as a regional effort to distribute the high cost involved in acquiring image data from which the required risk related base-data can be derived.
- A study of estimating population, (numbers, density, etc.) from high resolution imagery such as QUICKBIRD imagery should be explored.
- Since most information related to buildings and important infrastructure is normally available at municipalities, construction companies, or individual homes, municipalities in developing countries should develop a culture of collecting, properly archiving, and making these data available in a spatial data infrastructure. This strategy would significantly reduce the need for overhaul intensive data collection as the database would be updated as developments are being made.
- Cadastral or property value databases that are mainly available should also incorporate information on building materials and heights, which is very useful for flood risk assessment.

7.3 Summary and recommendations for flood disaster managers

Flood disaster management studies are challenging question that need continuous updating of risk related-base data for the purpose of monitoring the dynamic nature of floodplains, which might affect or be affected by development. Traditionally, gathering and analyzing hydrologic data related to floodplains and flood-prone areas has been a time-consuming effort requiring extensive field observations and calculations. In floodplain mapping, the requisite data and maps include the following: DEMs, maps (detailing river networks, soil and geology land cover/use maps, population density, infrastructure, and settlements), and hydrological data. For accurate flood assessment, this approach requires extensive and long term field surveys, with a network of gauging stations that can acquire the data needed for precise risk assessments. Such extensive long term information is seldom available for river systems in most developing countries.

Floods, hydraulic forces, engineering structures, and development on the floodplain can and do result in physical changes in the river channel, sedimentation patterns, and flood

boundaries, and it is very costly to continually update maps to accurately depict these changing conditions. Moreover, for large areas, such as major river valleys, time and funds available are often limited. Therefore, it is usually not possible to conduct expensive detailed hydrologic data gathering, analysis, and mapping of ever-changing conditions required for flood disaster management. Recent developments in RS sensor technology and image analysis methods now provide an economically feasible alternative means of providing data required for flood disaster related studies rapidly at convenient levels of detail for different levels of analysis (Table 7-2).

In line with these technological developments, this study explored the utility of object-oriented image analysis techniques to extract flood risk-related base-data from high resolution RS imagery. This summary and recommendation section is meant for those who would like to use RS imagery for flood risk-related base-data extraction. From the experience gained in this study and literature survey, suitable imagery and accompanying information extraction methods are suggested. However, no detailed explanations, background to and justifications for, methods are given. For such information, the entire thesis should be read. Other basic concepts of remote sensing can be found in *Lillesand et al (2004)* and *Richards and Jia (1999*). The detailed characteristics of the suggested imagery can found by searching the World Wide Web on http/www.itc.nl/research/products/sensordb. As mentioned above these studies are performed at different abstraction levels, required detail and available imagery. Each level and required imagery will be briefly discussed. But before discussing each level the following are the general advantages of digital image processing techniques:

- Automatic spatial measurements.
- Rapid way of extracting information.
- Thematic enhancements, such as linear contrast stretches, band rating, geometric and atmospheric corrections, edge enhancements, etc.
- Image scenes can easily be combined to form mosaics that cover extensive areas
- Maximum scene processing versatility.
- Offers reproducible solutions.
- Can easily be combined with other data in GIS for detailed quantitative risk analysis.

7.3.1 Detailed localised studies

This level requires detailed analysis of hazard and elements at risk for accurate damage estimates and vulnerability assessment. It is data intensive and the methods used to collect data in order of accuracy are: field methods, aerial RS imagery and high resolution satellite imagery. The mapping is normally done at scales 1: 10, 000 to 1: 5000 or better. Due to wide availability, large coverage, ease of processing and relatively low cost compared to other methods, high resolution imagery (Table 7-2) is becoming the most preferred alternative. The choice of which image type to employ depends on availability, cost and the task at hand. For example mapping of building footprints in areas with high density of buildings is a difficulty task using an image with resolution less than 1 m, and using an image with only panchromatic information is difficult interpret and has a limited number of features that can be discerned. However, even high resolution colour RS imagery still needs to be supplement with field methods for checks and ground truth in selected areas. These images have high information content that cannot be automatically extracted using pixel-based classification techniques.

Therefore, object-oriented classification is a suitable image analysis technique to manage this high information content as demonstrated in this study. However, these techniques require expensive specialised software and detailed knowledge about the objects of interest in order to define rules for extracting them. Furthermore, automatic extraction methods are still error prone and therefore, they are used for preliminary extraction of required detail followed by refined human editing on minor erroneous section of results. This provides the fastest approach for extracting the required information at this level, but the high cost of software might be a hindrance. Since urban features are clearly discernible by human eye on high resolution imagery, the alternative is labour intensive and subjective on screen digitising.

Due to the high cost involved in acquiring high resolution imagery, it is recommended to focus such detailed investigation on priority areas such as heavily built-up urban areas, with small-scale detailed measurements that cannot be detected using medium resolution imagery discussed in the next section. Moreover, they should only be employed in areas that require detailed flood modeling.

Table 7-1 Price comparison of aerial photos and high resolution imagery,; prices are based on a township size area of 121 (km^2) adapted from *(Bauer, 2002)*

	Product	Accuracy	Resolution	Product Type	Price Rate
Aerial Photo (scanned, non-rectified)	9-inch	N/A	1-meter	Colour	$4 -5,000
Aerial Photo (orthorectified)	9-inch	custom	1-meter	Colour	$10 -15,000
IKONOS	Reference	25-meter	1-meter	Panchromatic & Multispectral	$5,300
	Precision	4-meter	1-meter	Panchromatic & Mulitispectral	$10,000
QuickBird	Standard	23-meter	.61-meter	Panchromatic & Mulitspectral	$3,600
	Orthorectified	10 -12 meter Or custom	.61-meter	Panchromatic & Mulitspectral	$7,800

The cost of aerial images compared to high resolution RS imagery varies from country to country depending on availability of specialized companies, who conduct aerial surveys. For developed countries where there are many companies, more competitive prices for aerial images are available. For example *Bauer (2002),* made a cost comparison between QUICKBIRD, IKONOS and aerial photos in the USA (see Table 7-1). However, for most developing countries where specialized companies are unavailable, hiring of specialised company to carryout an aerial survey is more expensive and my take longer to time to deliver the required information. In that case high resolution imagery has an advantage. However, when more details are required than what can be acquired from RS imagery, it is imperative to go for aerial photos.

7.3.2 Medium scale studies

At this level, medium scale mapping of elements at risk is done at scales 1: 50, 000 – 1: 25 000 depending on the resolution of imagery. The medium resolution imagery (Table 7-2) gives synoptic coverage of a catchments area, which is the practical alternative to high

resolution imagery because of cost and time factors. Some of the imagery in this range such as ASTER is available free of charge or at low cost. Most common flood-related base-data extracted from these images include: catchment's characteristics (shape, drainage, density, swampy areas and boundary), land cover/use boundary, soil moisture, and agriculture development. The soil moisture content can be analysed in the water absorption bands of the electromagnetic spectrum, as the lower the reflectance the in those regions the higher the moisture content. The other method for measure by analysing the vegetation water content, which is related to the soil moisture content (e.g. *Doriaswamy et al., 2004; Jackson et al., 2004*) Soil moisture can serve as warning for subsequent flooding, if the soil has become too saturated to hold any further runoff or precipitation. Unlike the high resolution imagery these images can be processed using pixel-based classifiers available in most commercial image analysis software such as ERDAS, ILWIS and ENVI, which are relatively cheaper and user friendly. However, where available, contextual object-oriented image classification techniques still give superior results. The advantage of wide coverage and cost, easy processing has made these images popular for extracting flood risk-related base-data for some national early warning systems (e.g. Zhang et al., 2002a) and have produced promising results. This is the category recommended for most developing countries since it is easy to implement and cost effective and can only be supplemented by high resolution imagery in high priority areas.

7.3.3 Small scale studies

These are studies carried out using low resolution imagery at scales of about 1: 100 000 – 1: 3, 000 000 (Table 7-1). They are meant for global synoptic view of the study area, when conducting preliminary studies. They are also used for delineating maximum flood coverage of surface areas for the purpose of disseminating information about the flooding situation during and after the disaster events *(e.g. Dartmouth Flood Observatory, 2004).* Pixel-based classification methods are the most suitable for processing these data.

7.3.4 Real time flood extent and soil moisture

The all weather and cloud penetration capability of microwave radar has made SAR images a principal tool for real-time assessment of floods and mapping. However this is only possible if the satellite passes the area of interest at the time of the disaster. Otherwise airborne radar has to be used, which still requires suitable conditions for flying the aircraft. The other application of radar imagery is to map soil moisture conditions, as radar backscatter is affected by soil moisture, apart from topography, surface roughness and amount and type of vegetation cover. Therefore, if the latter variables are remain constant, multi-temporal radar images can show the change in soil moisture. Examples of applications of to soil mapping can be found in *Lee and Anagnostou*, (2004) and *Blumberg et al. (2004).*

Table 7-2 Remote sensing imagery characteristics for use in integrated flood management studies

Application		Image source	Resolution (m)		Swarth width (km)	suitable method
			PAN	MS		
Detailed scale floodplain management (building footprints, transportation and river networks, damage and risk assessment,) land use/cover ping (scale, 1:25 000- 1: 5000), flood hazards delineation, etc.	**High resolution**	QUICKBIRD	0.61	2.44	16.5	Digitizing and Object-oriented contextual image analysis
		IKONOS	1	4	11	
		ORBVIEW-3	1	4	8	
		KVR-1000	1-3		40 - 160	
		SPOT-5	2.5/5	10	60	
		IRS-1C/D/P6	5.8	23	70- 140	
		KOMPSAT-1	6.6		15	
Synoptic view of entire region Medium flood management (scale, 1: 25 000- 150 000) land use/cover boundary, damage assessment , hazard delineation	**Medium resolution**	SPOT-1/2/3/4	10	20	60	Object-oriented contextual and pixel based analysis
		LANDSAT ETM	15	28.50	185	
		LANDSAT TM		30		
		ASTER		15	60	
Synoptic view of entire region, small scale regional maps (1: 100, 000- 1: 3000, 000), preliminary studies	**Low resolution**	MODIS		250-1000	2330	Pixel based classification
		NOAA-AVHR		1 km	2399	
All weather measuring capability: real time flood mapping, water body discrimination	**Radar**	RADARSAT-1	8-100		50-500	Object-oriented contextual and pixel based analysis
		ERS-1/2	25-30		100	
		ENVISAT-ASAR	12.5- 150 m		56 400	

References

Alexander, D., 1993, Natural Disasters, UCL Press and Chapman & Hall, 632 p.

Alkema, D., 2004, RS and GIS applications in flood forecasting, National Workshop on Flood Disaster Management-Space Inputs, 3-4 june, 2004, NRSA, Hyderabad, India.

Anderson, J.R., Hardy, E.E., Roach, J.T., and Witmer, R.E., 1976, Land use and land cover classification system for use with remote sensing data: Professional paper 964, United States Geological Survey, Washington, D.C.

Annan, K., 1999, "An increasing vulnerability to natural disasters, The International Herald Tribune: **URL**:http://www.un.org/Overview/SG/nnan_press.htm (Accessed 3/01/05).

Aynekulu, E., 2003, Analysis of soil-vegetation interaction in relation to soil carbon sequestraction [Msc. thesis]: Enschede, International Institute for Geo-Information Science and Earth Observation. pp. 59-65.

Baatz, M., and Schape, A., 2000, Multiresolution Segmentation -an optimization approach for high quality multi-scale image segmentation, *in* Strobl, J., and Blaschke, T., eds., Angewandte Georaphische Informationsverarbeitung XII. Beitrage zum AGIT-Symposium salzburg 2000. Karlsruhe . Herbert Wichmann verlag, p. 12 -23.

Badji, M., Dautrebande, S., Mokaden, A.I., and Dewez, A., 1994, ERS-1 SAR imagery applied to rural basins hydrological studies: the flood inundation mapping and monitoring., Proceedings of the First Workshop on ERS-1 Pilot Projects: T oledo, Spain, p. pp. 117–124.

Ballard, A., and Brown, C.M., 1982, Computer vision: Prentice-Hall, Inc, Englewood Cliffs, N.j.

Baltsavias, E.P., 2004, Object extraction and revision by image analysis using existing geodata and knowledge: current status and steps towards operational systems: ISPRS Journal of Photogrammetry & Remote Sensing 58 (2004) 129– 151, v. 58 (2004), p. 129– 151.

Baltsavias, E.P., Gruen, A., and van Goo, L., 2001, Automatic man-made object extraction from aerial and satellite images (iii). Balkema, Lisse.

Baltsavias, E.P., Mason, S., and Stallmann, D., 1995, Use of DTMs/DSMa and orthorimages to supprot building extraction, *in* Gruen, A., Kuebler, O., and Agouris, eds.: Balkema, Basel.

Barber, D.G., Hochheim, K.P., Dixon, R., Mosscrop, D.R., and McMullan, M.J., 1996, The Role of Earth Observation Technologies in Flood Mapping: A Manitoba Case Study: Canadian Journal of Remote Sensing, v. 22, p. 137-143.

Bauer, M., 2002, High -resolution satellite imagery and resource mangement: **URL:** http://rsl.gis.umn.edu (accessed 31/01/2005).

Bauer, T., and Steinnocher, K., 2001, Per-parcel land use classification in urban areas applying a rule-based technique, GeoBIT/GIS 6(2001), p. 24-27.

Benz, U.C., Hofmann, P.W., G. , Lingenfelder, I., and Heynen, M., 2003, Multi-resolution, object-oriented fuzzy analysis of remote sensing data for GIS-ready information: ISPRS Journal of Photogrammetry & Remote Sensing, v. 58 (2004), p. 239– 258.

Blaikie, P., Canon, T., Davis, I., and Wisner, B., 1994, At Risk: Natural hazards, people's vulnerability,and disasters.: London, Routledge.

Blumberg, D.G., Neta, T., Margalit, N., Lazar, M., and Freilikher, V., 2004, Mapping exposed and buried drainage systems using remote sensing in Negev Desert, Israel: Geomorphology, v. 61(2004), p. 239-250.

Brivo, P.A., Colombo, R., Maggi, M., and Tomason, R., 2002, Integration of remote sensing data and GIS for accurate mapping of flooded areas: International Journal of Remote Sensing, v. 23, p. 429-441.

Bye, P., and Horner, M., 1998, Easter 1998 Floods.: Vol.1, London.

Campbell, J.B., 1996, Introduction to remote sensing: London, Taylor & Francis, 121-155 p.

Cannon, T., 1993, A hazard need not a disaster make: vulnerability and the causes of 'natural' disasters. In: P.A. Merriman and C.W.A. Browitt, Editors, Natural Disasters: Protecting Vulnerable Communities, Thomas Telford, London, p. 92-105.

Canny, J., 1986, A computational approach to edge detection: IEEE Transaction on Pattern Analysis and Manchine Intelligence, v. 8(6), p. 679-698.

Carlotto, M.J., 1998, Spectral shape classification of landsat thematic mapper imagery: Photogrammetric Engineering & Remote Sensing, v. 64(9), p. 905-913.

Chapman, G., Lenting, V., and Ashby, G., 2003, Thames coast flood risk assessment: Christchurch, New Zealand.

Clerke, W.H., 1994, Aerial Videography for Natural Resource Application in East Africa, USDA Forest Service, Antalanta, Geogia.

Company, M.R., 2001, Topics, annual review: Natural catastrophies, 2000, Munich Re, Munich.

Congalton, R., 1991, A review of assessing the accuracy of classification of remotely sensed data: Remote Sensing of Enviroment, v. 37, p. 35-46.

Corr, D.G., Tailor, A.M., Cross, A., Hogg, D.C., Lawrence, D.H., Mason, D.C., and Petrou, M.a., International journal of remote sensing, . 1989, Progress in automatic analysis of multi-temporal remotely sensed data: International Journal of Remote Sensing, v. 10(7), p. 1175-1195.

Cortijo, F.J., and Perez de la blanca, N., 1997, A Comparative Study of Multispectral Image Classifiers: Applications to Classification Problems with High-dimension Data and High-overlapping Spectral Signatures, DECSAI Technical Report: Depto. Ciencias de la Computacióne I. A. (DECSAI), Ingeieria informàtica, Universida de Granada, Granada, Spain.

CRED, Centre for Reserach on the Epidemiology of Disasters, 2004, EM-DAT: The OFDA/CRED International Disaster Database **URL**: www.em-dat.net (Acessed 24/01/2004).

Dartmouth Flood Observatory, 2004, 2004 Global Register of Major Flood Events: http://www.dartmouth.edu/~floods/index.html (Accessed August 12, 2004).

de By, R.A., 2001, Principles of Geographic Information Systems: Enchede, The Netherlands.

De Kok, R., Wever, T., and Fockelmann, R., 2003, Analysis of Urban Structure and Development Applying Procedures for Mapping of Large Area Data, The International Archives of the Photogrammetry, Remote Sensing and Spatial Information Sciences: Regensburg, Germany, 27-29 June 2003.

De Roo, A.P.J., 1999, LISFLOOD: A rainfall-runoff model for large river basins to assess the influence of land use changes on flood risk, RIBAMOD proceedings, Wallingford/European Commission EUR18287.

Dobson, J.E., Bright, E.A., Coleman, P.R., Durfee, R.C., and Worley, B.A., 2000, Landscan: A global population database for estimating population at risk: Photogrammetric Engineering & Remote Sensing, v. 66, p. 849-857.

Doriaswamy, P.C., Hatfield, J.L., Jackson, T.J., Akhmedov, B., Prueger, J., and Stern, A., 2004, Crop condition and yeild simulations using Landsat and MODIS: Remote Sensing of Enviroment, v. 92(2004), p. 548-559.

du Plessis, L.A., Viljoen, M.F., Weepener, H.L., and Berning, C., 1999, Flood damage functions, models and a computer program for irrigation and urban areas in South Africa, University of Orange Free State, p. 1-163.

Eckstein, W., and Munkelt, O., 1995, Extracting objects from digital terrain models, *in* Schenk, T., ed., Remote sensing and reconstraction for 3D objetcs and scenes. Proceedings of SPIE Symposium on Optical Science, Engineering, and Instrumentation, Volume 2572: San Diego.

eCognition, 2004, User guide, Technical report, Definies Imagine GmbH, Munich: Munich.

ERDAS field guide, 2003.

Fisher, P., 1997, The pixel: a snare and delusion: International Journal of Remote Sensing, v. 18(3), p. 679-685.

Fujii, K., and Arikwa, T., 2002, Urban object reconstruction using airbone laser elevation image and aerial image: IEEE Transaction on Geoscience and Remote Sensing, v. 40(10), p. 2234-2240.

Galy, G.M., and Sanders, S.A., 2000, Using SAR imagery for flood modelling, RGS-IBG Annual Conference: University of Sussex.

Gascuel, O., B.B. , Meunier, G., Caraux, P., Gallinari, A., Guenoche, Y., Guermeur, Y., Lechevallier, C., Marsala, L., Miclet, J., Nicolas, R., Nock, M., Ramdani, M., Sebag, B., Tallur, G., and Vitte, P., 1993, Twelve Numerical, Symbolic and Hybrid Supervised Classification Methods: International Journal of Pattern Recognition and Artificial Intelligence, p. 517-571.

Gerke, M., Butenuth, C., and Heipke, C., 2003, Automatic update of roads databases using aerial imagery and road construction data, ISPRS Archives, Volume XXXIV, Part3/W8: Munic, 17-19 Sept. 2003.

Glickman, T.S., Golding, D., and Silverman, E.D., 1992, Act of God and acts of man: Recent trends in natural disasters and major industrial accidents, Center for Risk Management: Worshington DC: Island Press.

Gong, P., and Howarth, P.J., 1989, Performance analyses of probabilistic relaxation methods for land-cover classiifcation: Remote Sensing of Enviroment, v. 30, p. 33-42.

—, 1990a, An assessment of factors influencing multispectral land-cover classification: Photogrammetric Engineering & Remote Sensing, v. 56(1), p. 67-73.

—, 1990b, The use of structural information for improving land-cover classification accuracies at rural-urban fringe: Photogrammetric Engineering & Remote Sensing, v. 56(1), p. 67-73.

—, 1992, Land-use classification of SPOT HRV data using a covedr -frequency method: International Journal of Remote Sensing, v. 13(8), p. 1459-1471.

Green, C.H., Parker, D.J., and Tunstall, S.M., 2000, Assessment of flood control and management options, Options Assessment: IV.4, Flood Hazard Research Centre, Middlesex University, p. 42-50.

Gruen, A., Baltsavias, E.P., and Henricsson, O., 1997, Automatic man-made object extraction from aerial and satellite images (II): Birkhäuser, Basel.

Gruen, A., Kuebler, O., and Agouris, P., 1995, Automatic man-made object extraction from aerial and satellite images (I): Balkema, Basel.

Guindon, B., 1997, Computer-based aerial image understanding: A review and assessment of its application to planimetric information extraction from very high resolution satellite images: Ottawa, Canada Centre for Remote Sensing.

Haala, N., and Brenner, C., 1999, Virtual city models from laser altimeter and 2D map data, Joint International Symposium on Geospatial Theory, Processing and Applications, Proceedings CD, Ottawa, Canada.

—, 1999a, Virtual City Models from Laser Altimeter and 2D map data, Joint International Symposium on Geospatial Theory, Processing and Applications, Proceedings CD, Ottawa, Canada.

Haralic, R., Shanmugam, K., and Dinstein, I., 1973, Texture features for image classification: IEEE Transaction on Systems, Man, and Cybernetics, v. SMC-3, p. 610-621.

Haralick, R., Shanmugam, K., and Dinstein, I., 1973, Texture features for image classification: IEEE Transaction on Systems, Man, and Cybernetics, v. SMC-3, p. 610-621.

Haralick, R.M., and Shapiro, L., 1992, Image segmentation techniques: Computer Vision and image processing, v. 29, p. 100-132.

Hardoy, J., and Satterthwaite, D., 1989, Squatter citizens: Life in the urban third world: London, Earth publications.

Heipke, C., Mayer, H., and Weidemann, C., 1999, Acquisition and updating of ATKIS using satellite remote sensing imagery, Remote Sensing Symposium on Remote Sensing of the System Earth A Challenge for the 21st Century: 28 June–2 July 1999, Hamburg.

Heipke, C., Pakzad, K., and Straub, B.M., 2000, Image analysis for GIS data aquisition: Photogrammetric Records, v. 16(96), p. 963-985.

Herold, M., Lui, X., and Clarke, K.C., 2003, Spatial metrics and image texture for mapping urban land use: Photogrammetric Engineering & Remote Sensing, v. 69(9).

Herold, M., and Scepan, J., 2002, Object-oriented mapping and analysis of urban land use/cover using IKONOS data, Proceedings of 22nd EARSEL Symposium "Geoinformation for European-wide integration: Prague, June 2002.

Hofmann, P., 2001a, Detecting informal settlements from IKONOS image data using methods of object oriented image analysis-an example from Cape Town (South Africa), *in* Jürgens, C., ed., Remote Sensing of Urban Areas: Regensburg.

—, 2001b, Detecting urban features from IKONOS data using an object-oriented approach, DEFiNiENS Imaging GmbH, Trappentreustr. 1, D-80339, Minich, Germany.

Holfman, P., 2001, Detecting Informal Settlements from IKONOS image data using methods of object oriented image analysis-an example from Cape Town (South Africa), *in* Jürgens, C., ed., Remote Sensing of Urban Areas: Regensburg.

Holfmann, P., 2001, Detecting informal settlements from IKONOS image data using methods of object oriented image analysis-an example from Cape Town (South Africa), *in* Jürgens, C., ed., Remote Sensing of Urban Areas: Regensburg.

Hui, A., Liew, S.C., Kwoh, L.K., and Lim, H., 2004, Extraction and utilization of geometrical and contextual information in very high resolution IKONOS batellite imagery: Singapore, Centre for Remote Imaging, Sensing and Processing, National University of Singapore Bkl.

Huurneman, G.C., and Jansen, L.L.F., 2001, Principles of remote sensing: International Institute for Aerospace Survey and Earth Observation, Enschede, second edition.

IDNDR, (International Decade for Natural Disaster Reduction), 1999, The mandate on disaster reduction, International Program Forum, Geneva, 5-9 july 1999: **URL**: www.unisdr.org/forum/mandate.htm (Accessed 28/12/04).

IFRCRS, (International Federation of Red Croos Red Cresent Societies), 1998, World disasiter report 1998: Oxford, p. 142- 147.

Inter.-Agency Secretariat of the International Strategy for Disaster Reduction (UN/ISDR), 2004, HAITI, Poverty generates disasters.

Jackson, J.T., Chen, D., Cosh, M., Li, F., Anderson, M., Wathall, C., Doriaswamy, E., and Hunt, E.R., 2004, Vegetation water content mapping using Landsat data derived normalised water index for corn and soyabeans: Remote Sensing of Enviroment, v. 92(2004), p. 475-482.

Jacobs, D.M., and Eggen-McIntosh, S., 1992, Airborne Vidoegraphy and GPS for Assessment of Forest Damage in Southern Louisan from Hurricane Andrew: Starkvillee, USA, USDA Forest Service, Southern Forest Experiment Station Forest Inventory and Analysis, p. 1-5.

Jensen, J.R., 1996, Introductory digital image processing: A remote sensing perspective.: 2nd ed. Englewood Cliffs, New Jersey: Prentice-Hall.

Kerle, N., and Stekelenburg, R., 2004, Advanced structural disaster damage assessment based on aerial oblique video imagery and intgrated auxiliary data sources, XXth ISPRS Congress: Istanbul, Turkey.

King, D.J., Jollineau, M., and B., F., 1999, Evaluation of MK-4 multispectral satellite photography in land cover classification of eastern Ontario: International Journal of Remote Sensing, v. 20(17), p. 3311-3331.

Kloer, B.R., 1994, Hybrid parametric/non-parametric image classification: Paper presented at the ACSM-ASPRS Anual Convention, Reno, Nevada, April 1994.

Kontoes, C.C., Raptis, V., Launter, M., and Oberstadler, R., 2000, The potential of kernel classification techniques for land use mapping in urban areas using 5m-spatial resolution IRS-1C imagery.: International Journal of Remote Sensing, v. 21(16), p. 3145-3151.

Kraus, K., and Pfeifer, N., 1998, Determination of terrain models in wooded areas with aerial laser scanner data: ISPRS Journal of Photogrammetry & Remote Sensing, v. 53(4), p. 193-203.

Lacroix, V., 1988, A three module strategy for edge-detection: IEEE Transactions on Pattern Analysis and Machine Intelligence, v. 10(6), p. 803-810.

Lee, K., and Anagnostou, E.N., 2004, A combined passive/active microwave remote sensing approach for surface variable retrival using Tropical Rainfall Measuring Mission observations: Remote Sensing of Enviroment, v. 92(2004), p. 112-125.

Lichtenegger, J., and Calabresi, G., 1995, ERS monitors flooding in The Netherlands. ESA, ESA Bulletin, Volume 81, p. p.94.

Lillesand, T.M., Kiefer, W.K., and Chipman, J.W., 2004, Remote sensing and image interpretation: John Wiley & Sons, New York, third edition,.

Lo, C.P., 1986, Accuracy of population estimates from medium-scale aerial photographs: Photogrammetric Engineering & Remote Sensing, v. 61, p. 1859-1869.

—, 1995, Automated population and dwelling estimates from high resolution imagery, a GIS approach: International Journal of Remote Sensing, v. 16(1), p. 17-34.

—, 2001, Modelling the population of China using DMSP operational linescan system night-time data: Photogrammetric Engineering & Remote Sensing, v. 67, p. 1037-1047.

Lucieer, A., 2004, Uncertainties in segmentation and their visualisation [PhD thesis]: Utrecht, Universiteit.

Marangoza, A.M., Oruc, M., and Buyuksalih, G., 2004, Object-oriented Image Analysis and Semantic Network for Extracting the Roads and Buildings from IKONOS Pan-sharpened Images, International Society for Photogrammetry and Remote Sensing, p. CD_ROM.

Martine, G., and Guzman, J.M., 2002, Population, poverty and vulnerability: Mitigating the effects of natural disasters, Environmental Change and Security Project (ECSP) Report , Issue 8, p. 45-68.

Mason, S.O., and Fraser, C.S., 1998, Image sources for informal settlements: Photogrammetric Records, v. 16(92), p. 313-330.

Mastin, M.C., 2002, Flood-hazard mapping in Honduras in response to Hurricane Mitch: Tacoma, Washington, U.S. GEOLOGICAL SURVEY, p. 1-52.

Matthews, J., and Gaffney, S., 1994, A study of flooding on Lough Corrib, Ireland during early 1994 using ERS-1 SAR data., Proceedings of First ERS-1 Pilot Project Workshop: Toledo, Spain, p. pp. 125-128.

Mausel, P.W., Everitt, J.H., Escobar, D.E., and King, D.J., 1992, Airborne vidography: current status and future perspectives: Photogrammetric Engineering & Remote Sensing, v. 58(8), p. 1181-1195.

Meitnel, G., Neubert, M., and Reder, J., 2001, The potential use of very high resolutions satellite data for uraban areas first experiences with IKONOS data, their classification and application in urban planning and environment monitoring, *in* Jurgens, C., ed., Remote Sensing of Urban Areas: Regensburg, Germany, p. 196-205.

Melching, C., and Pilon, P., 1999, Comprehensive risk assessment for natural hazards, *in* Melching, C., and Pilon, P., eds., WMO/TD No. 955: Geneva, World Meterological Organisation.

Mena, J.B., 2003, State of the art on automatic road extraction for GIS update: a novel classification: Pattern Recognition Letters, v. 24 (2003), p. 3037–3058.

Montoya, A.L., 2002, Urban Disaster Management: A Case Study of Earthquake Risk Assessment in Cartago, Costa Rica, ITC, Enschede.

Munich Reinsurance, 2000, Topics 2000. Natural Catastrophes - the current position. Special Millenium Issue, Munich Re Group, Munich 126pp.

—, 2003, GeoRisikoForschung, October.

Nirupama, S., and Simonovic, S., 2002, Role of Remote Sensing in Disaster Management MANAGEMENT, Institute of Catastrophic Loss Reduction, London, Ontario.

Ozisik, D., and Kerle, N., 2004, Post-earthquake damage assessment using satellite and airborne data in the case of the1999 Kocaeli earthquake, Turkey, XXth ISPRS Congress: Istanbul, Turkey.

Pal, N.R., and Pal, S.K., 1993, A review on image segmentation techniques: Pattern Recognition Letters, v. 26, p. 1277-1294.

Pal, S.K., and Wang, P.P., 1996, Genetic algorithms for pattern recognition: Boca Raton.

Qui, F., Woller, K.L., and Briggs, R., 2000, Modelling urban population growth from remote sensing imagery and TIGER GIS road data: Photogrammetric Engineering & Remote Sensing, v. 69(9), p. 1031-1042.

Ramala, T.V., 2001, Contribution of aerospace Imagery to assess flood risk on human settlements. A case study in Johannesburg, South Africa: Johannesburg, South Africa, CSIR, Satellite Applications Centre, p. 1-5.

Richards, J.A., and Jia, X., 1999, Remoten sensing digital image analysis.

Robinson, G.S., 1977, Edge detection by compass gradient masks: Computer graphics and image processing, v. 6, p. 492-501.

Rottenstein, F., and Jansa, J., 2002, Automatic extraction of buildings from LIDAR data and aerial images, Symposium on Geospatial Theory, Processing and Applications: Ottawa.

RSCC, Remote Sensing Core Curriculum, 2005, Photogrammetry, height and area measurements: **URL:** http://www.r-s-c-c.org/rscc/v112.html (accesed 31/01/2005).

Ruther, H., Martine, M.H., and Mtalo, E.G., 2002, Application of snakes and dynamic programming optimisation technique in modelling of buildings in informal settlement areas: ISPRS Journal of Photogrammetry & Remote Sensing, v. 56, p. 269-282.

Schiewe, J., 2003, Mult-Sensoral data processing for urban landscapa modelling: new meritis and new problems, The International Archives of the Photogrammetry, Remote Sensing and Spatial Information Sciences: Regensburg, Germany, 27-29 June 2003.

Schowengerdt, R., 1983, Techniques for images processing and classification in remote sensing: New York: Academic.

Scott, L., Shan, J., and Bethel, J.S., 2003, Class-guided building extraction from IKONOS imagery: Photogrammetric Engineering & Remote Sensing, v. 69, p. 143-150.

Shackelford, A.K., and Davis, C.H., 2003, A Combined fuzzy pixel-based and object-based approach for classification of high resolution multi-specral data over urban areas: IEEE Transaction on Geoscience and Remote Sensing, v. 41, p. 2354-2363.

Shufelt, J.A., 1999, Performance evaluation and analysis of monocular building extraction from aerial imagery. IEEE Pattern Analysis and Machine Intelligence, v. 21(4), p. 311-326.

Sithole, G., and Vosselman, G., 2004, Experimental comparison of filter algorithms for bare-Earth extraction from airborne laser scanning point clouds: ISPRS Journal of Photogrammetry & Remote Sensing, v. 59, p. 85-101.

Smith, M.E., Phillips, J.V., and Spahr, N.E., 2000, hurricane Mitch: peak discharge for selected river reaches in Hondurus, United States Geological Survey (USGS).

Smith, M.J., Asal, F.F.F., and Priestnall, G., 2004, The use of photogrammetry and LIDAR for landscape roughness estimation in hydrodynamics studies, *in* Altan Orhan, M., ed., International Society for Photogrammetry and Remote Sensing, Volume 35, p. CD-ROM.

Soille, P., 1999, Morphological image analysis: principles and applications: Springer-Verlag, Berlin Heidelberg.

—, 2002, Advances in mathematical morphology applied to goescience and remote sensing: IEEE Transaction on Geoscience and Remote Sensing, v. 40(9), p. 2042-2055.

Steger, C., Glock, C., Eckstein, W., Mayer, H., and Radig, B., 1995, Model-based road extraction from images, *in* Gruen, A., Kuebler, O., and Agouris, P., eds., Automatic extraction of man-made objects from aerial and space images: Berlin, German, Birkhauser Verlag, p. 275-284.

Steinnocher, K., and Bauer, T., 2001, Land use classification using IKONOS data: Per-parcel land use classification in urban areas applying a rule-based technique: Seibersdorf, Austrian Reserach Centres Seibersdorf, p. 5.

Strat, T.M., 1995, Using contex to control computer vision algorithms, *in* Gruen, A., Kuebler, O., and Agouris, p., eds., Automatic Extraction of Man-Made Objects from Aerial and Space Images: Berlin, Birkhauser, Swizerland.

Sun, W., Heidt, V., Gong, P., and Xu, G., 2003, Information fusion for rural land-use classification with high-resolution satellite imagery: IEEE Transaction on Geoscience and Remote Sensing, v. 41(4), p. 893-890.

Sutton, P., 1997, Modelling population density with night-time satellite imagery and GIS: Computers, Environment and Urban System, v. 21, p. 227-244.

Tempfli, K., 2004, Generation of framework data: Topography and orthophotography, GFM/2 lecture notes, International Institute for Earth Observation Science and Earth Observation: Enschede, The Netherlands.

Tennakoo, K.B.M., 2004, Parameterisation of 2D hydrodynamic models and flood hazard mapping for Naga city, Phillipines [Master of Science thesis], International I nstitute for Geo-information Science and Earth Observation Enschede, The Netherlands.

Thormodsgrad, J.M., and Feuguay, J.W., 1987, Large scale mapping with SPOT, Proceedings, SPOT-1 utilisation and assessment results: Paris, France.

Ton, J., Stricken, J., and Jain, A.K., 1991, Knowledge-based segementation of Landsat images: IEEE Transaction on Geoscience and Remote Sensing, v. 29(2), p. 222-232.

Townsand, F.E., 1986, The enhancement of computer classification by logical smoothening: Photogrammetric Engineering & Remote Sensing, v. 63(6), p. 691-666.

UN/ISDR, (Inter.-Agency Secretariat of the International Strategy for Disaster Reduction),, 2004, HAITI, Poverty generates disasters.

UN/ISDR, (United Nations/ Inter-Agency Secretariat of the International Strategy for Disasters Reduction), 2002, Guidelines for reducing flood looses: available online **URL:** www.unisdr.org (Accessed on 24/01/2003).

UNDP, (United Nations Development Programme), 2004, Reducing disaster risk, A challenge for development: New York, USA URL: www.undp.org/bcpr (Accessed, 21/01/2004).

UNDP/ECLAS, (United Nations Development Programme and United Nations Economic Commission for Latin American and the Caribean), 1998, A preliminary assessment of damages caused by the Hurricane Mitch.

United Nations Disaster Relief Co-ordinator, 1991, Mitigating Natural Disasters: Phenomena, Effects and Options., A Manual for Policy Makers and Planners: New York, USA.

van der Sande, C.J., Jong, S.M.d., and Roo, A.P.J.d., 2003, A segmentation and classification approach of IKONOS-2 imagery for land cover mapping to assist flood risk and flood damage assessment: International Journal of Applied Earth Observation, v. 4, p. 217-229.

van Westen, C., 2002, Geoinformation science and Earth observation for municipal risk management: The SLARIM project: Enschede, The Netherlands, International Institute for Geoinformation Science and Earth Observation, ITC.

van Westen, C., and Montoya, A.L., 2004, Use of LIDAR for building height determination a case study of flood risk in Tegucigalpa, Honduras, International Institute for Geo-Information Science and Earth Observation (ITC).

Vögtle, T., and Steinle, E., 2000, 3D modelling of buildings using laser scanning and spectral information, International Archives of Photogrammetry and Remote Sensing, Volume Vol. XXXIII, Part B3: Amsterdam, The Netherlands, p. 927-934.

Vögtle, T., Steinle, E., 2000, 3D modelling of buildings using laser scanning and spectral information, International Archives of Photogrammetry and Remote Sensing, Volume Vol. XXXIII, Part B3: Amsterdam, The Netherlands, p. 927-934.

Vosselman, G., 2000, Slope based filtering of laser altimetry data.: International Archives of Photogrammetry, Remote Sensingand Spatial Information Sciences, v. XXXIII part 3B, p. 935-942.

Vosselman, G., Gorte, B.G.H., Sithole, G., and Rabbani, T., 2004, Recognising structure in laser scanner point clouds: The International Archives of the Photogrammetry, Remote Sensing and Spatial Information Sciences.

Vosselman, G., and Suveg, I., 2001, Map based building reconstruction from laser data and images, *in* Baltsavias, E.P., ed., Automatic Extraction of Man-Made Objects from Aerial and Space Images (III), Balkema Publishers.

Wang, Y., Koopmans, B.N., and Pohl, C., 1995, The 1995 flood in The Netherlands monitored from space-a multisensor approach: International Journal of Remote Sensing, v. 16, p. 2735–2739.

Weber, C., and Puissant, A., 2003, Urbanization pressure and modeling of urban growth: example of the Tunis Metropolitan Area: Remote Sensing of Enviroment, v. 86, p. 341-352.

Welch, R., and Ehlers, W., 1987, Merging multiresolution SPOT HRV and Landsat TM data: Photogrammetric Engineering & Remote Sensing, v. 53(3), p. 301-303.

Wharton, S.W., 1987, A spectral-knowledge-based approach for urban land-cover discrimination: IEEE Transaction on Geoscience and Remote Sensing, v. 25.

Wilson, R., and Spann, M., 1988, Image segmentation and uncertainty: Letchworth, Hertfordshire, England.

Zedeh, L., 1965, Fuzzy sets: IEEE Transaction Information and Control, v. 8(3), 338-353.

Zhang, J., Zhou, C., Xu, K., and Watanabe, M., 2002a, Flood disaster monitoring and evaluation in China: Environmental Hazards, v. 4, p. 33-44.

Zhang, Q., 2003, A hierarchical object-based approach for urban land-use classification from remote sensing data [PHD thesis]: Wageningen, The Netherlands, Wageningen University.

Zhang, Q., Molenar, M., and Tempfli, K., 2002b, Heirarchical image object-based structural analysis toward urban land use classification using high-resolution imagery and airborne LIDAR data, The 3rd International Symposuim on Remote Sensing of Urban Areas, Volume 1: Istambu, Turkey, p. 251-258.

—, 2002d, Heirarchical image object-based structural analysis toward urban land use classification using high-resolution imagery and airborne LIDAR data, The 3rd International Symposuim on Remote Sensing of Urban Areas, Volume 1: Istambu, Turkey, p. 251-258.

Zhou, G., Song, C., Simmers, J., and Cheng, P., 2004, Urban 3D GIS from LIDAR and digital aerial images: Computers & Geosciences, v. 30(2004), p. 345-353.

Zucker, S., 1976, Region growing: Childhood and Adolescence: Computer graphics and image processing.